OPTIMAL SPACE TRAJECTORIES

Theodore N. Edelbaum

Analytical Mechanics Associates, Incorporated
Jericho, New York

December 1969

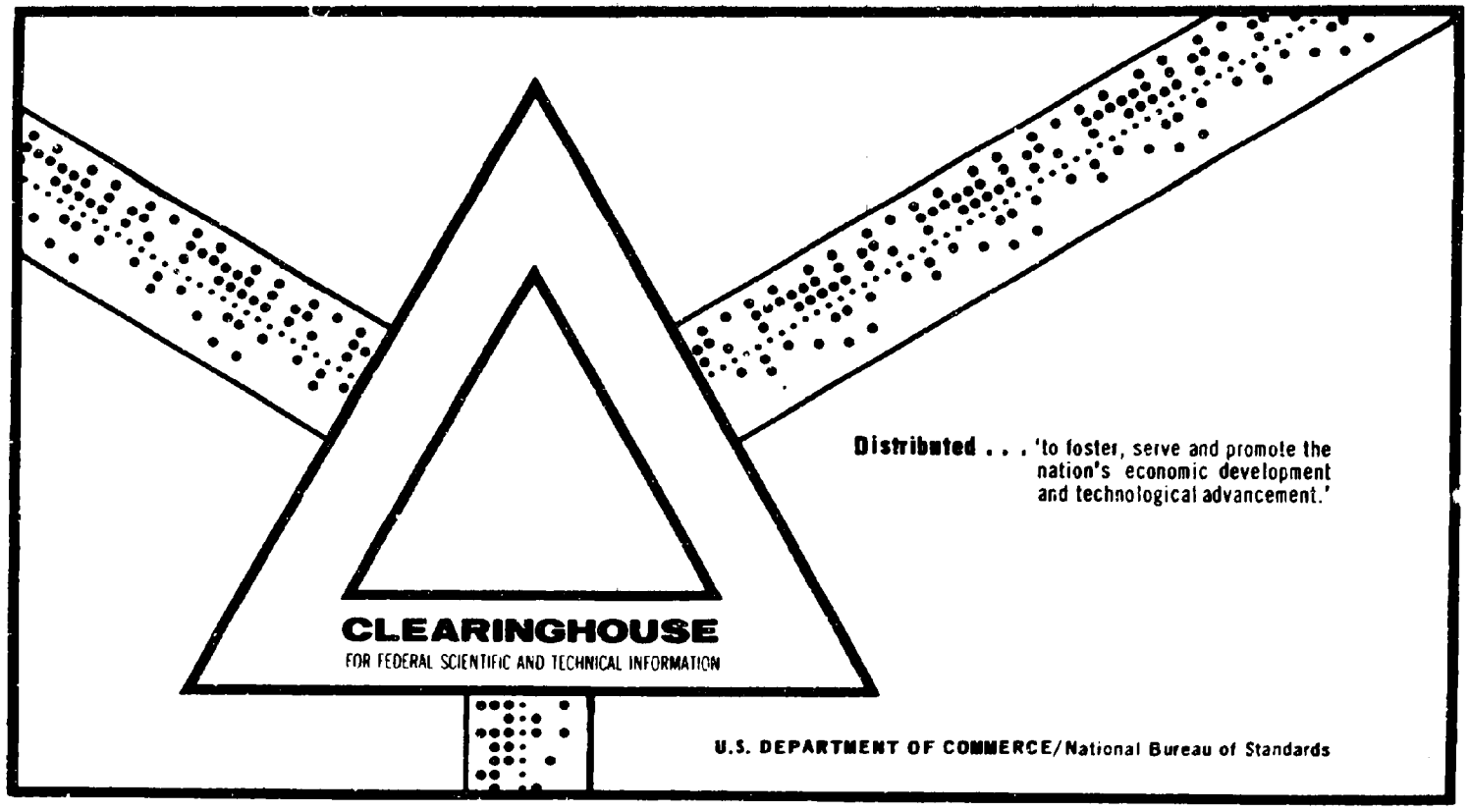

Final Report

OPTIMAL SPACE TRAJECTORIES

Theodore N. Edelbaum

Contract No. AF 49 (638) - 1648

December 1969

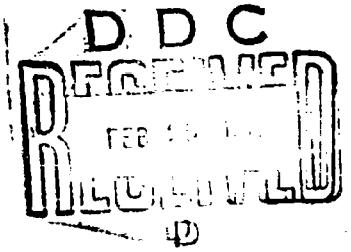

Analytical Mechanics Associates, Inc.

Jericho, N. Y.

1. This document has been approved for public release and sale; its distribution is unlimi

TABLE OF CONTENTS

CHAPTER 1: SPACE PROPULSION SYSTEMS

1.1 Rocket Propulsion Fundamentals

A rocket is a device which propels a vehicle by expelling mass. In space, where aerodynamic forces are negligible and where solar radiation pressure forces are assumed to be negligible, the equation of motion of a rocket powered vehicle is given by Eq. (1.1).

$$m\ddot{\bar{r}} = \dot{m}\bar{c} + m\bar{g} \tag{1.1}$$

In this equation m is the mass of the vehicle, $\bar{r}$ is the position vector, $\bar{c}$ is the exhaust velocity vector of the rocket, $\bar{g}$ is the gravitational acceleration, and $\dot{m}$ is the rate at which mass is expelled from the rocket. The rocket exhaust is assumed to be uniform in direction and magnitude. This equation gives the proper form of Newton's law for a variable mass body whose loss of mass is solely through a uniform rocket exhaust stream. The thrust of the rocket is defined by Eq. (1.2),

$$\bar{f} = \dot{m}\bar{c}, \tag{1.2}$$

and since the rate at which the vehicle loses mass is negative, the thrust will be directed opposite to the exhaust velocity vector of the rocket.

For electrically propelled vehicles, a quantity of some importance is the power in the exhaust stream since this power must be supplied from a power

source. The exhaust stream power is given by Eq. (1.3) for a uniform exhaust stream.

$$P = \frac{fc}{2} = -\frac{f^2}{2\dot{m}} \tag{1.3}$$

Throughout this monograph, we shall be attempting to minimize the mass of fuel consumed by the rocket. It is therefore important to have an expression for the rate at which mass is lost. This expression is given in two alternate forms by Eq. (1.4).

$$\dot{m} = -\frac{f}{c} = -\frac{f^2}{2P} \tag{1.4}$$

The rate of mass flow is proportional to the first power of thrust for a rocket with constant exhaust velocity and is proportional to the second power of thrust for a rocket with constant power. It is inversely proportional to either exhaust velocity or power, hence it is desirable to have high exhaust velocity or high power in rockets. Instead of exhaust velocity, rocket engineers normally speak of a quantity called specific impulse which is most conveniently defined as the exhaust speed divided by the standard acceleration of gravity, Eq. (1.5).

$$I = \frac{c}{g_0} \tag{1.5}$$

Specific impulse is normally measured in units of seconds.

The variation of thrust with mass flow rate for the two types of rockets is shown in Figure 1.1. It should be noted that the curves cross at two points.

Fig. 1.1 Variation of Thrust With Mass Flow Rate

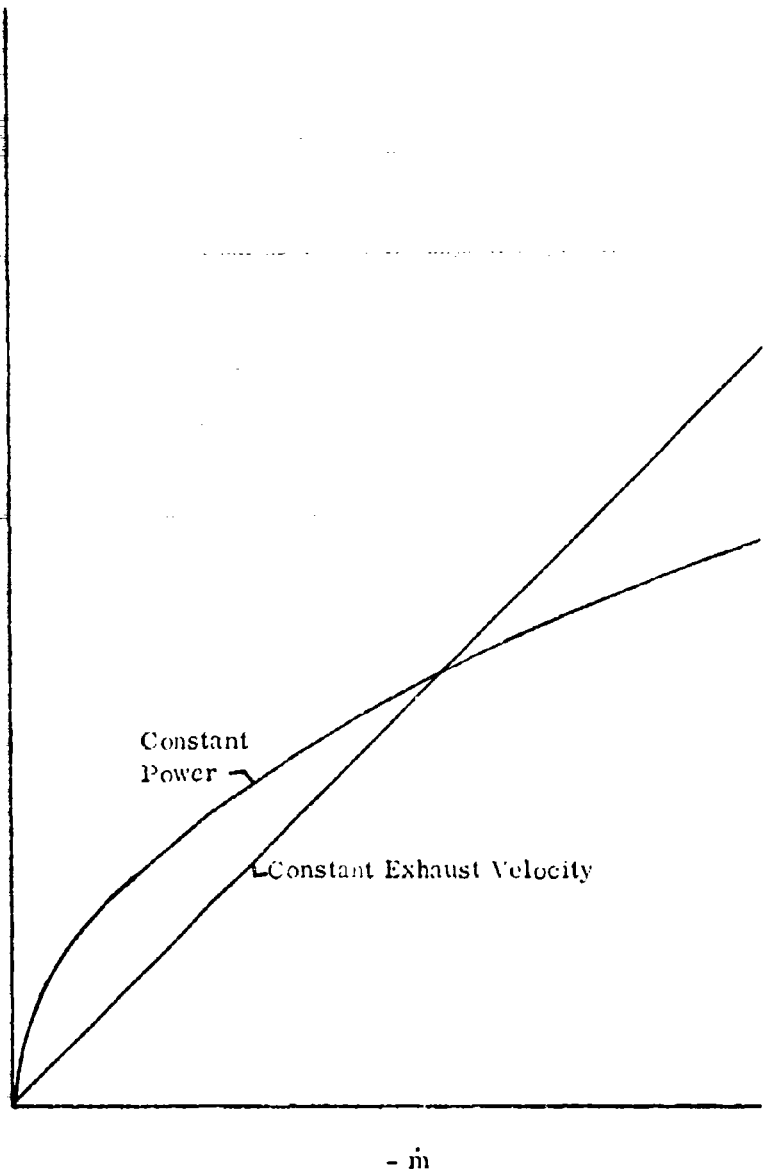

at the origin and at some finite thrust. Many rockets cannot be operated at various thrust levels but can be switched on and off. Such rockets may be considered as having either the same power or the same exhaust velocity at their operating point and when they are switched off.

1.2 The Spectrum of Space Propulsion Systems

Any rocket engine may be characterized by two important quantities which affect vehicle performance: the ratio of thrust to engine weight for the rocket and the specific impulse of the rocket. The ratio of thrust to engine weight is a measure of the mass of the engine required for a given thrust level, while the specific impulse gives a measure of the fuel required for various missions. The possible variations in these quantities for space propulsion systems are surprisingly wide, falling basically into two different areas. A plot of the ratio of the thrust to engine weight (at standard gravity) versus specific impulse is shown in Figure 1.2 for some of the more conventional types of rockets. All the way up in the left-hand corner of the figure, there is a block representing chemical rockets. Chemical rockets have large ratios of thrust to engine weight. The engines weigh very little for the thrust they produce, but they also have relatively low specific impulses. There are three major types of chemical rockets: those using liquid propellants which are stored in a tank and burned in a rocket engine, those which use solid propellants where the propellant tank is also the thrust chamber of the engine, and those using both liquids and solids where the

Fig. 1.2 Space Propulsion Engines

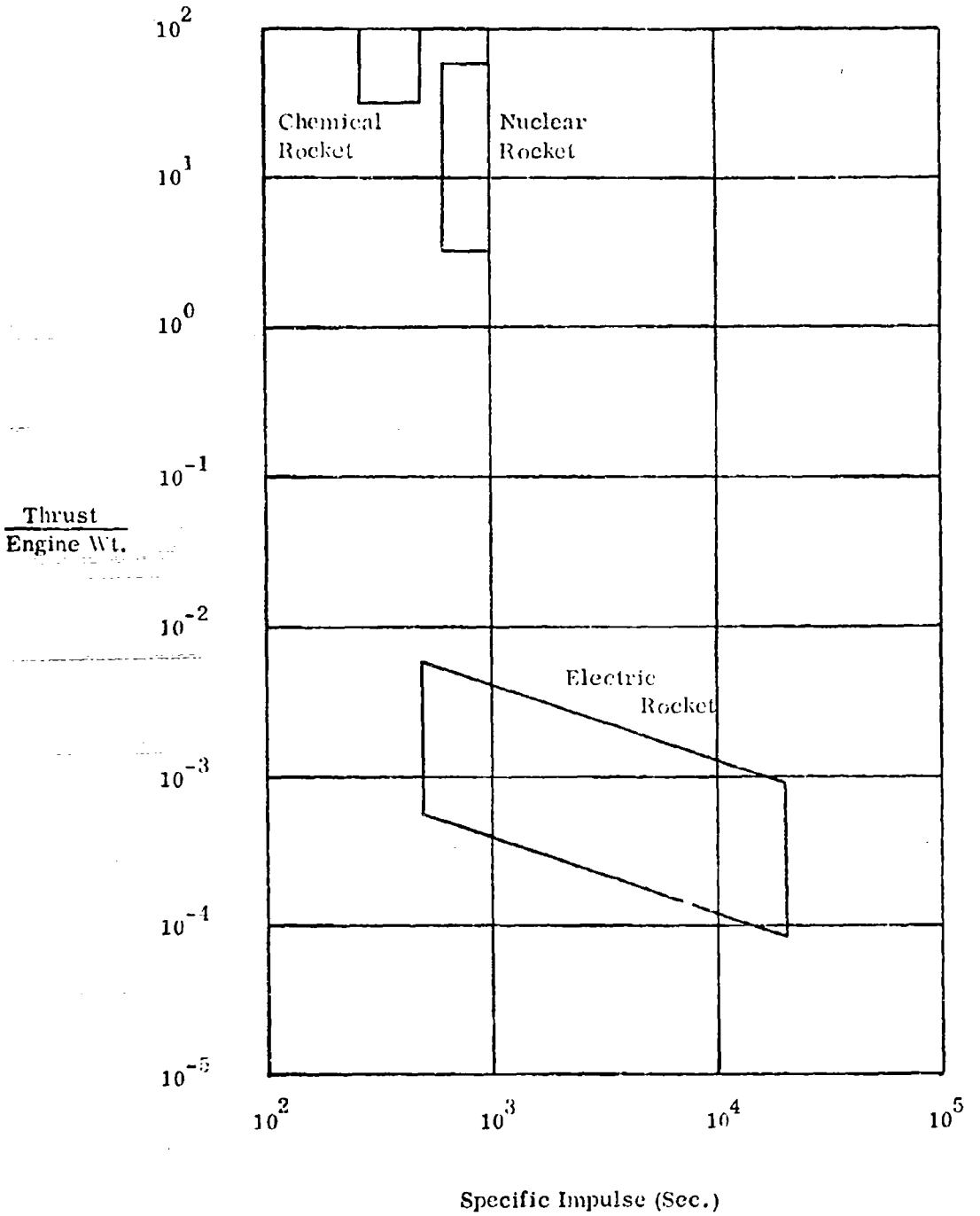

solid propellant is again stored in the thrust chamber while the liquid propellant is stored in a separate tank. Liquid propellants tend to offer higher performance than solid propellants, having both higher specific impulses and generally lighter overall system weight (including both tanks and engine). Solid propellants do have advantages such as storability, density, and economy which make them desirable for some missions. Hybrid rockets using both solids and liquids have not been developed very extensively yet but do give promise of fairly high specific impulses and may be promising for some missions. Only liquid rockets have been shown in the figure as it does not include tankage weights.

Liquid rockets used today with hydrogen-oxygen propellants are producing specific impulses of approximately 430 seconds and some more advanced systems have been proposed which may produce specific impulses on the order of 500 seconds. However, it does not seem likely that chemical rockets may produce performance much in excess of this if stable chemical species are used.

Liquid and hybrid chemical rockets may be designed so that they can be throttled. In this case, the engine can have any thrust varying from some maximum thrust down to some fairly low value. This throttling takes place essentially at constant specific impulse.

Because chemical rockets have relatively low specific impulse, a number of higher specific impulse devices have been proposed and some are under development. None of these, however, has yet reached the application stage for primary propulsion. One such scheme is the solid-core nuclear rocket shown

by a block next to the chemical rocket. These rockets utilize hydrogen exhausted through a very high temperature nuclear reactor operating near the material limits of graphite or tungsten and can produce specific impulses on the order of 800 seconds, about twice that obtainable with chemical rockets. This large improvement in specific impulse is obtained at the expense of some increase in both engine and tankage weights for this type of rocket, but they are advantageous for many missions and there is a current project to develop a solid-core nuclear rocket. Like chemical rockets, nuclear rockets may be designed to be throttled and may do this at essentially constant specific impulse.

Both chemical rockets and solid-core rockets are considered to be high-thrust devices that can be used for taking off from the surface of planets. They can provide high enough accelerations so that the rocket vehicle performance may often be approximated by replacing the finite burning time of these rockets by an impulse which requires zero time. Their primary limitation is exhaust velocity. Because of their throttling characteristics, they will be referred to as constant-exhaust-velocity rockets throughout this book.

Running along the bottom of Figure 1.2 is a class of electric propulsion systems which operate at much higher specific impulses than the high-thrust chemical and nuclear rocket systems, but also have orders of magnitude larger engine weights for a given thrust. These devices can only be used in orbit. Their thrust is very much smaller than local gravity for close planetary orbits and their whole mode of operation in a space mission is quite different. In a

chemical or nuclear rocket, the powered flight time is on the order of minutes or hours whereas for an electric propulsion system the powered flight time is on the order of months or years and generally constitutes the majority of the total mission time. An electric propulsion system is a combination of a power source and suitable power conditioning equipment with a thrust producing device or thrustor. The same types of thrustors might be used with different types of power sources and vice versa. A great variety of thrustors have been proposed and some of these have been developed to an operational state. The only currently operational thrustor types are resistojets which have relatively modest specific impulses of up to 800 seconds. Another highly developed type of thrustor is the ion rocket which operates efficiently at specific impulses above 3000 seconds. A number of other devices such as arcjets, MPD arcs and various plasma devices have been proposed and some of these are under development. Most of these engines can be operated only at or near a design point and cannot vary thrust effectively. It would be desirable to develop thrustors which could operate efficiently over a wide range of specific impulses at essentially constant power. This can be approximated to some extent by carrying several thrustors on a given power supply and switching from one to the other.

It will be noted that the thrust-to-weight ratio versus specific impulse for these electric propulsion devices is inversely proportional to the specific impulse and this is a simple consequence of Eq. (1.3) of the last section. The weight of an electric propulsion system is primarily in the power supply and as

the specific impulse is raised, the thrust must be decreased in order to keep the power constant. Most early studies of electric propulsion considered nuclear-electric power supplies. These are devices which take the heat from a nuclear reactor and convert it in some fashion or another to electricity. At the moment there is no active program in this country to develop a nuclear-electric power supply which would be suitable for electric propulsion and attention has switched to solar-electric propulsion systems. There are many possible ways of converting solar energy into electricity, but the most widely used and the most successful of these has been the photovoltaic cell. Unlike the nuclear-electric systems, the power of a solar cell system is a function of distance from the sun. In addition, the solar cell array must be in full sunlight and properly oriented towards the sun in order to develop full power. The power developed is not an inverse square function of distance from the sun because as the temperature of the cells changes, their efficiency varies. A typical curve for power as a function of distance from the sun is given in Figure 1.3.

A great variety of other propulsion devices has been proposed. Among these are solar heated rockets, radioisotope rockets, liquid core nuclear rockets, gaseous core nuclear rockets, nuclear pulse rockets and solar sails. With the exception of the last device, these are all rockets and may be treated by the methods to be developed in this book. The solar sail is a somewhat academic system which is easily treated by the general principles to be illustrated in this monograph.

Fig. 1.3 Solar Cell Power Variation

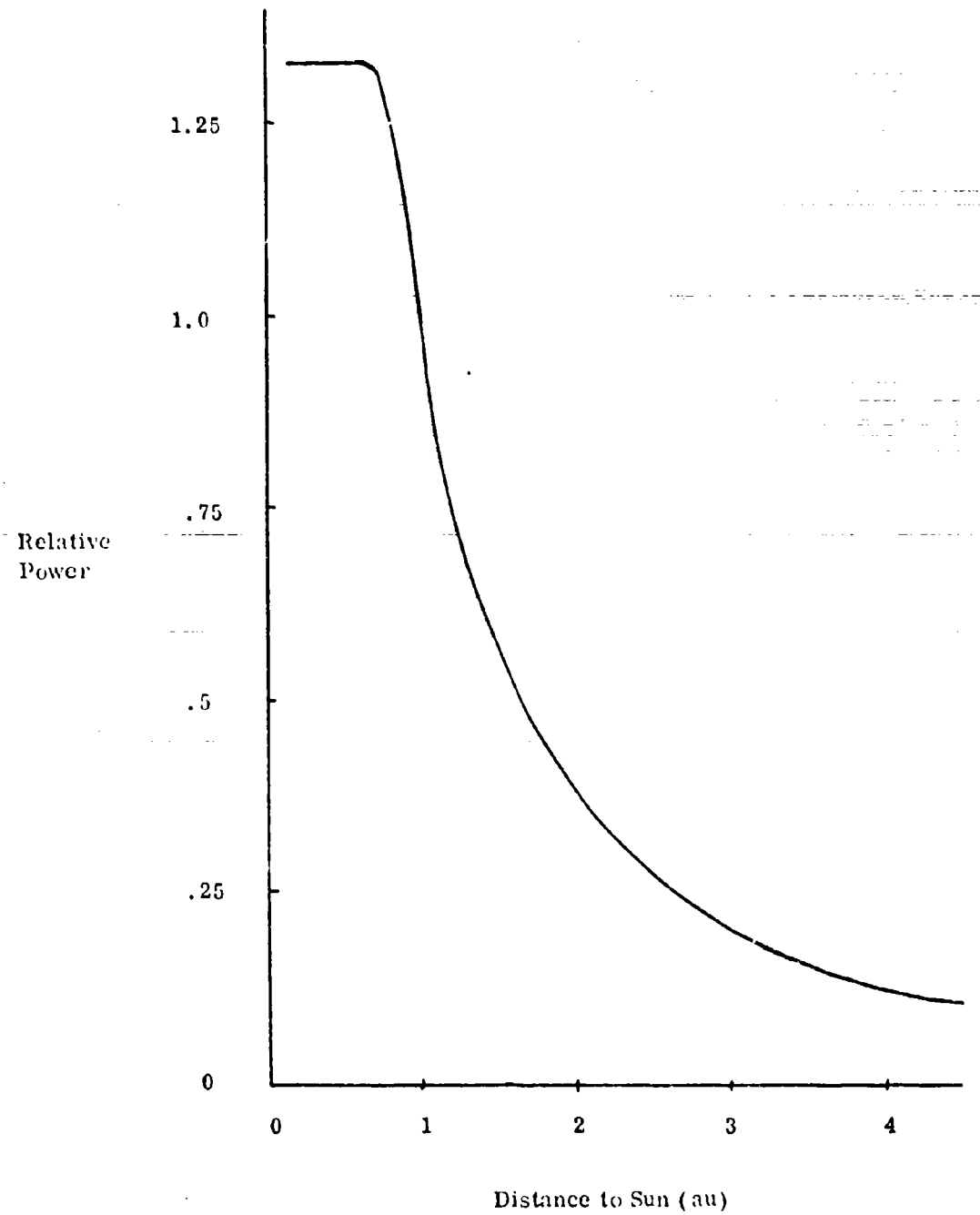

1.3 Payoff Functions

The payoff, the thing that we shall be trying to minimize, is the total fuel used and is given by integrating Eq. (1.4) to give Eq. (1.6).

$$m^0 - m^1 = \int_0^{t^1} \frac{f}{c}\, dt = \int_0^{t^1} \frac{f^2}{2P}\, dt \qquad (1.6)$$

Two forms of this equation are given: one applicable to systems with constant exhaust velocity and one applicable to the power-limited electric propulsion systems. For some purposes it is convenient to use alternate forms for these payoff functions, particularly for the idealized cases where the engines will have variable thrust. If we have a constant exhaust velocity system, Eq. (1.4) may be integrated by dividing through by the mass to form Eq. (1.7).

$$c\,\ell n\, \frac{m^0}{m^1} = \int_0^{t^1} \frac{f}{m}\, dt \equiv \Delta V \qquad (1.7)$$

The logarithm of the mass ratio of the system, a monotonic function of the fuel used, is proportional to the time integral of the thrust acceleration of the vehicle. This quantity is spoken of as characteristic speed, or velocity increment, or by a great variety of other names and will be used frequently. It is possible to use this payoff function instead of the fuel used as it is a monotonic function of the fuel used. The characteristic speed may be interpreted physically as the change in velocity that would be produced by thrusting in a single direction in the absence of a gravity field. Without gravity, the change in speed would be independent of

the acceleration program. Alternately, the characteristic speed may be looked upon as the sum of the absolute magnitude of the velocity increments that would be produced by impulsive thrusting in a gravity field.

It should be noted that the characteristic speed can be made much larger than the exhaust velocity. If the final mass could approach zero, the characteristic speed would approach infinity.

For a power-limited system, the corresponding quantity is found by dividing Eq. (1.4) through by the square of the mass to produce Eq. (1.8).

$$\frac{P^0}{m^1} - \frac{P^0}{m^0} = \int_0^{t^1} \frac{1}{2} \frac{P^0}{P} \left(\frac{f}{m}\right)^2 dt = J \tag{1.8}$$

This integral has never acquired a popular name and is generally known as J. The important thing here is that another monotonic function of the mass of the vehicle is proportional to the square of the thrust acceleration so that for a power-limited vehicle it is desirable to minimize the time integral of the square of the acceleration, whereas for a constant exhaust velocity system, it is desirable to minimize the time integral of the acceleration itself.

It was mentioned in the first section that a rocket that can be switched on and off and has only one operating point can be regarded as either a constant power or a constant exhaust velocity rocket. Either type of payoff may be used for such a rocket. In fact, in this case there is the following simple relation between the two payoff variables.

$$J = \frac{P^0}{m^0} \left[e^{\Delta V/c} - 1 \right] \tag{1.9}$$

1.4 Mass Relations for Exhaust-Velocity-Limited Systems

The total mass of the space vehicle is assumed to consist of four types of mass: payload, powerplant, structure and fuel (or propellant)

$$m^0 = m_L + m_P + m_S + m_F \tag{1.10}$$

The powerplant mass and part of the structure mass is assumed to be proportional to the maximum engine thrust.

$$m_P + m_{SP} = k_1 f_{max} \tag{1.11}$$

The remainder of the structure mass is assumed to be proportional to the mass of propellant.

$$m_{SF} = k_2 m_F \tag{1.12}$$

The ratio of the payload mass to the initial mass is then given by Eq. (1.13).

$$\frac{m_L}{m^0} = 1 - k_1 \frac{f}{m^0} - (1 + k_2) \frac{m_F}{m^0} \tag{1.13}$$

By using Eq. (1.7) of the last section, Eq. (1.13) may be put into the desired form, Eq. (1.14).

$$\frac{m_L}{m^0} = (1 + k_2)\, e^{-\Delta V/c} - \left(k_1 \frac{f}{m^0} + k_2\right) \tag{1.14}$$

This equation presents the relationship between the payload that can be carried and the payoff variable, characteristic speed, for a single-stage rocket. Equation (1.14) is plotted in Fig. 1.4 for several values of the tankage factor, k_2. Typical values of k_2 would be about .05 for typical propellants of about the density of water and about 0.1 for hydrogen.

1.5 Mass Relations for Power-Limited Systems

The constituent masses of a power-limited rocket are assumed to be the same as those of an exhaust-velocity-limited rocket and are again given by Eq. (1.10). As before, the powerplant mass and the structure required to support the powerplant are assumed to vary in the same way. In this case, they are assumed to be proportional to the power in the exhaust beam of the rocket.

$$m_P = \alpha P^0 \tag{1.15}$$

By combining Eq. (1.18) and (1.15), the following relationship for the mass of the vehicle is obtained.

Fig. 1.4 Single Stage Payload

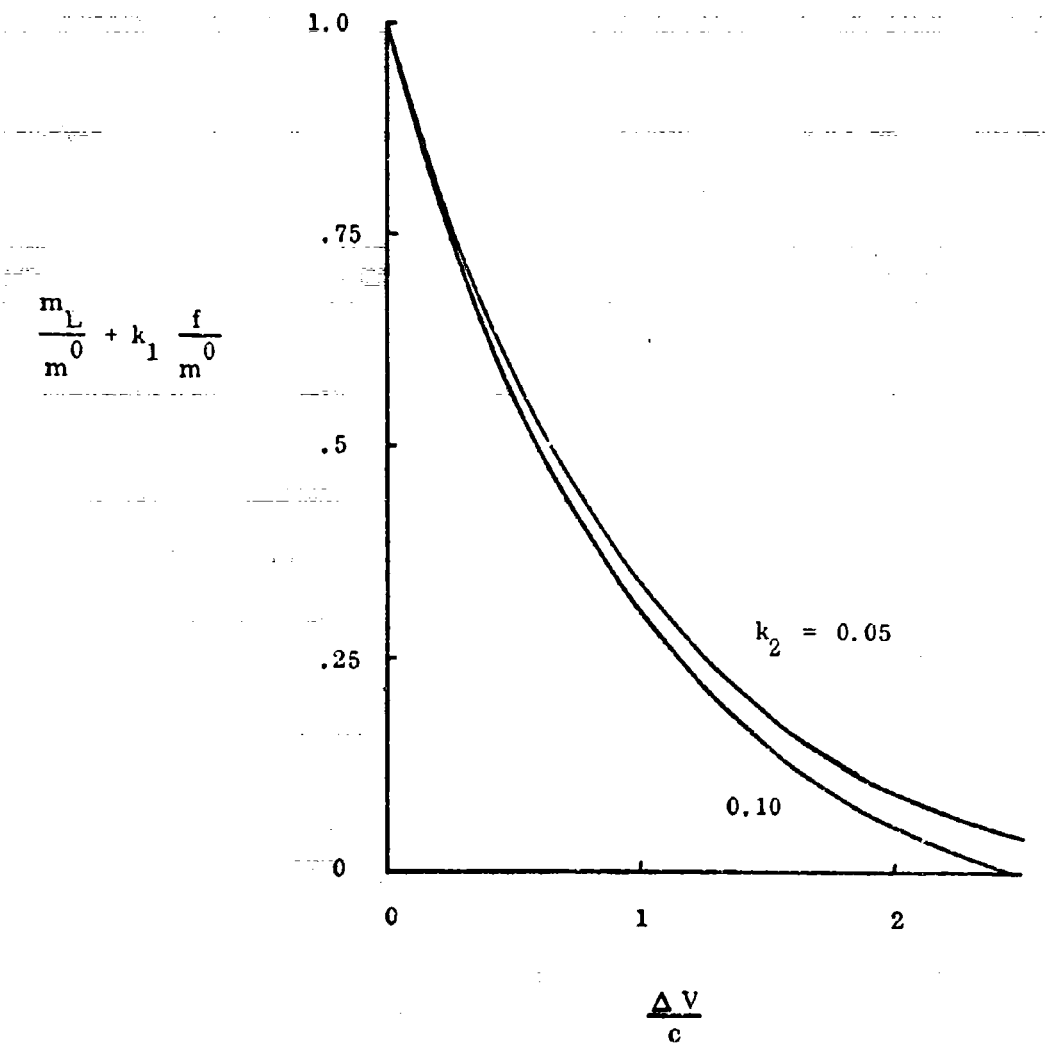

given value for exhaust beam power and powerplant mass. In this latter case, and only in this latter case, it is possible to optimize the mass distribution in the stage independently of the trajectory.

For the idealized power-limited rocket, having fully variable thrust, the value of J in Eq. (1.17) will depend only upon the particular mission and will be independent of the vehicle design. If the relationship between powerplant mass and exhaust-beam power is given by Eq. (1.15), Eq. (1.17) may then be optimized with respect to the powerplant mass. This may be done by simply differentiating Eq. (1.17) with respect to powerplant mass and setting the results equal to zero. The optimum mass distribution for a given value of the payoff, J, is then given by Eqs. (1.19) to (1.21).

$$\frac{m_P^*}{m^0} = \sqrt{(1+k_2)\,\alpha J} - \alpha J \qquad (1.19)$$

$$\frac{m_F^*}{m^0} = \sqrt{\frac{\alpha J}{1+k_2}} \qquad (1.20)$$

$$\frac{m_L^*}{m^0} = 1 - 2\sqrt{(1+k_2)\,\alpha J} + \alpha J \qquad (1.21)$$

1.6 Control Variables and Parameters

A control variable is a variable which may be manipulated so as to control the trajectory. This may be expressed symbolically as Eq. (1.22).

$$\frac{d\bar{x}}{dt} = \bar{f}(\bar{x}, \bar{u}, t) \tag{1.22}$$

In this equation, the rate of change of the state vector, $\bar{x}$, is a function of the state vector, $\bar{x}$, the control vector, $\bar{u}$, and the time, t. This equation represents a fairly general control problem and includes Eq. (1.1) as a special case. For a vehicle, the control vector, $\bar{u}$, is used to control the acceleration of the vehicle. Examples of control variables are throttle settings, thrust magnitudes, and thrust directions. The number of control variables may be greater or smaller than the dimensions of the acceleration vector. An example of the former is where there may be multiple engines, each with its own control variables. An example of the latter is a rocket which is controlled in three dimensions by a constant magnitude thrust at right angles to the radius vector. Only one control variable, a gimbal angle, can control all six components of position and velocity in an inverse square field.

Where the number of control variables is greater than the dimension of the acceleration vector, it will generally be possible to reduce the number of control variables by carrying out a partial optimization. This partial optimization will maximize the acceleration for a given rate of fuel consumption or, equivalently,

$$\frac{m^1}{m^0} = \frac{1}{1 + \frac{m^0}{m_P} \alpha J} \tag{1.16}$$

The fuel mass and the payload mass are then given by Eqs. (1.17) and (1.18).

$$\frac{m_F}{m^0} = \frac{\frac{m^0}{m_P} \alpha J}{1 + \frac{m^0}{m_P} \alpha J} \tag{1.17}$$

$$\frac{m_L}{m^0} = \frac{1 + k_2}{1 + \frac{m^0}{m_P} \alpha J} - \frac{m_P}{m^0} - k_2 \tag{1.18}$$

These equations are perfectly general and apply to rockets with either fixed or variable thrust. Equation (1.17) shows that, for a power-limited rocket, the fuel consumption depends upon the mass of the powerplant. It is possible for such rockets to decrease fuel mass by increasing powerplant mass. In general, there will be some optimum tradeoff between powerplant and fuel mass which will maximize payload for a given mission. For a fixed thrust rocket, it is necessary to carry out the optimization of the vehicle design and the trajectory design simultaneously. In this case, the value of J will depend upon the maximum acceleration available which will depend upon the powerplant mass. However, for a variable thrust rocket, it is possible to follow any required acceleration program with any

minimize the rate of fuel consumption for a given level of acceleration. An instructive example of this partial optimization is where a power-limited rocket and an exhaust-velocity-limited rocket are used in parallel. The total mass flow rate will be the mass flow rate of the two rockets.

$$-\dot{m} = \frac{f_1}{c_1} + \frac{f_2^2}{2P_2} = \frac{u_1}{c_1} + \frac{u_2^2}{2P_2} \tag{1.23}$$

The control variables will be taken as the magnitude of the thrust. The thrust of each engine will be assumed to be variable from zero up to some maximum value.

$$0 \leq u_1 \leq f_{1\,max} \tag{1.24}$$

$$0 \leq u_2 \leq f_{2\,max} \tag{1.25}$$

$$f_{2\,max} > P_2/c_1 \tag{1.26}$$

The total thrust will be the sum of the thrusts of the individual engines.

$$f = f_1 + f_2 = u_1 + u_2 \tag{1.27}$$

This equation may be used to eliminate one of the control variables and to express total mass flow rate in terms of the total thrust and the other control variable.

$$-\dot{m} = \frac{f-u_2}{c_1} + \frac{u_2^2}{2P_2} \tag{1.28}$$

The mass flow rate as a function of u_2 has a single maximum which is easily found to be given by Eq. (1.29).

$$u_2^* = \frac{P_2}{c_1} = f_2^* \tag{1.29}$$

The exhaust velocity at this optimum operating point of the power-limited-rocket is exactly twice the exhaust velocity of the exhaust-velocity-limited rocket,

$$c_2^* = \frac{2P_2}{f_2^*} = 2\ c_1 \tag{1.30}$$

With this relationship, it can be seen that there are three different regimes of operation for the two engines in parallel (see Fig. 1.5). In the first regime, for small thrusts, only the power-limited rocket is utilized.

$$0 \leq f < \frac{P_2}{c_1} \qquad -\dot{m} = \frac{f^2}{2P_2} \tag{1.31}$$

In the second regime, for intermediate thrust levels, the power-limited rocket is used at this optimum operating point and the thrust of the exhaust-velocity-limited rocket increases from zero to its maximum value.

$$\frac{P_2}{c_1} \leq f \leq \frac{P_2}{c_1} + f_{1\,\max} \qquad -\dot{m} = \frac{f}{c_1} - \frac{P_2}{2c_1^2} \tag{1.32}$$

In the third regime, the exhaust-velocity-limited rocket has reached its maximum value of thrust and the thrust of the power-limited rocket is increased to meet the total required thrust.

Fig. 1.5 Variation of Thrust With Mass Flow Rate

(Combination Propulsion)

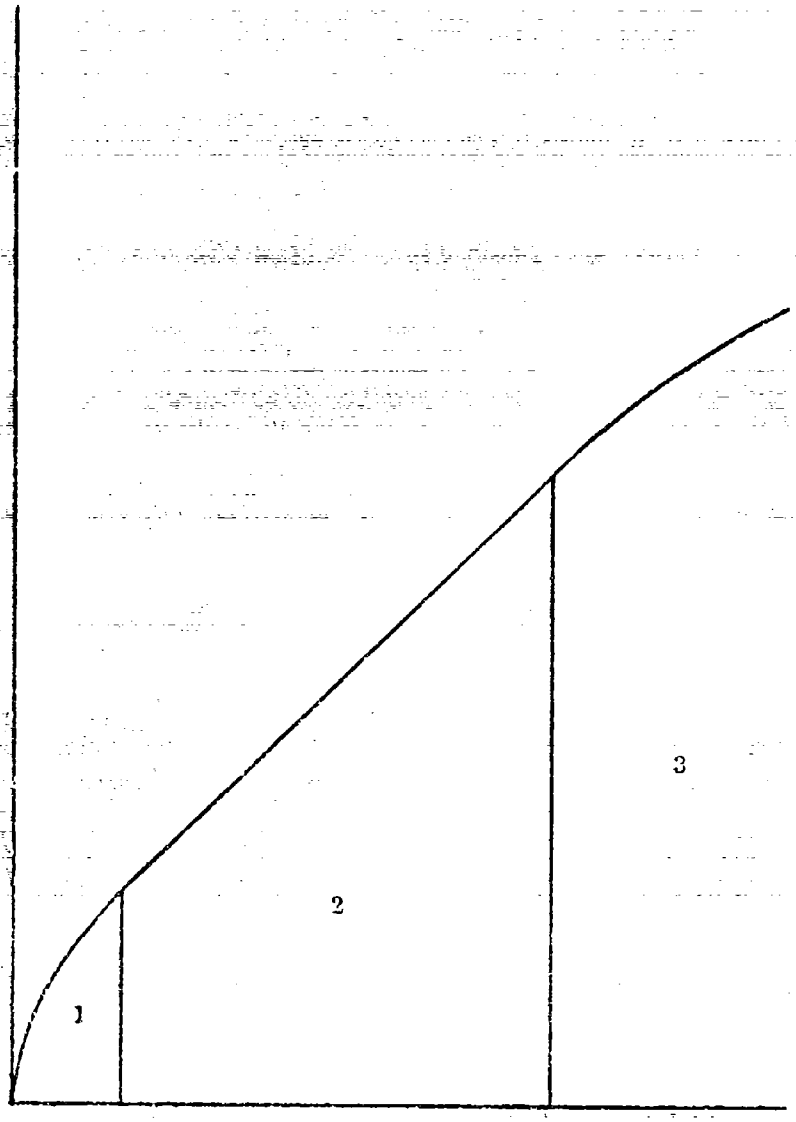

$$\frac{P_2}{c_1} + f_{1\,max} < f \leq f_{1\,max} + f_{2\,max} \quad -\dot{m} = \frac{f_{1\,max}}{c_1} + \frac{(f-f_{1\,max})^2}{2P_2} \tag{1.33}$$

The first and third regions are examples of regions in which the maximum occurs at a boundary of one of the control variables, in this case, the thrust of the exhaust-velocity-limited rocket. In region two, we have a stationary maximum for the second control variable, the thrust of the power-limited rocket.

There are many possible formulations for the control variables for a given rocket propulsion system. As further examples of such formulations, some of the propulsion systems of Section 1.2 will be considered. In general, it will be assumed that the engines are gimbaled so that the thrust may be pointed freely in any direction. The control vector will be taken to be the thrust vector of the vehicle.

$$\bar{f} = \bar{u} \tag{1.34}$$

Then the mass flow rate may be taken to be a function of position, time, and the magnitude of the thrust.

$$\dot{m} = \dot{m}\,(\bar{r}, t, u) \tag{1.35}$$

For a chemical or nuclear rocket, the mass flow rate will be given by Eq. (1.36), while the control variable will have a bound on its absolute magnitude.

$$\dot{m} = -\frac{|\bar{u}|}{c} \tag{1.36}$$

$$|\bar{u}| \leq f_{max} \tag{1.37}$$

If the nuclear rocket derives its source of heat from isotope decay rather than from a reactor, the decay of the isotope will produce a continuing decrease in the amount of power available, so that the maximum value of thrust will be given by Eq. (1.38).

$$f_{max} = f^0 e^{-k(t-t^0)} \tag{1.38}$$

For an idealized nuclear-electric rocket, the mass flow rate will be given by Eq. (1.39).

$$\dot{m} = - \frac{\bar{u} \cdot \bar{u}}{2P} \tag{1.39}$$

In this case, it will usually not be necessary to set an upper bound upon the magnitude of the thrust as large thrusts will be undesirable because of their exorbitant fuel consumption.

$$|\bar{u}| < \infty \tag{1.40}$$

If the rocket is a solar-electric rocket rather than a nuclear-electric rocket, the available power will be a function of distance from the sun.

$$P = P(r) \tag{1.41}$$

For practical engines, where the engine may only operate at a single design point, the magnitude of the control vector may only have two discreet values. In this case, the equations for the mass flow rate will be the same for a chemical rocket.

a nuclear rocket or a nuclear-electric rocket,

$$\dot{m} = -\frac{|\bar{u}|}{c} \tag{1.42}$$

$$|\bar{u}| = 0. \; f_{max} \tag{1.43}$$

A somewhat idealized version of a practical solar-electric rocket may be represented by Eqs. (1.44) and (1.45).

$$\dot{m} = -\frac{|\bar{u}|}{c} \tag{1.44}$$

$$|\bar{u}| \leq \frac{2P(r)}{c} \tag{1.45}$$

In this case, the rocket is assumed to be capable of using all the available power at constant exhaust velocity.

In addition to control variables, the problem may also contain a fixed vector of control parameters which do not change their values with time. The control problem is then represented by Eq. (1.46), where $\bar{\ell}$ is the vector of control parameters.

$$\frac{d\bar{x}}{dt} = \bar{f}(\bar{x}, \bar{u}, \bar{\ell}, t) \tag{1.46}$$

This problem arises when we wish to consider the optimization of the vehicle and trajectory for a given space mission, such as the determination of the maximum payload which can be carried by a fixed-thrust nuclear-electric rocket on a given mission. In this case the powerplant size, which will determine the value of the

fixed-thrust level, would be one of the parameters of the problem. In the same example, the exhaust velocity of the rocket might be another parameter to be optimized.

CHAPTER 2: THE MAXIMUM PRINCIPLE

2.1 Extrema of Functions

The problem of maximizing or minimizing a function is basic to all problems in space trajectory optimization. The word "extremum" is used to indicate a maximum or a minimum without specifying one or the other. The problem to be considered in this section is to maximize a scalar function y of a control vector u.

$$y = f(\bar{u}) \tag{2.1}$$

The control vector $\bar{u}$ is assumed to be contained in a closed domain U. If y is a continuous function of $\bar{u}$, then the theorem of Weierstrass guarantees that the function y always contains both a maximum and a minimum.

> "Every function which is continuous in a closed domain, U, of the variables possesses a largest and a smallest value in the interior or on the boundary of the domain."

If the function is differentiable and the maximum or minimum occurs at an interior point, then the partial derivatives of y with respect to each component of $\bar{u}$ must vanish. Such a point where the gradient of y vanishes is spoken of as a stationary point. While an interior maximum or minimum of a differentiable function must occur at a stationary point, a stationary point need not yield an extremum. For example, the stationary point may correspond to a

saddle point where both greater and smaller values of the function occur in the near vicinity of the point. A one-dimensional example of a saddle point would be a point of inflection where the first and second derivatives of y with respect to a scalar u would vanish. If y possesses second partial derivatives, then the second partial derivative matrix would be indefinite for a saddle point, positive definite for a minimum, and negative definite for a maximum. In general, these extrema would only be local extrema; that is, extrema within some subdomain of U rather than with respect to all of U.

The extrema of the function y may also occur on the boundary of U or at "corners" where y does not possess partial derivatives with respect to $\bar{u}$. The theorem of Weierstrass also applies to the boundary of U, which is a lower dimensional subdomain of U. For example, if the domain U is a 3-dimensional polyhedron. stationary extrema must be sought within the interior of U, on the faces of the polyhedron, and on the edges of the polyhedron. In order to determine the absolute extrema of y in such a domain (if y has continuous first partial derivatives), all of these stationary extrema must be considered and compared with the values of y at the vertices of the polyhedron. If y is a linear function of U, there will generally be no stationary extrema and the extrema must occur at the vertices of the n-dimensional polyhedron. This is the basis of linear programming.

2.2 The Optimal Control Problem

An important class of optimal control problems is to maximize the final value of the payoff variable x_0 subject to the differential Eqs. (2.3) with the control vector $\bar{u}$ contained in some closed domain U.

$$x_0^1 = \min. \tag{2.2}$$

$$\frac{dx}{dt} = \bar{f}(\bar{x}, u, t) \tag{2.3}$$

The initial and final times are specified as are the initial and final values of the state x. This problem is a generalization of the elementary problem considered in the previous section. The cost, or payoff, x_0^1 depends on the complete time history of the values of the control vector $\bar{u}$, rather than upon its value at any one time. The payoff variable is what is called a functional as it depends upon a continuous sequence of values of the vector $\bar{u}$.

This problem is much more difficult than the elementary problem considered in Section 2.1 and far less is known about its solution. There is no general existence theorem corresponding to the theorem of Weierstrass and the sufficiency theorems that have been developed are generally difficult to use and are of limited applicability. There is a satisfactory theory concerning necessary conditions for this problem and this theory is the basis of the analysis in this monograph.

2.3 The Maximum Principle

The maximum principle is a necessary condition for a maximizing solution of the optimal control problem considered in the previous section. Any solution which does maximize the payoff x_0^1 must satisfy the maximum principle. However, solutions which satisfy the maximum principle may not be maximizing. A solution which does satisfy the maximum principle will be referred to as an extremal.

The maximum principle is stated in terms of a Hamiltonian defined by Eq. (2.4).

$$H = H(\bar{x}, \bar{\lambda}, \bar{u}, t) \equiv \bar{\lambda} \cdot \bar{f}(\bar{x}, \bar{u}, t) \tag{2.4}$$

The vector $\bar{\lambda}$ is a vector of Lagrange multipliers of the same dimension as the state vector $\bar{x}$. There is one component of this vector for each component of the state vector. The differential equations of motion and the differential equations governing the Lagrange multipliers are given by the canonical Eqs. (2.5) and (2.6).

$$\frac{dx_i}{dt} = \frac{\partial H}{\partial \lambda_i} \qquad i = 0, 1, \ldots, n \tag{2.5}$$

$$\frac{d\lambda_i}{dt} = -\frac{\partial H}{\partial x_i} \qquad i = 0, 1, \ldots, n \tag{2.6}$$

These equations are often stated in the equivalent vector form (2.7) and (2.8).

$$\frac{d\bar{x}}{dt} = \frac{\partial H}{\partial \bar{\lambda}} \tag{2.7}$$

$$\frac{d\bar{\lambda}}{dt} = -\frac{\partial H}{\partial \bar{x}} \tag{2.8}$$

The maximum principle of Pontryagin states that the Hamiltonian H of Eq. (2.4) must be maximized with respect to the value of the control vector $\bar{u}$ contained within the closed domain U at all times from t^0 to t^1. The maximum principle reduces the optimal control problem to an infinite sequence of maximization problems in Euclidean space and to a 2-point boundary value problem. The maximization problem is the problem of maximizing H with respect to $\bar{u}$ at each time. The 2-point boundary value problem is the problem of determining the initial values of the Lagrange multipliers λ_i that will cause the extremal to go to the correct final state.

Equations (2.6) are a set of linear homogeneous equations in the Lagrange multipliers λ_i. These equations are adjoint to the linearized variational equations of Eqs. (2.5). A natural scaling of this homogeneous system of equations will be chosen by taking the terminal value of the Lagrange multiplier associated with the cost to be unity (Eq. (2.9)).

$$\lambda_0^1 = 1 \tag{2.9}$$

Because the Lagrange multipliers are adjoints to the linearized equations of motion, and because of the scaling used in Eq. (2.9), they may be interpreted as influence functions for the cost and obey the relationship of Eq. (2.10) at all times.

$$\lambda_i(t) = \frac{\partial x_0^1}{\partial x_i} \qquad i = 0, 1, \ldots, n \tag{2.10}$$

The Hamiltonian itself is the negative of the influence function for time and obeys Eq. (2.11).

$$H = - \frac{\partial x_0^1}{\partial t} \tag{2.11}$$

The system of equations of Eqs. (2.5) and (2.6) also possesses a first integral which gives the value of the Hamiltonian at all times (Eq. (2.12)).

$$H(t) = H^1 - \int_t^{t^1} \frac{\partial H}{\partial t} \, dt \tag{2.12}$$

If the system is autonomous, i.e., the functions f_i are independent of time, then this integral will be a constant of the motion.

If all the maxima of H with respect to $\bar{u}$ are stationary maxima, then the optimal control problem is reduced to a problem in the classical calculus of variations. This classical theory possesses a more satisfactory and useful theory of sufficiency conditions than has yet been developed for the more complex optimal control problem.

2.4 Control Parameters and Free Boundary Conditions

The problem considered in Section 2.3 may be generalized somewhat by assuming that the boundary conditions are not fixed but may vary over some terminal hypersurface. This problem may also be generalized by assuming that $\bar{f}$

may depend upon a constant vector of control parameters $\bar{\ell}$. This makes the Hamiltonian a function of four vectors and time.

$$H = \bar{\lambda} \cdot \bar{f}(\bar{x}, \bar{u}, \bar{\ell}, t) = H(\bar{\lambda}, \bar{x}, \bar{u}, \bar{\ell}, t) \tag{2.13}$$

For any given set of values for the control vector $\bar{\ell}$, the cost may be computed by solving a standard optimal control problem. The cost may then be represented as a function of the boundary conditions and the parameter vector, Eq. (2.14).

$$x_0^1 = x_0^1(\bar{x}^0, \bar{x}^1, t^0, t^1, \bar{\ell}) \tag{2.14}$$

The problem of determining the optimal values for the boundary conditions and the parameter vector has now been reduced to a problem in the theory of extrema of functions. If the cost given in Eq. (2.14) is differentiable, then a set of transversality conditions may be derived which determine the optimal values for the boundary conditions. For example, if the initial conditions are fixed and the terminal conditions are variable, then the variation in cost due to variations in the terminal conditions must be stationary and will be given by Eq. (2.15).

$$\delta x_0^1 = -\sum_{i=1}^{n} \lambda_i^1 \delta x_i^1 + H^1 \delta t^1 = 0 \tag{2.15}$$

This equation must be satisfied for all variations which are consistent with the terminal conditions. For example, if one component of the terminal state is unspecified, then by Eq. (2.15) the corresponding component of the Lagrange

multiplier must be zero. If the initial or final time is unspecified, then the Hamiltonian H must be zero at that time. More generally, if the terminal state must lie on some hypersurface in the space of the state variables, then the terminal Lagrange multiplier vector must be normal to the hypersurface. Equation (2.15) may also be used where the terminal hypersurface is a specified function of time and the state.

If the payoff x_0^1 is differentiable with respect to the parameter vector $\bar{\ell}$, then the following conditions must hold with respect to each component ℓ_k of the parameter vector.

$$\int_{t^0}^{t^1} \frac{\partial H}{\partial \ell_k} \, dt = 0 \qquad (2.16)$$

This condition may be derived by considering each component of the parameter vector as a new state variable whose derivative is equal to zero.

2.5 Singular Arcs

The maximum principle determines the optimal control only if the Hamiltonian H has a unique maximum value with respect to the control vector $\bar{u}$. When H has two or more equal maxima, the problem becomes more complicated. One important case arises when H is linear in one or more components of $\bar{u}$. If the coefficient of the linear term is nonzero, the maximum of H will occur at the boundary of $\bar{u}$. However, if the coefficient is zero, then all values of that component of $\bar{u}$ yield the same value of H and the maximum principle does not

determine the control. This is the case in which singular arcs may arise. A singular arc is a segment of an optimal trajectory of finite duration where the control does not lie on the boundary and the coefficient of the linear term in the Hamiltonian is identically zero over the finite time interval.

If the problem is linear in the state and control, then the singular arc will arise when the solution is non-unique and may be replaced by non-singular arcs having the same cost. However, if the problem is nonlinear in the state $\bar{x}$ but linear in one component of the control $\bar{u}$, then singular arcs may represent all or part of a unique minimizing solution.

In practice it may not be possible to operate a control between its maximum and minimum limits. However, an approximation to such intermediate controls may be obtained by operating the control alternately at its maximum and minimum values. If this is done rapidly, a chattering approximation to the intermediate control is obtained. Anytime that a Hamiltonian possesses two equal maxima, chattering may be used to connect the two maxima and the possibility of a singular arc arises.

2.6 Impulsive Controls

If the Hamiltonian is linear in a component of $\bar{u}$ and this component of $\bar{u}$ is unbounded, then a positive coefficient for this component in the Hamiltonian implies that the control should be infinite. The usual derivations of the maximum principle do not hold for this case. However, the scope of the maximum

principle has been extended so that this important case may be treated. The details of the results will be presented in the next chapter for the rocket problem.

2.7 Sufficiency

The maximum principle is merely a necessary condition for an extremum and its satisfaction is no guarantee that the solution to a particular problem has been found. In special cases it may be possible to establish that there is a unique solution that satisfies the maximum principle. In these cases the maximum principle will be sufficient for an extremum. However, in general, it is not possible to show that the problem possesses a unique solution. In fact, it is often impossible to show that the problem possesses any well-behaved solution.

The only way by which one can determine absolute extrema is by calculating all extremals and comparing their costs. There are a few techniques which can sometimes be used to determine local extrema. If the control never lies on a boundary, then the problem may be treated by the classical calculus of variations which possesses a local sufficiency theory based on the second variation. This theory is a generalization of the local sufficiency theory for the extrema of functions. If the controls do lie on the boundary for part of the solution, a more general approach must be used. Such an approach has recently been developed by Boltyanski for determining absolute extrema within a given domain. Unfortunately, this theory requires the generation of the complete families of extremals in this domain. This is usually impractical if the state vector $\bar{x}$ has more than two components in addition to the payoff.

CHAPTER 3: GENERAL THEORY OF OPTIMUM ROCKET TRAJECTORIES

3.1 Application of the Maximum Principle

The equations of motion of a rocket moving in an arbitrary time-varying gravitational field are given by Eq. (1.1) of Chapter 1. This equation will be re-written as two first-order equations, Eq. (3.1) and (3.2), so that they will be the first-order form to which the maximum principle is applicable.

$$\dot{\bar{V}} = \frac{\bar{f}}{m} + \bar{g}(\bar{r}, t) \tag{3.1}$$

$$\dot{\bar{r}} = \bar{V} \tag{3.2}$$

The rate of loss of mass of the rocket is assumed to be a general function of position, time, and the thrust vector.

$$\dot{m} = \dot{m}(\bar{r}, t, \bar{f}) \tag{3.3}$$

This system of vector and scalar equations are the state equations for a general rocket trajectory optimization problem. They will form a fifth-order system for planar flight in two spatial dimensions and a seventh-order system for flight in three spatial dimensions.

The Hamiltonian of this system is given by Eq. (3.4). This Hamiltonian represents a Mayer formulation of the optimization problem. The vector $\bar{\lambda}$ is

adjoint to the velocity vector, the vector $\bar{\mu}$ is adjoint to the position vector, and the scalar σ is adjoint to the scalar mass of the rocket.

$$H = \frac{\bar{\lambda} \cdot \bar{f}}{m} + \bar{\lambda} \cdot \bar{g} + \bar{\mu} \cdot \bar{V} + \sigma \dot{m} \tag{3.4}$$

$$H = H(\bar{V}, \bar{r}, m, \bar{\lambda}, \bar{\mu}, \sigma, \bar{f}, t) \tag{3.5}$$

The Hamiltonian H is a function of the state variables, the adjoint variables, the control vector, and the time. The differential equations for the adjoint variables are given by Eqs. (3.6), (3.7) and (3.8).

$$\dot{\bar{\lambda}} = - \frac{\partial H}{\partial \bar{V}} = - \bar{\mu} \tag{3.6}$$

$$\dot{\bar{\mu}} = - \frac{\partial H}{\partial \bar{r}} = - \bar{\lambda} \cdot \frac{\partial \bar{g}}{\partial \bar{r}} - \sigma \frac{\partial \dot{m}}{\partial \bar{r}} \tag{3.7}$$

$$\dot{\sigma} = - \frac{\partial H}{\partial m} = \frac{\bar{\lambda} \cdot \bar{f}}{m^2} \tag{3.8}$$

Because of the simple relationship between the adjoint vectors for position and velocity, Eqs. (3.6) and (3.7) are often written in the second-order form given by Eq. (3.9).

$$\ddot{\bar{\lambda}} = \bar{\lambda} \cdot \frac{\partial \bar{g}}{\partial \bar{r}} + \sigma \frac{\partial \dot{m}}{\partial \bar{r}} \tag{3.9}$$

The adjoint vecotr $\bar{\lambda}$ plays an important part in the theory of optimum space trajectories and is often called the primer vector, a name originally introduced by Lawden.

The maximum principle states that the Hamiltonian, Eq. (3.4), should be maximized with respect to the control vector, in this case the thrust vector. Only two of the terms in the Hamiltonian are affected by the thrust so that the maximum principle reduces to the maximization of these two terms (Eq. (3.10)).

$$\frac{\bar{\lambda} \cdot \bar{f}}{m} + \sigma \dot{m} = \max \tag{3.10}$$

Equation (3.10) is a general equation applying to a great many types of rocket propulsion devices. Among these types are those where the thrust magnitude must lie within a given time-varying set, and to the case where the thrust magnitude is a fixed function of time, but the direction may be freely varied. The one important case not covered by Eq. (3.10) is where the maximum thrust magnitude is a function of both position and time. This case can be conveniently handled by expressing the thrust as the product of a throttle variable k, which may vary from zero to one, and the maximum thrust of the rocket.

$$\bar{f} = k \bar{f}_{max} (\bar{r}, t) \tag{3.11}$$

As the thrust is now a function of the position vector $\bar{r}$, the equation for the primer vector, Eq. (3.9), must be modified as Eq. (3.12).

$$\ddot{\bar{\lambda}} = \bar{\lambda} \cdot \frac{\partial \bar{g}}{\partial \bar{r}} + \sigma \frac{\partial \dot{m}}{\partial \bar{r}} + \frac{k}{m} \bar{\lambda} \cdot \frac{\partial \bar{f}_{max}}{\partial \bar{r}} \tag{3.12}$$

At this point it will be assumed that the engine may be rotated freely in space so that the maximum thrust is not a function of direction and so that the fuel flow rate depends only upon the magnitude of the thrust. In this case, Eq. (3.10) implies that the thrust should be aligned with the primer vector to produce Eq. (3.13).

$$\frac{\lambda f}{m} + \sigma \dot{m} = \max \tag{3.13}$$

This equation may now be used to maximize the Hamiltonian H with respect to thrust magnitude as well as thrust direction. It is convenient to re-write Eq. (3.13) as Eq. (3.14).

$$f + \frac{\sigma m}{\lambda} \dot{m} = \max \tag{3.14}$$

There are two important cases that arise depending upon the curvature of the curve of thrust versus fuel flow rate. The two cases are illustrated in Figs. 3.1 and 3.2.

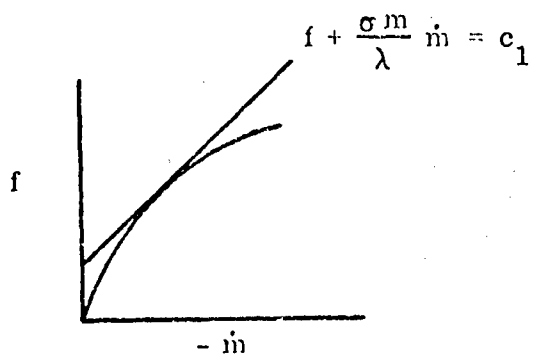

Fig. 3.1

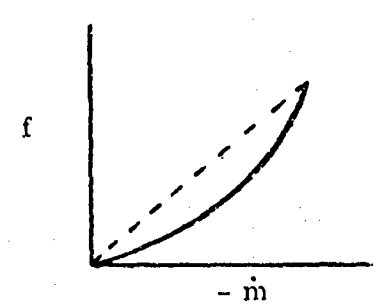

Fig. 3.2

In the first case illustrated in Fig. 3.1 the maximization of H will generally lead to a stationary maximum point away from the boundaries on the thrust. This case is characteristic of the idealized power-limited rocket. The second case illustrated in Fig. 3.2 always has a maxima of the Hamiltonian occurring at the maximum and minimum values of the thrust. The thrust is never operated at intermediate values except in the particular case where the thrust is a linear function of the mass flow rate. It is possible to approximate to a linear relationship between thrust and mass flow rate for these engines by operating the engine alternately for short periods of time at both maximum and minimum thrust, a process known as chattering. If the optimal trajectory contains a singular arc, such chattering behavior will form part of the optimal solution.

3.2 Constant Exhaust Velocity

In the particular case of a rocket with a constant exhaust velocity, the mass flow rate is given by Eq. (3.15), where c is a constant. Equation (3.14) is then replaced by Eq. (3.16).

$$\dot{m} = -\frac{f}{c} \tag{3.15}$$

$$f = \frac{\sigma m}{\lambda c} \quad f = \max \tag{3.16}$$

In this case the criteria for the magnitude of the thrust are given by Eqs. (3.17).

$$\lambda > \frac{\sigma m}{c} \qquad f^* = f_{max}$$

$$\lambda < \frac{\sigma m}{c} \qquad f^* = f_{min} \tag{3.17}$$

$$\lambda = \frac{\sigma m}{c} \qquad f_{min} \leq f \leq f_{max}$$

If the magnitude of the primer vector is greater than $\sigma m/c$, the thrust is turned on full throttle. If the magnitude of the primer vector is less than $\sigma m/c$, the engine will operate at its minimum thrust level, which will be taken to be zero. Finally, in the particular case of a singular arc the magnitude of the primer vector will remain equal to $\sigma m/c$ along the arc, and the value of the thrust will lie between its limits.

3.3 Impulsive Controls

It is interesting to determine what happens to Eqs. (3.17) if impulses are allowed. Using the results of Chapter 1, Eq. (1.7), Eq. (3.4) may be rewritten as Eq. (3.18).

$$H = \frac{f}{m}\left(\lambda - \frac{\sigma m}{c}\right) + \bar{\lambda} \cdot \bar{g} - \dot{\bar{\lambda}} \cdot \bar{V} \tag{3.18}$$

The rate of change of the quantity σm may be determined from Eq. (3.19).

$$\frac{d(\sigma m)}{d\Delta V} = \frac{m\, d\sigma}{\frac{f}{m}\, dt} + \frac{\sigma\, dm}{\frac{f}{m}\, dt} = \lambda - \frac{\sigma m}{c} \tag{3.19}$$

When λ is less than $\sigma m/c$, the thrust will be zero and the rate of change of ΔV will be zero so that there will be no change in the quantity σm. When λ is equal to $\sigma m/c$, the rate of change of σm with respect to ΔV, given by Eq. (3.19), will be zero. During an impulsive thrust, the value of the primer vector and its first two time derivatives will not change. As a result, the right-hand side of Eq. (3.19) will remain equal to zero during an impulsive thrust and along a singular arc. This means that as long as the value of thrust is allowed to vary between zero and infinity, the quantity $\sigma m/c$ will be a constant of the motion, which may be taken as unity.

The magnitude of the primer vector must be less than unity when the rocket is turned off and must be equal to unity when the vehicle is powered. It can never be greater than unity for an optimum trajectory. Since the primer vector and its first two time derivatives are continuous, all impulses between the initial and final times must occur at local maxima of the primer vector. In this case the primer vector and its derivative will be orthogonal and the last term in Eq. (3.18) will not change across the impulse. The first term will be zero on both sides of an interior impulse and may be defined to be zero during such an impulse. As a result the Hamiltonian for the constant exhaust velocity problem with unconstrained thrust may be taken as in Eq. (3.20).

$$H = \bar{\lambda} \cdot \bar{g} - \dot{\bar{\lambda}} \cdot V \tag{3.20}$$

This equation will not apply during the terminal impulses where the Hamiltonian will not be defined. It will apply in the open interval from the initial to the terminal time.

3.4 Power-Limited Rocket

In the case of a power-limited rocket where the power may be a function of time and position, the mass flow rate will be given by Eq. (3.21).

$$\dot{m} = -\frac{f^2}{2P} \tag{3.21}$$

Equation (3.14) in this case becomes Eq. (3.22).

$$f - \frac{\sigma m}{2\lambda P} f^2 = \max \tag{3.22}$$

This equation is of the type illustrated in Fig. 3.1 and always has the stationary maximum given by Eq. (3.23).

$$f^* = \frac{\lambda P}{\sigma m} \tag{3.23}$$

The equation for the Lagrange multiplier for the mass, σ, is given by Eq. (3.24) and the equation for the rate of change of mass is given by Eq. (3.25).

$$\dot{\sigma} = \frac{\lambda^2 P}{\sigma m^3} \tag{3.24}$$

$$\dot{m} = -\frac{\lambda^2 P}{2\sigma^2 m^2} \tag{3.25}$$

These equations may be combined to yield Eq. (3.26), which is readily integrated to yield Eq. (3.27).

$$\frac{\dot{\sigma}}{\sigma} = -\frac{2\dot{m}}{m} \tag{3.26}$$

$$\sigma m^2 = \sigma^0 (m^0)^2 \tag{3.27}$$

The acceleration of the rocket is then given by Eq. (3.28) and the Hamiltonian by Eq. (3.29).

$$\frac{f^*}{m} = \frac{P}{\sigma m^2} \lambda \tag{3.28}$$

$$H = \lambda^2 \frac{P}{\sigma m^2} + \bar{\lambda} \cdot \bar{g} - \dot{\bar{\lambda}} \cdot \bar{V} + \sigma m^2 \frac{\dot{m}}{m^2} \tag{3.29}$$

As this is a homogeneous system, we may set the Lagrange multiplier σ^0 equal to the value given by Eq. (3.30) to produce the Hamiltonian given by Eq. (3.31).

$$\sigma^0 = \frac{P^0}{(m^0)^2} \tag{3.30}$$

$$H = \lambda^2 \frac{P}{P^0} + \bar{\lambda} \cdot \bar{g} - \dot{\bar{\lambda}} \cdot \bar{V} - \frac{d(P^0/m)}{dt} \tag{3.31}$$

The quantity on the right may be recognized as equal to the quantities given by Eq. (3.32). This produces the final form of the Hamiltonian H for the power-limited problem, Eq. (3.33).

$$\frac{d}{dt}\left(\frac{P^0}{m}\right) = \frac{1}{2}\frac{P^0}{P}\left(\frac{f}{m}\right)^2 = \frac{dJ}{dt} = \frac{\lambda^2}{2}\frac{P}{P^0} \tag{3.32}$$

$$H = \bar{\lambda}\cdot\bar{g} - \dot{\bar{\lambda}}\cdot\bar{V} + \frac{\lambda^2}{2}\frac{P}{P^0} \tag{3.33}$$

It should be noted that in both cases where there are no bounds on the thrust, the mass has disappeared from the problem. This is because for these problems the thrust may be replaced by the thrust acceleration as a control variable. It should also be noted that Eq. (3.33) applies to an arbitrary time-varying gravity field and to a power level that is an arbitrary function of time and position.

3.5 Summary of Results

From this point on this monograph will be primarily concerned with three different trajectory optimization problems. The first problem, to be referred to as Problem C1, is concerned with minimum fuel trajectories for a constant exhaust velocity rocket having a fixed bound on the maximum thrust level. In general, the thrust level will be assumed to be variable, but in the special case of minimum time trajectories the thrust will be assumed to be fixed at its maximum value. In such a case the minimum fuel trajectory is also a minimum time trajectory. The

second problem, to be referred to as Problem C2, will be concerned with a constant exhaust velocity rocket with no upper bound on the thrust magnitude. Here the solution will consist of impulses and coasting arcs except in the exceptional case of singular arcs. The payoff to be maximized will be the negative of the total velocity increment as the velocity increment should be minimized. For this problem minimum time trajectories are meaningless as they require a consumption of infinite amounts of fuel.

The third problem, to be referred to as Problem P1, is the minimum fuel problem for a constant power rocket with unbounded variable thrust. In general, the power may be a function of position and time, although most results will be for the constant power case. For this problem both minimum time and time-open problems are not of interest because they correspond respectively to zero time, infinite fuel consumption and infinite time, zero fuel consumption solutions. Table 3.1 summarizes some of the pertinent characteristics of these three problems.

TABLE 3.1

Problem	C1	C2	P1
Exhaust velocity - c	constant	constant	variable
Maximum thrust level - f_{max}	bounded	unbounded	unbounded
Power level - P	variable	variable	function of position and time
Payoff - x_0^1	m^1	$-\Delta V$	$-J$
Terminal value of adjoint to mass - σ^1	1	c/m^1	$\left(\frac{1}{m^1}\right)^2$
Hamiltonian - H	$\bar{\lambda} \cdot \bar{g} - \dot{\bar{\lambda}} \cdot \bar{V} + \frac{f}{m}\left(\lambda - \frac{\sigma m}{c}\right)$	$\dot{\bar{\lambda}} \cdot \bar{g} - \dot{\bar{\lambda}} \cdot \bar{V}$	$\bar{\lambda} \cdot \bar{g} - \dot{\bar{\lambda}} \cdot \bar{V} + \frac{\lambda^2}{2} \frac{P}{P^0}$

3.6 Boundary Conditions

This section will consider what effect various types of boundary conditions have on the terminal values of the Lagrange multipliers for the three problems defined in the previous section. These boundary conditions will be determined from the general transversality condition, Eq. (2.15) of Chapter 2. Applying this transversality condition to the rocket trajectory problems of this chapter produces Eq. (3.34). This equation must be stationary for allowable variations in the terminal conditions.

$$\delta x_0^1 = \bar{\lambda} \cdot \overline{\delta V} - \dot{\bar{\lambda}} \cdot \overline{\delta r} - H \delta t \tag{3.34}$$

In the case of interception trajectories the terminal velocity at interception is unspecified. Equation (3.34) then indicates that at interception all three components of the primer vector must be zero (Eq. (3.35)).

$$\bar{\lambda}^1 = \bar{0} \tag{3.35}$$

For time fixed interception this equation must be satisfied for all three problems — C1, C2, and P1. Because the primer vector is zero at the time of interception, the thrust will be zero at that time in all cases. For time open interception the terminal position will be a specified function of time (Eq. (3.36)).

$$\bar{r} = \bar{r}_t(t) \tag{3.36}$$

The variation in position due to a variation in interception time will then be given by Eq. (3.37).

$$\delta \bar{r} = \bar{V}_t \delta t \tag{3.37}$$

The stationary condition of Eq. (3.34) for this problem is given by Eq. (3.38).

$$-\dot{\bar{\lambda}} \cdot \overline{\delta r} = H^1 \delta t \tag{3.38}$$

This equation yields a terminal value of the Hamiltonian for problems C1 and C2 where use has been made of the fact that the thrust is turned off at interception.

$$H^1 = -\dot{\bar{\lambda}} \cdot \bar{V} = \dot{\bar{\lambda}} \cdot \bar{V}_t \tag{3.39}$$

Equation (3.39) implies that the derivative of the primer vector must be perpendicular to the relative velocity vector at interception. In the special case where the target is stationary the Hamiltonian must be zero at interception and the derivative of the primer vector must be perpendicular to the velocity vector. For minimum time interception only Problem C1 is of interest. Equation (3.34) then yields Eq. (3.40), resulting in Eqs. (3.41) and (3.42).

$$0 = (-\dot{\bar{\lambda}} \cdot V_t + \dot{\bar{\lambda}} \cdot \bar{V} - \frac{f}{c}) \delta t \tag{3.40}$$

$$\frac{f}{c} = \dot{\bar{\lambda}} \cdot (\bar{V} - V_t) \tag{3.41}$$

$$H^1 = \dot{\bar{\lambda}} \cdot V_t \tag{3.42}$$

The problem of time fixed rendezvous provides no freedom in the terminal conditions so that no transversality conditions may be imposed. However, there are several variable time rendezvous problems of interest. It will be assumed that the target vehicle is falling freely under the action of gravity. Its position and velocity are given by Eqs. (3.43), while the variations in these quantities are given by Eqs. (3.44).

$$\bar{r} = \bar{r}_t(t) \qquad \bar{V} = \bar{V}_t(t) \tag{3.43}$$

$$\delta\bar{r} = \bar{V}_t(t) \qquad \delta\bar{V} = \bar{g}(t) \tag{3.44}$$

Applying Eq. (3.34) to this problem yields Eq. (3.45).

$$\delta x_0^1 = (\bar{\lambda}\cdot\bar{g} - \dot{\bar{\lambda}}\cdot\bar{V}_t - H)\,\delta t \tag{3.45}$$

For the time open case for Problem C1 the stationary condition of Eq. (3.45) results in Eq. (3.46).

$$\lambda = \frac{\sigma m}{c} \tag{3.46}$$

This equation indicates that the thrust should cut off at the time of rendezvous and that a coasting arc should begin at that time. Applying Eq. (3.45) to Problem C2 requires some care because the Hamiltonian may not be defined at a terminal impulse. However, Eq. (3.45) may be used with the value of the Hamiltonian immediately prior to the impulse, resulting in Eq. (3.47).

$$\dot{\bar{\lambda}} \cdot (\bar{V}_t - V) = \dot{\bar{\lambda}} \cdot \Delta\bar{V} = 0 \tag{3.47}$$

This equation may be replaced by Eq. (3.48) as the primer vector must point in the direction of the terminal impulse.

$$\dot{\bar{\lambda}} \cdot \bar{\lambda} = 0 \tag{3.48}$$

This equation indicates that the primer vector magnitude must have a stationary maximum at the terminal time. This implies that for this problem as well as Problem C1 a coasting arc must begin at the time of rendezvous.

The minimum time rendezvous problem is only of interest for Problem C1. Applying Eq. (3.45) yields Eq. (3.49).

$$\lambda^1 = \frac{m^1}{c} \tag{3.49}$$

This equation is not very useful as all it does is determine a natural scaling for the values of the primer vector.

An interesting rendezvous problem occurs when the transfer time from one body in free fall to another body in free fall is specified, but the time at which the maneuver starts is not specified. This case is of interest for all three problems — C1, C2, and P1. Applying Eq. (3.45) to these problems yields, respectively, Eqs. (3.50), (3.51), and (3.52).

$$\text{C1} \qquad \frac{f}{m}\left(\lambda - \frac{\sigma m}{c}\right)\Bigg|^{t^0} = \frac{f}{m}\left(\lambda - \frac{\sigma m}{c}\right)\Bigg|^{t^1} \tag{3.50}$$

$$\text{C2} \qquad \dot{\bar{\lambda}} \cdot \overline{\Delta V}^0 = -\dot{\bar{\lambda}} \cdot \overline{\Delta V}^1 \tag{3.51}$$

$$\text{P1} \qquad \frac{\lambda^2}{2}\Bigg|^{t^0} = \frac{\lambda^2}{2}\,\frac{P}{P^0}\Bigg|^{t^1} \tag{3.52}$$

Many of the interesting problems in space trajectory optimization are problems of orbit transfer. In order to define such problems, it is usually necessary to assume that the gravitational field is only a function of position and not of time. This assumption will be made here. Such an assumption will result in the Hamiltonian being constant for Problems C1, C2, and those examples of Problem P1 where the power is independent of the time. The variations in position and velocity on the target orbit will be given by Eqs. (3.53), where the variable τ refers to a fictitious motion on the target orbit and does not correspond to time on the actual trajectory.

$$\delta \bar{r} = \bar{V}_t \, \delta\tau \qquad\qquad \delta \bar{V} = \bar{g} \, \delta\tau \tag{3.53}$$

For time fixed orbit transfer for Problem C1, Eq. (3.34) yields Eq. (3.54) which will be true at both ends of the trajectory.

$$\bar{\lambda} \cdot \bar{g} - \dot{\bar{\lambda}} \cdot \bar{V} = 0 \tag{3.54}$$

Because the Hamiltonian will be constant for this problem, Eq. (3.55) may also be obtained.

$$H = \frac{f}{m}\left(\lambda - \frac{\sigma m}{c}\right)\Big|^{t^0} = \frac{f}{m}\left(\lambda - \frac{\sigma m}{c}\right)\Big|^{t^1} \tag{3.55}$$

For Problem C2 with time fixed the variations in position and velocity will be assumed to be given by Eqs. (3.56).

$$\delta \bar{r} = (\bar{V} \pm \overline{\Delta V})\,\delta\tau \qquad\qquad \delta \bar{V} = \bar{g}\,\delta\tau \tag{3.56}$$

This results in Eqs. (3.57) and (3.58).

$$\delta x_0^1 = 0 = (\bar{\lambda}\cdot\bar{g} - \dot{\bar{\lambda}}\cdot\bar{V} \mp \dot{\bar{\lambda}}\cdot\overline{\Delta V})\,\delta\tau \tag{3.57}$$

$$H = -\dot{\bar{\lambda}}\cdot\overline{\Delta V}\Big|^{t^0} = +\dot{\bar{\lambda}}\cdot\overline{\Delta V}\Big|^{t^1} \tag{3.58}$$

For Problem P1, Eq. (3.54) is again obtained and if the power is not a function of time, Eq. (3.59) may also be obtained.

$$H = \frac{\lambda^2}{2}\Big|^{t^0} = \frac{\lambda^2}{2}\,\frac{P}{P^0}\Big|^{t^1} \tag{3.59}$$

For time open orbit transfer for Problem C1, Eq. (3.54) still holds and, in addition, Eq. (3.60) holds. The Hamiltonian will be zero.

$$\lambda = \frac{\sigma m}{c} \tag{3.60}$$

The terminal times for this time open problem must represent the beginning of coasting arcs.

For time open orbit transfer for Problem C2, Eq. (3.58) must hold. However, in this case, because the time is not specified, the Hamiltonian must be zero. Therefore, Eq. (3.61) must hold.

$$\dot{\bar{\lambda}} \cdot \bar{\lambda} = 0 \tag{3.61}$$

Once again, as in Problem C1, the terminal powered arcs must join onto coasting arcs.

For minimum time orbit transfer in Problem C1, Eq. (3.54) must hold and Eq. (3.62) must hold.

$$\lambda^1 = \frac{m^1}{c} \tag{3.62}$$

As for minimum time rendezvous, this provides a natural scaling for the Lagrange multipliers.

Another interesting problem is the problem of reaching a given energy. The energy in a time varying gravitational field may be represented as in Eq. (3.63) where U is the time varying gravitational potential.

$$E = \frac{\bar{V} \cdot \bar{V}}{2} + U(\bar{r}, t) \tag{3.63}$$

For the time fixed problem the allowable variations in velocity and position must satisfy Eq. (3.64).

$$\bar{V}_t \cdot \overline{\delta V} - \bar{g} \cdot \delta \bar{r} = 0 \tag{3.64}$$

The change in cost from Eq. (3.34) is given by Eq. (3.65).

$$\delta x_0^1 = \bar{\lambda} \cdot \overline{\delta V} - \dot{\bar{\lambda}} \cdot \delta \bar{r} = 0 \tag{3.65}$$

In order for both (3.64) and (3.65) to be satisfied, Eqs. (3.66) must be satisfied.

$$\bar{\lambda} = \frac{\lambda}{V_t} \bar{V}_t \qquad \dot{\bar{\lambda}} = \frac{\lambda}{V_t} \bar{g} \tag{3.66}$$

For all three problems the quantity on the left-hand side of Eq. (3.67) is equal to the right-hand side.

$$\bar{\lambda} \cdot \bar{g} - \bar{\lambda} \cdot \bar{V} = \frac{\lambda}{V_t} \bar{g} \cdot (\bar{V}_t - \bar{V}) \tag{3.67}$$

For both Problem C1 and P1 the velocity is continuous so that both quantities will be equal to zero. For Problem C2 the value of H will not be zero but will be given by the right-hand side of Eq. (3.67). It should be noted that the terminal impulse for Problem C2 will be in the direction of the velocity vector so that V_t and V will be colinear.

To consider the problem of reaching a given energy with variable terminal time, it will be assumed that the gravitational potential is not a function

of time. For the time open problem of reaching a given energy for Problem C1, the transversality conditions will result in Eqs. (3.66), (3.67) and (3.60). For Problem C2 the corresponding equations will be (3.66), (3.67) and (3.61). This implies that for this problem, Eq. (3.68) must be satisfied.

$$\bar{V} \cdot \bar{g} = 0 \tag{3.68}$$

This equation has a simple, physical interpretation. The rate of change of energy is proportional to velocity so that the terminal orbit must be entered at a point where the velocity is a maximum. The stationary condition for this to be true is given by Eq. (3.68), which will be satisfied at an apse of the terminal orbit. For minimum time transfer to a given energy level in Problem C1, the transversality conditions will result in Eqs. (3.66), (3.67) and (3.62).

CHAPTER 4: TRAJECTORY OPTIMIZATION IN FIELD-FREE SPACE

4.1 Integration of the Adjoint Equations

If the mass flow rate of the rocket is independent of position, then the adjoint equations become uncoupled from the equations of motion for linearized gravity fields. An important special case of such fields is field-free space far from any massive body.

In field-free space the differential equation for the primer vector is given by Eq. (4.1)

$$\ddot{\bar{\lambda}} = \bar{0} \tag{4.1}$$

This equation is readily integrated to yield Eq. (4.2).

$$\bar{\lambda} = \bar{\lambda}^0 + \dot{\bar{\lambda}}^0 (t - t^0) \tag{4.2}$$

The tip of the primer vector moves along a straight line at constant velocity. This line may be spoken of as the locus of the primer vector. The primer vector always lies in a plane determined by the origin and this locus. The magnitude of the primer vector is given by Eq. (4.3).

$$|\lambda| = \sqrt{\bar{\lambda}^0 \cdot \bar{\lambda}^0 + 2\bar{\lambda}^0 \cdot \dot{\bar{\lambda}}^0 (t-t^0) + \dot{\bar{\lambda}}^0 \cdot \dot{\bar{\lambda}}^0 (t-t^0)^2} \tag{4.3}$$

This equation represents a hyperbola which is concave upwards. Because of the shape of this curve there will be, at most, one coasting arc for Problem C2 and either one or two impulses. For Problem C2 there will be, at most, one coasting arc with either one or two thrusting arcs. If the final position is open, the derivative of the primer vector will be identically zero and the primer vector will be constant in magnitude. This will be a singular case for Problems C1 and C2, the thrust direction will be specified but the time of application and magnitude of the thrust will be unspecified.

4.2 Constant Exhaust Velocity Propulsion with Unbounded Thrust Magnitude

For interception the previous chapter has shown that the primer vector must be zero at the terminal time, Eq. (4.4).

$$|\lambda^1| = 0 \tag{4.4}$$

The primer vector can only become zero if its rate of change is directed antiparallel to its initial direction. This result implies that the direction of thrust during interception must be constant. This constant thrust direction for interception is independent of any consideration of the type of propulsion and holds for all propulsion systems in field-free space.

The magnitude of the primer vector must decrease linearly to zero at interception. There will be only one impulse represented by Eq. (4.5), which may be re-written as (4.6).

$$\overline{\Delta V} = \frac{\bar{r}_t^{\,1} - \bar{r}^{\,0}}{t^1 - t^0} - \bar{V}^{\,0} \tag{4.5}$$

$$\overline{\Delta V} = \frac{\bar{r}_t^{\,0} - \bar{r}^{\,0}}{t^1 - t^0} + \bar{V}_t^{\,0} - \bar{V}^{\,0} \tag{4.6}$$

The magnitude of the required velocity increment may be found by taking the dot product of Eq. (4.6) with itself. The velocity increment is a function of the initial relative position, the relative velocity, and the total time allowed. For given initial conditions there is an optimum time for interception which minimizes the velocity increment. This optimum time may be found by determining the stationary point of the norm of Eq. (4.6). Carrying out this computation yields the two minimizing roots given by Eq. (4.7).

$$t^1 - t^0 = - \frac{(\bar{r}_t^{\,0} - \bar{r}^{\,0}) \cdot (\bar{r}_t^{\,0} - \bar{r}^{\,0})}{(\bar{r}_t^{\,0} - \bar{r}^{\,0}) \cdot (\bar{V}_t^{\,0} - \bar{V}^{\,0})} \quad , \quad \infty \tag{4.7}$$

The left-hand root represents the optimum interception time when the vehicle is approaching the target, while the right-hand root represents the optimum interception time when the vehicle is receding from the target. The left-hand root has an interesting physical interpretation as it is the negative of the range to the target divided by the rate of change of range. The minimum velocity increment for these optimum times is given by Eq. (4.8), the left-hand expression again applying to vehicles approaching the target and the right-hand expression for vehicles receding from the target.

$$\Delta V = \frac{|(\bar{V}_t^0 - \bar{V}^0) \times (\bar{r}_t^0 - \bar{r}^0)|}{|\bar{r}_t^0 - \bar{r}_0|} \quad , \quad |\bar{V}_t^0 - \bar{V}^0| \tag{4.8}$$

The left-hand term in Eq. (4.8) is equal to the magnitude of the relative velocity multiplied by the sine of the angle between the relative velocity vector and the line-of-sight to the target. It applies only when the vehicle is approaching the target. When the vehicle is receding from the target the optimum maneuver is to stop the relative motion except for an infinitesimal residual velocity which will accomplish interception as the time becomes infinite.

When the vehicle is moving towards the target, the optimum interception has several interesting geometric properties. As required by Eq. (3.39) of the previous chapter, the rate of change of the primer vector must be perpendicular to the relative velocity at interception. The thrust is also directed from the unperturbed position that the intercepter would have at the terminal time to the position that the target has at the terminal time. This last result will be true for any interception in field-free space with any propulsion system.

Another interesting interception problem is when the transfer time is fixed but the time at which the initial orbit is left is not specified. The required velocity increment for this case is given by Eq. (4.9), which may be re-written as Eq. (4.10).

$$\overline{\Delta V} = \frac{\bar{r}_t^0 - \bar{r}^0 + (\bar{V}_t^0 - \bar{V}^0)(t - t^0)}{t^1 - t} + \bar{V}_t^0 - \bar{V}^0 \tag{4.9}$$

$$\overline{\Delta V} \quad \frac{\bar{r}_t^{\,0} - \bar{r}^{\,0}}{\Delta t} + \frac{\bar{V}_t^{\,0} - \bar{V}^{\,0}}{\Delta t} \; (t^1 - t^0) \tag{4.10}$$

The quantity t in these equations refers to the time at which the impulse is applied. The quantity Δt is the allowable maneuver time $t^1 - t$.

This maneuver is the field-free version of the optimum interception of one planet by a vehicle that departs from another planet with a specified transfer time. By taking the dot product of Eq. (4.10) with itself and finding the stationary point when t^1 is allowed to vary holding the quantity Δt fixed, yields Eq. (4.11).

$$t^1 - t^0 = - \frac{(\bar{r}_t^{\,0} - \bar{r}^{\,0}) \cdot (\bar{V}_t^{\,0} - \bar{V}^{\,0})}{(\bar{V}_t^{\,0} - \bar{V}^{\,0}) \cdot (\bar{V}_t^{\,0} - \bar{V}^{\,0})} \tag{4.11}$$

The optimum value of the interception time is the same as the time of closest approach of the two vehicles when no propulsion is applied. The magnitude of the velocity increment for this case is given by Eq. (4.12).

$$\Delta V = \frac{|(\bar{V}_t^{\,0} - \bar{V}^{\,0}) \times (\bar{r}_t^{\,0} - \bar{r}^{\,0})|}{|\bar{V}_t^{\,0} - \bar{V}^{\,0}| \, \Delta t} \tag{4.12}$$

This velocity increment is equal to the unperturbed closest approach distance divided by the given transfer time. For this case the rate of change of the primer vector and the primer vector are perpendicular to the relative velocity vector.

For rendezvous there will be two impulses which will always be given at the beginning and end of the maneuver. The first impulse puts the vehicle on a collision course with the target. This is the same impulse as is required for interception. The second impulse cancels the relative velocity between the two vehicles at interception. The total velocity increment required is given by Eq. (4.13).

$$\Delta V = \frac{|\bar{r}_t^{\,0} - \bar{r}^{\,0} + (\bar{V}_t^{\,0} - \bar{V}^{\,0})(t^1 - t^0)|}{t^1 - t^0} + \frac{|\bar{r}_t^{\,0} - \bar{r}^{\,0}|}{t^1 - t^0} \tag{4.13}$$

The magnitude of the second impulse depends only upon the initial range to the target and the allowable rendezvous time. The total velocity increment required for rendezvous is a monotonically decreasing function of the time allowed. The optimum time for rendezvous is always infinite. This optimum rendezvous time is the same as the optimum time for interception when the vehicle is receding from the target.

If the transfer time is fixed but the time of initiating the maneuver is open, the rendezvous may be analyzed by the same type of analysis as was used for the corresponding interception case. Once again, the first impulse will be the same as that required for interception and the second impulse will cancel the relative velocity difference. The total velocity increment is given by Eq. (4.14).

$$\Delta V = \frac{|\bar{r}_t^0 - \bar{r}^0 + (\bar{V}_t^0 - \bar{V}^0)(t^1 - t^0)|}{\Delta t} + \frac{|\bar{r}_t^0 - \bar{r}^0 + (\bar{V}_t^0 - \bar{V}^0)(t^1 - t^0 - \Delta t)|}{\Delta t} \tag{4.14}$$

The optimum time for initiating the rendezvous maneuver may be found by determining the stationary minimum of Eq. (4.14) with respect to the terminal time. The optimum terminal time is given by Eq. (4.15).

$$t^1 - t^0 = -\frac{(\bar{r}_t^0 - \bar{r}^0) \cdot (\bar{V}_t^0 - \bar{V}^0)}{(\bar{V}_t^0 - V^0) \cdot (\bar{V}_t^0 - V^0)} + \frac{\Delta t}{2} \tag{4.15}$$

Unlike the corresponding interception case, the times to start and end the maneuver are centered around the unperturbed closest approach time rather than terminating at that time. The total velocity increment for this case is given by Eq. (4.16).

$$\Delta V = \sqrt{(\bar{V}_t^0 - \bar{V}^0) \cdot (\bar{V}_t^0 - \bar{V}^0) + 4\left[\frac{|(\bar{V}_t^0 - \bar{V}^0) \times (\bar{r}_t^0 - \bar{r}^0)|}{|\bar{V}_t^0 - \bar{V}^0| \, \Delta t}\right]^2} \tag{4.16}$$

The two velocity increments are equal in magnitude. They each have a component normal to the relative velocity whose magnitude is the same as that for interception in the same transfer time. These two velocity components cancel each other. Each velocity increment also has a component which is equal to half of the relative velocity and opposed to the relative velocity direction.

This minimum velocity increment for rendezvous with a fixed transfer time is the same as the minimum velocity increment for transfer from the first

orbit to the second orbit in the same transfer time. This is because the unperturbed motion of the two vehicles will produce all possible relative positions of the two vehicles on each orbit. This result will not generally be true for orbits in more complex gravity fields. One other example for which it is true is for coplanar circular orbits in a central gravity field.

4.3 Power-Limited Propulsion with Unbounded Thrust Magnitude

For power-limited propulsion the acceleration vector will be taken as identical with the primer vector as was done in Chapter 3. With the primer vector given by Eq. (4.2), the equations of motion may be integrated to yield Eqs. (4.17) and (4.18).

$$\bar{V} = \bar{V}^0 + \bar{\lambda}^0 (t - t^0) + \frac{1}{2} \dot{\bar{\lambda}}^0 (t - t^0)^2 \tag{4.17}$$

$$\bar{r} = \bar{r}^0 + \bar{V}^0 (t - t^0) + \frac{1}{2} \bar{\lambda}^0 (t - t^0)^2 + \frac{1}{6} \dot{\bar{\lambda}}^0 (t - t^0)^3 \tag{4.18}$$

Similarly, the payoff may be determined by integrating its differential equation to yield Eq. (4.19).

$$J = \frac{1}{2} \bar{\lambda}^0 \cdot \bar{\lambda}^0 (t - t^0) + \frac{1}{2} \bar{\lambda}^0 \cdot \dot{\bar{\lambda}}^0 (t - t^0)^2 + \frac{1}{6} \dot{\bar{\lambda}}^0 \cdot \dot{\bar{\lambda}}^0 (t - t^0)^3 \tag{4.19}$$

For interception the primer vector and the thrust acceleration must go to zero at the terminal time. The initial value of the primer vector must then be given by Eq. (4.20).

$$\bar{\lambda}^0 = -\dot{\bar{\lambda}}^0 (t^1 - t^0) \tag{4.20}$$

At the terminal time the position of the vehicle must be the same as the position of the target. Using this fact and substituting Eq. (4.20) into Eq. (4.18) yields Eq. (4.21).

$$\dot{\bar{\lambda}}^0 = -3\frac{\bar{r}_t^1 - \bar{r}^0}{(t^1 - t^0)^3} + \frac{3V^0}{(t^1 - t^0)^2} = -3\frac{\bar{r}_t^0 - \bar{r}^0}{(t^1 - t^0)^3} - 3\frac{\bar{V}_t^0 - \bar{V}^0}{(t^1 - t^0)^2} \tag{4.21}$$

Equations (4.21) and (4.20) provide the solution of the boundary value problem and allow the determination of all quantities of interest, including the payoff. Eq. (4.22).

$$J = \frac{3}{2}\frac{\left|\bar{r}_t^0 - \bar{r}^0 + (\bar{V}_t^0 - \bar{V}^0)(t^1 - t^0)\right|^2}{(t^1 - t^0)^3} \tag{4.22}$$

This expression for J has an absolute minimum of zero at infinite time. It also has a local minimum with respect to t^1 if the angle between the realtive velocity and position vectors is less than 30^o and the intercepting vehicle is approaching the target. The time at which this local minimum occurs is given by Eq. (4.23).

$$t^1 - t^0 = -2\frac{(\bar{r}_t^0 - \bar{r}^0)\cdot(\bar{V}_t^0 - \bar{V}^0)}{(\bar{V}_t^0 - \bar{V}^0)\cdot(\bar{V}_t^0 - \bar{V}^0)} - \sqrt{\left[2\frac{(\bar{r}_t^0 - \bar{r}^0)\cdot(\bar{V}_t^0 - \bar{V}^0)}{(\bar{V}_t^0 - \bar{V}^0)\cdot(\bar{V}_t^0 - \bar{V}^0)}\right]^2 - 3} \tag{4.23}$$

During an optimal interception the thrust acceleration will decrease linearly to zero. However, for guidance purposes it is useful to have a closed loop synthesis of the optimal control in terms of the current state of the vehicle, the current state of the target, and of the time to go. Such a synthesis is easily achieved by regarding the initial state in Eqs. (4.20) and (4.21) as the current state to yield Eq. (4.24).

$$\bar{A} = 3\,\frac{\bar{r}_t - \bar{r}}{(t^1 - t)^2} + 3\,\frac{\bar{V}_t - \bar{V}}{t^1 - t} \tag{4.24}$$

The numerator in Eq. (4.22) for the payoff is simply the square of the unperturbed distance between the two vehicles at the terminal time. For interception with a given transfer time but a variable terminal time, the optimum terminal time will obviously be the time of closest approach. This is the same as the optimum terminal time for the impulsive case, Eq. (4.11). The minimum payoff, J, for this case will then be given by Eq. (4.25).

$$J = \frac{3}{2}\,\frac{\left|(\bar{V}_t^0 - \bar{V}^0) \times (\bar{r}_t^0 - \bar{r}^0)\right|^2}{\left|\bar{V}_t^0 - \bar{V}^0\right|^2 \Delta t^3} \tag{4.25}$$

For rendezvous, Eqs. (4.17) and (4.18) must be solved simultaneously to yield the initial values of the adjoint vector given by Eqs. (4.26) and (4.27).

$$\dot{\bar{\lambda}}^0 = -\frac{12}{(t^1 - t^0)^3}\left[\bar{r}_t^0 - \bar{r}^0 + \frac{1}{2}(\bar{V}_t^0 - \bar{V}^0)(t^1 - t^0)\right] \tag{4.26}$$

$$\bar{\lambda}^0 = \frac{6}{(t^1 - t^0)^2}\left[\bar{r}_t^0 - \bar{r}^0 + \frac{2}{3}(\bar{V}_t^0 - \bar{V}^0)(t^1 - t^0)\right] \tag{4.27}$$

The corresponding value of the payoff J is given by Eq. (4.28).

$$J = 2\frac{|\bar{V}_t^0 - \bar{V}^0|^2}{t^1 - t^0} + 6\frac{(\bar{V}_t^0 - \bar{V}^0)\cdot(\bar{r}_t^0 - \bar{r}^0)}{(t^1 - t^0)^2} + 6\frac{|\bar{r}_t^0 - \bar{r}^0|^2}{(t^1 - t^0)^3} \tag{4.28}$$

This payoff J is a monotonically decreasing function of the transfer time. The optimum time for rendezvous is once again infinite as it was for the impulsive case.

The optimum control for rendezvous may be synthesized exactly as it was for the interception case to yield Eq. (4.29).

$$\bar{A} = \frac{6}{(t^1 - t)^2}\left[\bar{r}_t - \bar{r} + \frac{2}{3}(\bar{V}_t - \bar{V})(t^1 - t)\right] \tag{4.29}$$

In this case the magnitude of the acceleration during an optimum rendezvous will vary hyperbolically with time.

For the case where the transfer time is specified but the time of starting or terminating the maneuver is not, the payoff is given by Eq. (4.30).

$$J = \frac{|\bar{V}_t^0 - \bar{V}^0|^2}{\Delta t}\left[2 - 6\frac{t^1-t^0}{\Delta t} + 6\frac{(t^1-t^0)^2}{\Delta t^2}\right] - \frac{(\bar{V}_t^0 - \bar{V}^0)\cdot(\bar{r}_t^0 - \bar{r}^0)}{\Delta t^2}\left[6 - 12\frac{t^1-t^0}{\Delta t}\right] + 6\frac{|\bar{r}_t^0 - \bar{r}^0|^2}{\Delta t^3} \tag{4.30}$$

This equation has a stationary minimum at precisely the same time as that for impulsive rendezvous given by Eq. (4.15). The corresponding payoff for this case is given by Eq. (4.31).

$$J = \frac{1}{2}\frac{|\bar{V}_t^0 - \bar{V}^0|^2}{\Delta t} + 6\frac{|(\bar{V}_t^0 - \bar{V}^0) \times (\bar{r}_t^0 - \bar{r}^0)|^2}{|\bar{V}_t^0 - \bar{V}^0|^2 \Delta t^3} \tag{4.31}$$

The first term in Eq. (4.31) represents the cost of a constant deceleration which cancels the relative velocity between the two vehicles. The second term represents the cost of a change in position with no change in velocity at right angles to the velocity change. The latter thrust component varies linearly with time and passes through zero at the unperturbed closest approach time.

CHAPTER 5: TRAJECTORY OPTIMIZATION IN AN INVERSE SQUARE-FIELD

5.1 Integrals of Motion

The Hamiltonian for optimal trajectories in an inverse square-field is given by Eq. (5.1) where γ is the gravitational constant of the central body.

$$H = \frac{\lambda f}{m} - \gamma \frac{\bar{\lambda} \cdot \bar{r}}{r^3} - \dot{\bar{\lambda}} \cdot \dot{\bar{r}} + \sigma \dot{m} \tag{5.1}$$

The mass flow rate will be assumed to be independent of position and time. The equation of motion is given in second order form by Eq. (5.2).

$$\ddot{\bar{r}} = \frac{\bar{f}}{m} - \gamma \frac{\bar{r}}{r^3} \tag{5.2}$$

The mass flow rate is given By Eq. (5.3) for the constant exhaust velocity rocket and for the constant power rocket.

$$\dot{m} = -\left(\frac{f}{c}, \frac{f^2}{2P} \right) \tag{5.3}$$

This notation with a comma separating the expressions for the two types of rockets will be used consistently through this chapter.

The equation for the primer vector is given in second order form by Eq. (5.4).

$$\ddot{\bar{\lambda}} = -\gamma \frac{\bar{\lambda}}{r^3} + 3\gamma \frac{\bar{r} \cdot \bar{\lambda}}{r^5} \bar{r} \tag{5.4}$$

The final equation for the Lagrange multiplier for mass is given by Eq. (5.5).

$$\dot{\sigma} = \frac{\lambda f}{m^2} \tag{5.5}$$

The first integral of this system of equations is given by the Hamiltonian, which is constant for an optimal trajectory as the equations have no explicit dependence on time. Three more integrals are given by a vector integral which results from the spherical symmetry of the problem. Taking the vector cross product of the primer vector with Eq. (5.2) produces Eq. (5.6).

$$\bar{\lambda} \times \ddot{\bar{r}} = -\gamma \frac{\bar{\lambda} \times \bar{r}}{r^3} \tag{5.6}$$

Taking the vector cross product of the position vector with Eq. (5.4), produces Eq. (5.7).

$$\bar{r} \times \ddot{\bar{\lambda}} = -\gamma \frac{\bar{r} \times \bar{\lambda}}{r^3} \tag{5.7}$$

Adding Eqs. (5.6) and (5.7), produces Eq. (5.8).

$$\frac{d}{dt}(\bar{\lambda} \times \dot{\bar{r}} + \bar{r} \times \dot{\bar{\lambda}}) = 0 \tag{5.8}$$

This equation may be integrated to produce Eq. (5.9) where $\bar{\Lambda}$ is a vector constant of the motion.

$$\bar{\lambda} \times \dot{\bar{r}} + \bar{r} \times \dot{\bar{\lambda}} = \bar{\Lambda} \tag{5.9}$$

An additional integral may be derived when the thrust is unbounded (cases C-2 and P-1) where the mass multiplier is given by Eq. (5.10).

$$\sigma = \left(\frac{c}{m} , \frac{P}{m^2} \right) \tag{5.10}$$

For these two cases the Hamiltonian is given by Eq. (5.11).

$$H = -\gamma \frac{\bar{\lambda} \cdot \bar{r}}{r^3} - \dot{\bar{\lambda}} \cdot \dot{\bar{r}} + \left(\quad , \frac{\lambda^2}{2} \right) \tag{5.11}$$

Taking the dot product of the primer vector with Eq. (5.2), produces Eq. (5.12).

$$\bar{\lambda} \cdot \ddot{\bar{r}} = \lambda \frac{f}{m} - \gamma \frac{\bar{\lambda} \cdot \bar{r}}{r^3} \tag{5.12}$$

Taking the dot products of the position vector with Eq. (5.4), produces Eq. (5.13).

$$r \cdot \ddot{\bar{\lambda}} = 2\gamma \frac{\bar{\lambda} \cdot \bar{r}}{r^3} \tag{5.13}$$

Adding twice Eq. (5.13) to Eq. (5.12), produces Eq. (5.14).

$$2\bar{r} \cdot \ddot{\bar{\lambda}} + \bar{\lambda} \cdot \ddot{\bar{r}} = 3\gamma \frac{\bar{\lambda} \cdot \bar{r}}{r^3} + \lambda \frac{f}{m} \tag{5.14}$$

The time derivative of the left-hand side of Eq. (5.15) is equal to its right-hand side. Substituting Eq. (5.14) into the right-hand side produces Eq. (5.16).

$$\frac{d}{dt} (\bar{\lambda} \cdot \dot{\bar{r}} + 2\bar{r} \cdot \dot{\bar{\lambda}}) = 2\bar{r} \cdot \ddot{\bar{\lambda}} + \bar{\lambda} \cdot \ddot{\bar{r}} + 3\dot{\bar{\lambda}} \cdot \dot{\bar{r}} \tag{5.15}$$

$$\frac{d}{dt} (\bar{\lambda} \cdot \dot{\bar{r}} + 2\bar{r} \cdot \dot{\bar{\lambda}}) = 3\gamma \frac{\bar{\lambda} \cdot \bar{r}}{r^3} + 3\dot{\bar{\lambda}} \cdot \dot{\bar{r}} + \lambda \frac{f}{m} \tag{5.16}$$

Substituting Eq. (5.11) into Eq. (5.16), produces Eq. (5.17).

$$\frac{d}{dt}\left(\bar{\lambda}\cdot\dot{\bar{r}} + 2\bar{r}\cdot\dot{\bar{\lambda}}\right) + 3H - \left(\lambda\frac{f}{m}\,,\ 5\frac{\lambda^2}{2}\right) = 0 \tag{5.17}$$

Eq. (5.17), may be integrated with respect to time to produce the additional integral of motion for these two problems — Eq. (5.18).

$$\bar{\lambda}\cdot\dot{\bar{r}} + 2\bar{r}\cdot\dot{\bar{\lambda}} + 3Ht - (\Delta V,\ 5J) = \text{const.} \tag{5.18}$$

The integration can be carried out for the constant exhaust velocity case because the thrust is turned on only when the primer vector has unit magnitude. The integral holds on the open interval from the initial time to the final time even if there are singular arcs.

5.2 Variation of Parameters

For many problems it is convenient to rewrite the equations of motion in terms of the variation of orbital elements, instead of the position and velocity vectors used in the previous section. The orbital element formulation is useful for both coasting arcs where the vehicle is unpowered and for low thrust trajectories where the elements of the orbit may be expected to vary slowly. Eq. (5.2) is replaced by six first order equations for the rates of change of the orbital elements. The elements chosen are semimajor axis a, eccentricity e, argument of perigee ω, inclination i, longitude of the node Ω, and mean anomaly M. Results for other sets of elements can be derived in the same way. The rates of change of these elements may be found in any standard text celestial mechanics and are given by (5.19) through (5.24).

$$\frac{da}{dt} = 2\sqrt{\frac{a^3}{\gamma}}\,\frac{F_r e f_1 + F_\theta f_5}{m f_3} \tag{5.19}$$

$$\frac{de}{dt} = \sqrt{\frac{a}{\gamma}}\,\frac{F_r f_1 f_5 + F_\theta (f_4 + f_2 f_3)}{m f_3} \tag{5.20}$$

$$\frac{d\omega}{dt} = \sqrt{\frac{a}{\gamma}}\,\frac{-F_r f_4 f_5 + F_\theta (f_3 + f_5^2) f_1}{m e f_3} - \sqrt{\frac{a}{\gamma}}\,\frac{F_z (f_1 f_5 \cos\omega + f_4 \sin\omega)}{m f_5 \tan i} \tag{5.21}$$

$$\frac{di}{dt} = \sqrt{\frac{a}{\gamma}}\,\frac{F_z (f_4 \cos\omega - f_1 f_5 \sin\omega)}{m f_5} \tag{5.22}$$

$$\frac{d\Omega}{dt} = \sqrt{\frac{a}{\gamma}} \frac{F_z(f_1 f_5 \cos \omega + f_4 \sin \omega)}{m f_5 \sin i} \tag{5.23}$$

$$\frac{dM}{dt} = \sqrt{\frac{\gamma}{a^3}} + \sqrt{\frac{a}{\gamma}} \frac{F_r(f_4 f_5^2 - 2e f_3^2) - F_\theta f_1 f_5 (f_3 + f_3^2)}{me f_3} \tag{5.24}$$

The mean and eccentric anomalies are related by Kepler's Eq. (5.25) and the f_i are given by Eqs. (5.26).

$$M = E - e \sin E \tag{5.25}$$

$$\left.\begin{aligned} f_1 &\equiv \sin E & f_3 &\equiv 1 - e \cos E \\ f_2 &\equiv \cos E & f_4 &\equiv \cos E - e \\ & & f_5 &\equiv \sqrt{1 - e^2} \end{aligned}\right\} \tag{5.26}$$

The Hamiltonian for this formulation is given by Eq. (5.27).

$$H = \lambda_a \dot{a} + \lambda_e \dot{e} + \lambda_\omega \dot{\omega} + \lambda_i \dot{i} + \lambda_\Omega \dot{\Omega} + \lambda_M \dot{M} + \sigma \dot{m} \tag{5.27}$$

This Hamiltonian is the same as the Hamiltonian given by Eq. (5.1). The transformation between the two formulations may be found by the standard techniques of canonical transformation. A different technique will be utilized herein. The

basis of this technique is noting that the instantaneous values of $\bar{\lambda}$ and $\dot{\bar{\lambda}}$ are independent of the thrust level so that $\bar{\lambda}$ and $\dot{\bar{\lambda}}$ have the same value on the osculating unpowered conic and on the powered trajectory. For the osculating conic the thrust will be zero which yields Eq. (5.28) when Eq. (5.1) and (5.27) are equated.

$$-\bar{\lambda}\cdot\bar{r}\frac{\gamma}{r^3} - \dot{\bar{\lambda}}\cdot\dot{\bar{r}} = \lambda_M\sqrt{\frac{\gamma}{a^3}} \tag{5.28}$$

The components of the primer vector in the cylindrical coordinate systems whose axis is perpendicular to the orbital plane may be determined by equating the components of the primer vector in Eq. (5.1) and (5.28).

$$\lambda_r = \sqrt{\frac{a}{\gamma}}\,\frac{2\lambda_a ae^2 f_1 + \lambda_e ef_1 f_5^2 - (\lambda_\omega - f_5\lambda_M)f_4 f_5 - 2\lambda_M ef_3^2}{ef_3} \tag{5.29}$$

$$\lambda_\theta = \sqrt{\frac{a}{\gamma}}\,\frac{2\lambda_a aef_5 + \lambda_e ef_5(f_4 + f_2 f_3) + (\lambda_\omega - f_5\lambda_M)(f_3 + f_5^2)f_1}{ef_3} \tag{5.30}$$

$$\lambda_z = \sqrt{\frac{a}{\gamma}}\,\frac{f_4\beta_1 + f_1 f_5\beta_2}{f_5} \tag{5.31}$$

The quantities β_1 and β_2 are given by Eqs. (5.32).

$$\beta_1 \equiv \lambda_i \cos\omega + \lambda_\Omega \sin\omega \csc i - \lambda_\omega \sin\omega \cot i$$

$$\beta_2 \equiv -\lambda_i \sin\omega + \lambda_\Omega \cos\omega \csc I - \lambda_\omega \cos\omega \cot i \tag{5.32}$$

The derivative of the primer vector is calculated by determining its value on the osculating unpowered ellipse. The Hamiltonian on this ellipse is given by Eq. (5.33).

$$H = \lambda_M \sqrt{\frac{\gamma}{a^3}} \tag{5.33}$$

With this Hamiltonian, the rates of change of the Lagrange multipliers for all the elements except the semimajor axis are zero. The rate of change of the Lagrange multiplier for the semimajor axis is given by Eq. (5.34).

$$\dot{\lambda}_a = \frac{3}{2}\lambda_M \sqrt{\frac{\gamma}{a^5}} \tag{5.34}$$

The components of the derivative of the primer vector in the r, θ, z directions are given by Eqs. (5.35), (5.36), and (5.37).

$$\dot{\lambda}_r = \frac{\partial \lambda_r}{\partial E}\dot{E} + \frac{\partial \lambda_r}{\partial \lambda_a}\dot{\lambda}_a - \lambda_\theta \dot{\theta} \tag{5.35}$$

$$\dot{\lambda}_\theta = \frac{\partial \lambda_\theta}{\partial E}\dot{E} + \frac{\partial \lambda_\theta}{\partial \lambda_a}\dot{\lambda}_a + \lambda_r \dot{\theta} \tag{5.36}$$

$$\dot{\lambda}_z = \frac{\partial \lambda_z}{\partial E}\dot{E} + \frac{\partial \lambda_z}{\partial \lambda_a}\dot{\lambda}_a \tag{5.37}$$

The first two terms on the right-hand side represent the rates of change due to the variables in the equations while the last terms on the right-hand side are due to the rotation of the coordinate system. The rates of change of the eccentric anomaly and central angle are given by standard two-body formulas.

$$\dot{E} = \sqrt{\frac{\gamma}{a^3}}\,\frac{1}{f_3} \qquad \dot{\theta} = \sqrt{\frac{\gamma}{a^3}}\,\frac{f_5}{f_3^2}$$

Carrying out these operations results in Eqs. (5.38), (5.39), and (5.40).

$$\dot{\lambda}_r = \frac{-2\lambda_a ae - \lambda_e e f_2 f_5 - (\lambda_\omega - f_5\lambda_M) f_1 f_5 + \lambda_M e^2 f_1 f_3}{aef_3^2} \tag{5.38}$$

$$\dot{\lambda}_\theta = \frac{-\lambda_e e r_1 f_5 + (\lambda_\omega - f_5\lambda_M) f_2 + \lambda_M e f_5}{aef_3} \tag{5.39}$$

$$\dot{\lambda}_z = \frac{-\beta_1 f_1 f_5 + \beta_2 f_2}{af_3 f_5} \tag{5.30}$$

These six expressions for the primer vector and its rates of change are general expressions which are true both for powered and unpowered orbits. They represent the results of a canonical transformation between the two forms of the equations of motion. In the particular case of an unpowered coasting arc, the osculating orbit will be identical with the coasting arc at all points and Eq. (5.34) may be integrated to yield Eq. (5.41).

$$\lambda_a = \lambda_a^o + \frac{3}{2}\lambda_M\sqrt{\frac{\gamma}{a^5}}\,(t - t^o) \tag{5.41}$$

On a coasting arc, the Lagrange multipliers for all elements except the semi-major axis will be constant. It should also be noted that the equations for the primer vector and its derivative on a coasting arc are the same as the variational equations for position and velocity respectively. This means that any of the innumerable solutions of the

variational equations of two-body orbits may be used to determine the primer vector time history during coast. The present formulation has the possible advantage of identifying the integration constants in terms of the Lagrange multipliers of the orbital elements.

The integrals of motion derived in section (5.1) will now be expressed in terms of the orbital elements and their multipliers. This will be done by direct calculation of the dot and cross products of the primer vector with the position and velocity vectors. The components of position and velocity are given by the following standard two-body equations.

$$r = af_3 \qquad \dot{r} = \sqrt{\frac{\gamma}{a}}\frac{ef_1}{f_3} \qquad r\dot{\theta} = \sqrt{\frac{\gamma}{a}}\frac{f_5}{f_3}$$

The first constant of the motion, the Hamiltonian, is given by Eq. (5.42) for the constant exhaust velocity problem and for the constant power problem.

$$H = \sqrt{\frac{\gamma}{a^3}}\lambda_M + \left(\quad , \frac{\lambda^2}{2} \right) \tag{5.42}$$

It should be noted that for the constant exhaust velocity problem, this provides a determination of λ_M in terms of the current state. The value of the primer vector for the power limited problem may be determined by squaring and adding Eqs. (5.29), (5.30) and (5.31).

The vector constant will be determined by direct calculation to be given by Eq. (5.43) where the components of the column vector on the right side are in the r, θ, and z directions.

$$\dot{\bar{r}}x\bar{\lambda} + \dot{\bar{\lambda}}x\bar{r} = \begin{pmatrix} \dfrac{f_4\beta_1 + f_1 f_5 \beta_2}{f_3} \\ \dfrac{f_1 f_5 \beta_1 - f_4 \beta_2}{f_3} \\ \lambda_\omega \end{pmatrix} \tag{5.43}$$

This result is precisely the result obtained by Moyer (AIAA J. 7, 1232-1235) for the time-open constant exhaust velocity problem. It is shown in that paper that Eq. (5.43) yields the following equations for the Lagrange multipliers of the Euler angles of the orbit.

$$\lambda_\Omega = \lambda_\Omega^o \tag{5.44}$$

$$\lambda_\omega = \lambda_\Omega^o \cos i + \sin i \,(C_1 \sin \Omega - C_2 \cos \Omega) \tag{5.45}$$

$$\lambda_i = C_2 \sin \Omega + C_1 \cos \Omega \tag{5.46}$$

The two constants in these equations are given by Eqs. (5.47) and (5.48).

$$C_1 = \lambda_i^o \cos \Omega^o - \lambda_\Omega^o \cot i^o \sin \Omega^o + \lambda_\omega^o \sin \Omega^o \csc i^o \tag{5.47}$$

$$C_2 = \lambda_i^o \sin \Omega^o + \lambda_\Omega^o \cot i^o \cos \Omega^o - \lambda_\omega^o \cos \Omega^o \csc i^o \tag{5.48}$$

It should be noted that equations (5.44), (5.45), and (5.46) are simply the dot products of the vector constant with the axes of rotation of the Euler angles.

Finally, the quantity in the last integral may be determined by direct calculation to be given by Eq. (5.49).

$$\bar{\lambda}\cdot\dot{\bar{r}} + 2\bar{r}\cdot\dot{\bar{\lambda}} = -2\lambda_a a \tag{5.49}$$

Equation (5.18) then provides a direct representation of the Lagrange multiplier for the semimajor axis in terms of the Hamiltonian, the time, the cost, and the semimajor axis. It should be noted that Eq. (5.18) reduces to Eq. (5.41) on a coasting arc.

5.3 Maxima of the Primer Vector

For the constant exhaust velocity case, the thrust may only be applied at absolute maxima of the primer vector having unit magnitude.

$$\bar{\lambda}\cdot\bar{\lambda} = 1 \tag{5.50}$$

Since the primer vector is continuous and has continuous first and second time derivatives, all maxima except those at the initial and final time must be stationary maxima.

$$\bar{\lambda}\cdot\dot{\bar{\lambda}} = 0 \tag{5.51}$$

A necessary condition for these stationary values to be local maxima is that the second derivative of Eq. (5.50) with respect to time must be negative.

$$\dot{\bar{\lambda}}\cdot\dot{\bar{\lambda}} + \bar{\lambda}\cdot\ddot{\bar{\lambda}} \leq 0 \tag{5.52}$$

The dot product of the primer vector with its second derivative may be found from Eq. (5.4) to be given by Eq. (5.53)

$$\bar{\lambda}\cdot\ddot{\bar{\lambda}} = -\frac{\gamma}{r^3}(1 - 3\lambda_r^2) \tag{5.53}$$

As the dot product of any vector with itself is necessarily positive, Eq. (5.52) yields the additional inequality of Eq. (5.54).

$$\bar{\lambda}\cdot\ddot{\bar{\lambda}} \leq 0 \tag{5.54}$$

Equations (5.53) and (5.54) together yield Eq. (5.55).

$$\lambda_r^2 \leq \frac{1}{3} = \sin^2 35.264^o \tag{5.55}$$

A necessary condition for the primer vector to have a stationary maximum is that the thrust direction must be within 35.264 degrees of the local horizontal direction.

Equation (5.52) may be used to obtain a bound on the rate of change of the primer vector given by Eq. (5.56).

$$\dot{\bar{\lambda}} \cdot \dot{\bar{\lambda}} \leq \frac{\gamma}{r^3}(1 - 3\lambda_r^2) \tag{5.56}$$

The maximum rate of rotation of the primer vector at a stationary maxima is equal to the rate of rotation of a satellite in a circular orbit at the same radial distance. This maximum rotation rate can only be realized if the radial component of the primer vector is zero. If the radial component of the primer vector has the maximum allowable value given by Eq. (5.55), then the rate of rotation of the primer vector must be zero.

For the case of singular arcs, the magnitude of the primer vector must remain unity over a finite time interval. In these cases, the inequality in Eqs. (5.52) and (5.56) must be replaced by an equality.

Chapter 6: LINEARIZED POWER-LIMITED TRANSFER IN THE VICINITY OF AN ELLIPTIC ORBIT

6.1 Optimum Thrust Program

In Chapter 4 it was mentioned that if the maximum flow rate of a rocket is independent of position then the adjoint equations become uncoupled from the equations of motion for linearized gravity fields. This may be seen by writing Eq. (3.9) for this case as Eq. (6.1).

$$\ddot{\bar{\lambda}} = \bar{\lambda} \cdot \frac{\partial \bar{g}}{\partial \bar{r}} \tag{6.1}$$

The differential equation for the primer vector depends only upon the time history of the gravity gradient. In a linearized analysis the change in the gravity gradient due to a change in position is neglected. Therefore, the adjoint equations for the primer vector become uncoupled from the equations of motion. The gravity vector and gravity gradient matrix are evaluated along a nominal trajectory. As long as position deviations from the nominal are small, such an analysis will give a good approximation to the motion.

The nominal trajectory may be powered or unpowered. A particularly important case is where the nominal trajectory is an unpowered elliptic orbit. Optimal low-thrust trajectories in the vicinity of such an elliptic orbit may be found analytically by linearizing around this elliptic orbit. Since the primer vector history along a coasting arc was found in the previous chapter this primer vector history will constitute the optimal control for the linearized problem.

One consequence of the linearization will be that the Hamiltonian for the power limited problem will no longer be a constant of the motion. The reason for this is that the gravity gradient matrix in Eq. (6.1) is now a function of time. In order to have a constant Hamiltonian it would be necessary to solve the exact nonlinear equations of motion. The fact that the Hamiltonian is not a constant for the linear problem creates no difficulty as a full set of integrals for this problem is obtained during the course of the explicit solution of the problem.

The linearized motion in the vicinity of an elliptic orbit is conveniently solved in a variation of parameter formulation. The equations of motion are written as Eqs. (6.2) to (6.7).

$$\frac{da}{dt} = 2\sqrt{\frac{a^3}{\gamma}}\,\frac{F_r e f_1 + F_\theta f_5}{m f_3} \tag{6.2}$$

$$\frac{de}{dt} = \sqrt{\frac{a}{\gamma}}\,\frac{F_r f_1 f_5 + F_\theta (f_4 + f_2 f_3)}{m f_3} \tag{6.3}$$

$$\frac{d\theta}{dt} = \sqrt{\frac{a}{\gamma}}\,\frac{-F_r f_4 f_5 + F_\theta (f_3 + f_5^2) f_1}{me f_3} \tag{6.4}$$

$$\frac{d\alpha}{dt} = \sqrt{\frac{a}{\gamma}}\,\frac{F_2 f_4}{m f_5} \tag{6.5}$$

$$\frac{d\beta}{dt} = \sqrt{\frac{a}{\gamma}} \frac{F_2 f_1}{m} \tag{6.6}$$

$$\frac{dM}{dt} = \sqrt{\frac{\gamma}{a^3}} + \sqrt{\frac{a}{\gamma}} \frac{F_r(f_4 f_5^2 - 2e f_3^2) - F_\theta f_1 f_5 (f_3 + f_5^2)}{mef_3} \tag{6.7}$$

The angular variables θ, α, and β represent small rotations of the elliptic orbit in its own plane, around the major axis, and around the latus rectum, respectively. As the linearization of the problem only involves small rotations it is convenient to use orthogonal rotations rather than Euler angles. The angular variables are defined by Eqs. (6.8) through (6.10) in terms of variations in the conventional Euler angles.

$$\theta \equiv \delta\omega + \cos i \, \delta\Omega \tag{6.8}$$

$$\alpha \equiv \cos \omega \delta i + \sin i \sin \omega \, \delta\Omega \tag{6.9}$$

$$\beta \equiv -\sin \omega \delta i + \sin i \cos \omega \, \delta\Omega \tag{6.10}$$

The Lagrange multipliers for the linear problem will be exactly the same as for the coasting arc. That is, the Lagrange multipliers for each of the orbit elements except the semimajor axis will be constant. The Lagrange multiplier for the semimajor axis will be a linear function of time given by Eq. (6.11) and evaluated on the unpowered coasting ellipse.

$$\lambda_a = \lambda_a^o + \frac{3}{2}\lambda_M \sqrt{\frac{\gamma}{a^5}}\, t \tag{6.11}$$

For this set of orbit elements the optimal thrust acceleration program is given by Eqs. (6.12) through (6.14).

$$\frac{F_r}{m} = \lambda_r = \sqrt{\frac{a}{\gamma}}\, \frac{2\lambda_a a e^2 f_1 + \lambda_e e f_1 f_5^2 - (\lambda_\theta - f_5 \lambda_M) f_4 f_5 - 2\lambda_M e f_3^2}{e f_3} \tag{6.12}$$

$$\frac{F_\theta}{m} = \lambda_\theta = \sqrt{\frac{a}{\gamma}}\, \frac{2\lambda_a a e f_5 + \lambda_e e f_5 (f_4 + f_2 f_3) + (\lambda_\theta - f_5 \lambda_M)(f_3 + f_5^2) f_1}{e f_3} \tag{6.13}$$

$$\frac{F_z}{m} = \lambda_Z = \sqrt{\frac{a}{\gamma}}\, \frac{\lambda_\alpha f_4 + \lambda_\beta f_1 f_5}{f_5} \tag{6.14}$$

Thr thrust acceleration program represents the vector sum of six different acceleration programs corresponding to the initial values of each of the Lagrange multipliers. As the thrust acceleration vector for this problem is identical with the primer vector on a coasting ellipse, these acceleration programs are also of interest for impulsive transfers. The programs corresponding to the first five Lagrange multipliers are illustrated in Figures (6.1) through (6.5) for an eccentricity equal to the square root of 1/2. Each of these programs will maximize the change in its orbital element for a given fuel consumption during a fixed time period. In general, each program will also produce changes in the other orbital elements.

The optimum program for changing semimajor axis is illustrated in Figure (6.1). For this program the primer vector is always directed along the velocity vector and its magnitude is proportional to the magnitude of the velocity. The locus of the tip of the primer vector will describe a circle, as this circle is known to be the hodograph of the velocity vector for Keplerian motion. The primer vector will have a stationary maximum at periapsis and a minimum at apoapsis. At an eccentricity of zero, the primer vector will remain constant in magnitude as it moves around the circular orbit. As the eccentricity goes to unity, the magnitude of the primer vector at periapsis will approach infinity. If this magnitude is constrained to be finite then the primer vector will consist of a discontinuous function having finite magnitude at periapsis and being zero everywhere else.

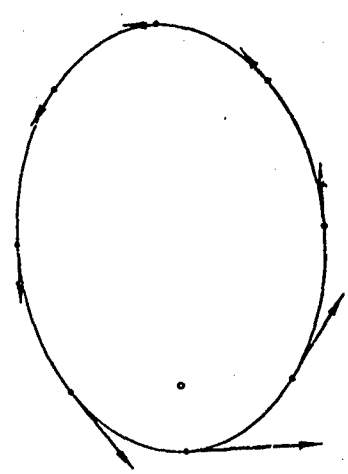

Fig. (6.1) Optimum thrust program for change in a (e = 0.707).

The optimum thrust program for changing eccentricity is illustrated in Figure (6.2). This program always has two equal maxima at apoapsis and at periapsis for all eccentricities. The primer vector solution corresponding to this Lagrange multiplier on a coasting arc allows for two impulse transfers with this coasting arc in between the two impulses. The direction of the thrust always approximates the direction of the semiminor axis of the ellipse. For small eccentricities, there is relatively little variation in the magnitude of the acceleration. At an eccentricity of unity, the magnitude of the acceleration vector varies linearly from zero at the origin to its maximum value at apoapsis. Like the semimajor axis program at unit eccentricity there is also an isolated value at periapsis which in this case is equal to the value of the primer vector at apoapsis. For this eccentricity of unity, the thrust is directed exactly at right angles to the major axis.

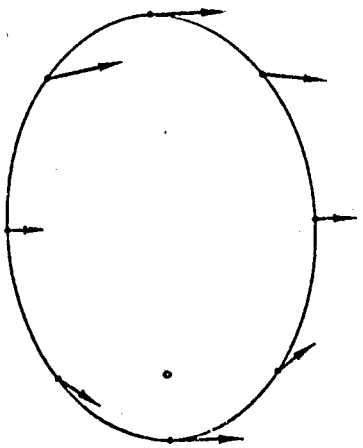

Fig. (6.2) Optimum thrust program for change in e(e = 0.707).

The optimum thrust program for rotating the orbit in its own plane is shown in Figure (6.3). In this case, the primer vector also has two equal maxima which constitute possible locations for impulses in the impulsive problem. These maxima occur in the vicinity of the semiminor axis and are exactly at the semiminor axis for eccentricities of zero and one. For an eccentricity of zero, this program is the same as the program for changing eccentricity but is moved 90^{o} around the orbit. For an eccentricity of unity the thrust is directed at right angles to the major axis instead of lying close to it. At this eccentricity, the acceleration program varies smoothly from zero at apoapsis and periapsis to a maximum at the semiminor axis. At this eccentricity, this program is the same as the program for rotating the orbit around the latus rectum except that it lies in the plane of the orbit.

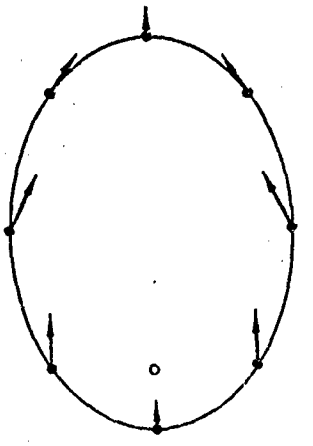

Fig (6.3) Optimum thrust program for change in θ ($e = 0.707$).

Figure (6.4) shows the optimum program for rotating the orbit around the semimajor axis. In this case, the magnitude of the primer vector is proportional to its perpendicular distance from the latus rectum. Figure (6.5) shows the primer vector solution for rotating the orbit around the latus rectum. In this case, the magnitude of the primer vector is proportional to the perpendicular distance from the major axis.

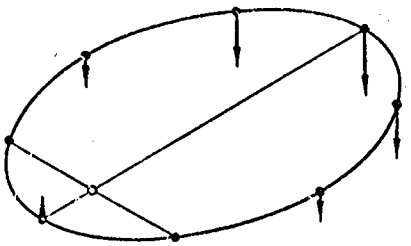

Fig. (6.4) Optimum thrust program for change in α (e = 0.707).

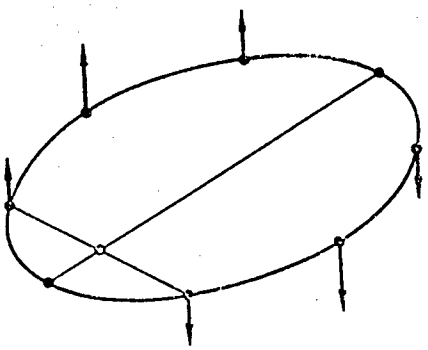

Fig. (6.5) Optimum thrust program for change in β (e = 0.707).

The sixth thrust program, the program for changing the mean anomaly, is a combination of three programs, the program for rotating the orbit in its own plane, a purely radial program whose magnitude is proportional to radius and the semimajor axis program with a linear time variation superimposed upon it. Because of the change in the semimajor axis program with time, this is the only program that will not be periodic and will not repeat itself.

6.2 Integration of the Equations

The correct first order terms for the rates of change of all elements except the mean anomaly may be found by simply substituting Eqs. (6.12) through (6.14) into Eqs. (6.2) through (6.6) and integrating. For these integrations the orbit elements are taken as the elements of the unperturbed ellipse. The independent variable used for the integrations is the eccentric anomaly of the unperturbed orbit. The first order perturbations in semimajor axis produce first order perturbations in mean anomaly so that Eq. (6.15) must be used to calculate the perturbations in the mean anomaly. The double integration implied by this equation may be avoided by rewriting the perturbation in semimajor axis in terms of the identity of Eq. (6.16).

$$\frac{dM}{dt} \approx \sqrt{\frac{\gamma}{a^3}} - \frac{3}{2}\sqrt{\frac{\gamma}{a^5}}\,\Delta a + \sqrt{\frac{a}{\gamma}}\,\frac{F_r(f_4 f_5^2 - 2ef_3^2) - F_\theta f_1 f_5(f_3 + f_5^2)}{mef_3} \tag{6.15}$$

$$\Delta a = \frac{d(t\Delta a)}{dt} - t\,\frac{da}{dt} \tag{6.16}$$

The integration of the equations of motion with the optimum thrust program is straight forward and results in Eqs. (6.17) through (6.24). The various integrals occuring in these integrations are expressed by the Φ functions given following Eq. (6.24).

$$\Delta a = \lambda_a \Phi_{aa} + \lambda_e \Phi_{ae} + \lambda_\theta \Phi_{a\theta} + \lambda_M \Phi_{aM} \tag{6.17}$$

$$\Delta e = \lambda_a \Phi_{ae} + \lambda_e \Phi_{ee} + \lambda_\theta \Phi_{e\theta} + \lambda_M \Phi_{eM} \tag{6.18}$$

$$\Delta_\theta = \lambda_a \Phi_{a\theta} + \lambda_e \Phi_{e\theta} + \lambda_\theta \Phi_{\theta\theta} + \lambda_M \Phi_{\theta M} \tag{6.19}$$

$$\Delta\alpha = \lambda_\alpha \Phi_{\alpha\alpha} + \lambda_\beta \Phi_{\alpha\beta} \tag{6.20}$$

$$\Delta\beta = \lambda_\alpha \Phi_{\alpha\beta} + \lambda_\beta \Phi_{\beta\beta} \tag{6.21}$$

$$M = \sqrt{\frac{\gamma}{a^3}}\, t + \lambda_a \Phi_{aM} + \lambda_e \Phi_{eM} + \lambda_\theta \Phi_{\theta M} + \lambda_M \Phi_{MM} - \frac{3}{2}\sqrt{\frac{\gamma}{a^5}}\, t\Delta a \tag{6.22}$$

$$J = \frac{1}{2}(\lambda_a \Delta a + \lambda_e \Delta e + \lambda_\theta \Delta_\theta + \lambda_\alpha \Delta\alpha + \lambda_\beta \Delta\beta + \lambda_a \lambda_M \Phi_{aM} + \lambda_e \lambda_M \Phi_{eM} + \lambda_\theta \lambda_M \Phi_{\theta M} + \lambda_M^2 \Phi_{MM}) \tag{6.23}$$

$$t = \sqrt{\frac{\gamma}{a^3}}\,(E - e \sin E - M^o) \tag{6.24}$$

$$\Phi_{aa} = \left(a^9/\gamma^3\right)^{1/2} 4[E + e \sin E]_{E_o}^{E}$$

$$\Phi_{ac} = \left(a^7/\gamma^3\right)^{1/2} 4(1 - e^2)\,[\sin E]_{E_o}^{E}$$

$$\Phi_{a\theta} = -\left(\frac{a^7}{\gamma^3}\right)^{1/2} 4\frac{(1 - e^2)^{1/2}}{e}\,[\cos E]_{E_o}^{E}$$

$$\Phi_{aM} = \left(\frac{a^7}{\gamma^3}\right)^{1/2} [3E^2 + 6eE \sin E + 4\frac{1 + 3e^2}{e} \cos E + e^2 \cos^2 E - 6M^o(E + e \sin E)]_{E_o}^{E}$$

$$\Phi_{ee} = \left(\frac{a^5}{\gamma^3}\right)^{1/2} (1 - e^2)\,[\frac{5}{2} E - 4e \sin E + \frac{3}{2} \sin E \cos E + \frac{e}{3} \sin^3 E]_{E_o}^{E}$$

$$\Phi_{e\theta} = \left(\frac{a^5}{\gamma^3}\right)^{1/2} (1 - e^2)^{1/2}\,[\cos E - \frac{3 - e^2}{2e} \cos^2 E + \frac{1}{3} \cos^3 E]_{E_o}^{E}$$

$$\Phi_{eM} = \left(\frac{a^5}{\gamma^3}\right)^{1/2} (1 - e^2)\,[6E \sin E + 7 \cos E + \frac{3(1 + e^2)}{2e} \cos^2 E - \frac{\cos^3 E}{3} - 6M^o \sin E]_{E_o}^{E}$$

$$\Phi_{\theta\theta} = \left(\frac{a^5}{\gamma^3}\right)^{1/2} \left[\frac{5 - 4e^2}{2e^2} E - \frac{1 - e^2}{e} \sin E - \frac{3 - 2e^2}{2e^2} \sin E \cos E - \frac{\sin^3 E}{3e}\right]_{E^o}^{E}$$

$$\Phi_{\theta M} = \left(\frac{a^5}{\gamma^3}\right)^{1/2} (1 - e^2)^{1/2} \left[- \frac{5 + 8e^2}{2e^2} E - \frac{6E \cos E}{e} + \frac{9 + e^2}{e} \sin E + \right.$$

$$\left. \frac{3 + 2e^2}{2e^2} \sin E \cos E + \frac{\sin^3 E}{3e} + \frac{6}{e} M^o \cos E\right]_{E^o}^{E}$$

$$\Phi_{\alpha\alpha} = \left(\frac{a^5}{\gamma^3}\right)^{1/2} \frac{1}{1 - e^2} \left[\frac{1 + 4e^2}{2} E - e(3 + e^2) \sin E + \frac{1 + e^2}{2} \sin E \cos E + \right.$$

$$\left. \frac{e}{3} \sin^3 E\right]_{E^o}^{E}$$

$$\Phi_{\alpha\beta} = \left(\frac{a^5}{\gamma^3}\right)^{1/2} \frac{1}{(1 - e^2)^{1/2}} \left[e \cos E - \frac{1 + e^2}{2} \cos E + \frac{e}{3} \cos^3 E\right]_{E^o}^{E}$$

$$\Phi_{\beta\beta} = \left(\frac{a^5}{\gamma^3}\right)^{1/2} \left[\frac{E}{2} - \frac{\sin E \cos E}{2} - \frac{e}{3} \sin^3 E\right]_{E^o}^{E}$$

$$\Phi_{MM} = \left(\frac{a^5}{\gamma^3}\right)^{1/2} \left[3E^3 + \frac{5 + 23e^2 + 13e^4}{2e^2} E + 9eE^2 \sin E + \right.$$

$$\frac{3}{2} e^2 E(\cos^2 E - \sin^2 E) + 12 \frac{1 + 3e^2}{e} E \cos E - \frac{17 + 46e^2 + e^4}{e} \sin E -$$

$$3 \frac{1 + e^2 + 2e^4}{2e^2} \sin E \cos E - \frac{1 - e^2 - e^4}{3e} \sin^3 E - 3M^o (3E^2 + 6eE \sin E +$$

$$\left. 4 \frac{1 + 3e^2}{e} \cos E + e^2 \cos^2 E) + 9(M^o)^2 (E + e \sin E)\right]_{E^o}^{E}$$

These equations represent a complete first order solution for optimum transfers in the neighborhood of an elliptic orbit. They are linear in both the changes and in the state and the corresponding Lagrange multipliers. By using the proper boundary conditions or transversality conditions, it is possible to solve any desired interception,rendezvous or orbit transfer problem. For interception the transversality condition is that the final value of the thrust acceleration given by Eqs. (6.12) through (6.14) must be zero. For rendezvous the initial values of all the Lagrange multipliers must be found so as to drive the terminal state deviations to zero. For orbit transfer, the transversality condition is that the Lagrange multiplier for the mean anomaly must be zero. The other five Lagrange multipliers must be determined so as to reduce the deviations in their five state variables to zero.

6.3 Secular Changes in the Orbit

While Eqs. (6.17) through (6.24) represent a complete solution of the problem they are rather complex and contain a large number of terms. If the time for rendezvous or orbit transfer is large, so that the maneuver requires many revolutions in the elliptic orbit, then the equations can be greatly simplified and an explicit solution is easily obtained. This is done by neglecting the bounded periodic terms in Eqs. (6.17) to (6.24) in comparison with the dominant secular terms to yield Eqs. (6.25) to (6.32).

$$\Delta a = \lambda_a \sqrt{\frac{a^9}{\gamma^3}}\, 4E + \lambda_M \sqrt{\frac{a^7}{\gamma^3}}\, 3E^2 \tag{6.25}$$

$$\Delta e = \lambda_e \sqrt{\frac{a^5}{\gamma^3}}\, \frac{5}{2}(1 - e^2)\, E \tag{6.26}$$

$$\Delta\theta = \lambda_\theta \sqrt{\frac{a^5}{\gamma^3}} \frac{5 - 4e^2}{2e^2} E - \lambda_M \sqrt{\frac{a^5}{\gamma^3}(1 - e^2)} \frac{5 + 8e^2}{2e^2} E \tag{6.27}$$

$$\Delta\alpha = \lambda_\alpha \sqrt{\frac{a^5}{\gamma^3}} \frac{1 + 4e^2}{2(1 - e^2)} E \tag{6.28}$$

$$\Delta\beta = \lambda_\beta \sqrt{\frac{a^5}{\gamma^3}} \frac{E}{2} \tag{6.29}$$

$$M = E - \lambda_a \sqrt{\frac{a^7}{\gamma^3}} 3E^2 - \lambda_\theta \sqrt{\frac{a^5}{\gamma^3}(1 - e^2)} \frac{5 + 8e^2}{2e^2} E - \lambda_M \sqrt{\frac{a^5}{\gamma^3}} \frac{3}{2} E^3 \equiv E - \Delta M \tag{6.30}$$

$$2J = \lambda_a^2 \sqrt{\frac{a^9}{\gamma^3}} 4E + \lambda_a \lambda_M \sqrt{\frac{a^7}{\gamma^3}} 6E^2 + \lambda_e^2 \sqrt{\frac{a^5}{\gamma^3}} \frac{5}{2}(1 - e^2) E + \lambda_\theta^2 \sqrt{\frac{a^5}{\gamma^3}} \frac{5 - 4e^2}{2e^2} E$$
$$- 2\lambda_\theta \lambda_M \sqrt{\frac{a^5}{\gamma^3}(1 - e^2)} \frac{5 + 8e^2}{2e^2} E + \lambda_\alpha^2 \sqrt{\frac{a^5}{\gamma^3}} \frac{1 + 4e^2}{2(1 - e^2)} E + \lambda_\beta^2 \sqrt{\frac{a^5}{\gamma^3}} \frac{E}{2} + \lambda_M^2 \sqrt{\frac{a^5}{\gamma^3}} 3E^3 \tag{6.31}$$

$$t = \sqrt{\frac{a^3}{\gamma}} E \tag{6.32}$$

For rendezvous or orbit transfer, the Lagrange multipliers that satisfy the boundary value problem are easily determined and the payoff may be written directly in terms of the changes in the elements and the total transfer time.

$$J = \frac{\gamma}{2at'} \left[\frac{\Delta a^2}{4a^2} + \frac{2}{5} \frac{\Delta e^2}{1 - e^2} + \frac{2(1 - e^2)\Delta\alpha^2}{1 + 4e^2} + 2\Delta\beta^2 \right]$$
$$+ \frac{2a^2}{3} \frac{(\Delta M - \Delta M^*)^2}{(t')^3} \tag{6.33}$$

$$\Delta M^* \equiv -\frac{3}{4}\sqrt{\frac{\gamma}{a^5}}\, t' \Delta a - \sqrt{1-e^2}\,\frac{5+8e^2}{5-4e^2}\,\Delta\theta \qquad (6.34)$$

If only long time-orbit transfer is considered, all the cross product terms in Eqs. (6.25) through (6.32) disappear. The thrust program corresponding to the Lagrange multiplier for each orbit element not only maximizes the rate of change of that element, but produces no change in the other four elements. This particular set of orbit elements was chosen because they have this orthogonality property. Not all sets of orbit elements will have this property.

Equations (6.12) through (6.14) show that there are no secular changes in the thrust acceleration programs for orbit transfer. The averaged thrust acceleration will, therefore, remain constant from revolution to revolution, and the orbit elements will,on the average, change linearly with time.

For rendezvous problems the final value of the mean anomaly, the sixth orbit element must be considered. Equation (6.33) represents the fuel requirement for changing all six elements over long time periods. The quantity ΔM^* defined by Eq. (6.34) represents the perturbation in the mean anomaly produced by the thrust programs for changing semimajor axis and for rotating the semimajor axis in its own plane. The fuel required to change the mean anomaly depends upon the square of the difference between the desired perturbation and this particular perturbation. The thrust program that produces the desired perturbation in the mean anomaly is the semimajor axis program of Figure (6.1) with an averaged thrust acceleration that is a linear function of time. The terms involving λ_M in Eq. (6.12) and (6.13) have a negligable effect on long-time motion but are significant for short time rendezvous. Since Eq. (6.33) holds only in the case of long time motion, the mean

anomaly term of Eq. (6.33) will generally be negligable compared to the terms in brackets because it is inversely proportional to time cubed. The fuel required for rendezvous will be only slightly greater than the fuel required for orbit transfer for these long-time cases.

CHAPTER 7: OPTIMUM POWER-LIMITED ORBIT TRANSFER IN STRONG GRAVITY FIELDS

7.1 Integrals of Motion

In section 6.3 of the previous chapter, the secular rates of change of the orbit elements in the presence of small perturbing thrusts were determined. In the present chapter, these rates of change of the orbit elements will be integrated over many revolutions to determine the optimum sequence of orbit elements between the initial orbit and the final orbit. The changes in the orbit elements will no longer be assumed to be small, but the rates of change of the orbit elements due to a small perturbing thrust will be assumed to be small. Only the first order terms in the equations of motion will be considered. The analysis is an application of what is known as Kryloff Bogoliuboff averaging. The errors of this type of averaging will be on the order of the square of the ratio of the thrust acceleration to the acceleration of gravity. For typical electric propulsion systems with accelerations of about 10^{-4} g's, the error in this approximation will be on the order of 1 percent at about 10 earth radii.

Using the results of section 6.3 of the previous chapter an averaged Hamiltonian may be written as Eq. (7.1).

$$\tilde{H} = \frac{a}{2\gamma}\left[4\lambda_a^2 a^2 + \frac{5}{2}\lambda_e^2(1-e^2) + \frac{5-4e^2}{2e^2}\lambda_\theta^2 + \frac{1+4e^2}{2(1-e^2)}\lambda_\alpha^2 + \frac{1}{2}\lambda_\beta^2\right] \qquad (7.1)$$

For this Hamiltonian the Lagrange multiplier for the mean anomaly has been assumed to be zero as only orbit transfer and not rendezvous will be treated. The Lagrange

multipliers for the angular variables in Eqs. (7.1) may be expressed in terms of the Lagrange multipliers of the conventional Euler angles by Eqs. (7.2), (7.3), and (7.4).

$$\lambda_\theta = \lambda_\omega \tag{7.2}$$

$$\lambda_\alpha = \beta_1 = \lambda_i \cos \omega + \lambda_\Omega \sin \omega \csc i - \lambda_\omega \sin \omega \cot i \tag{7.3}$$

$$\lambda_\beta = \beta_2 = -\lambda_i \sin \omega + \lambda_\Omega \cos \omega \csc i - \lambda_\omega \cos \omega \cot i \tag{7.4}$$

The use of the conventional Euler angles will allow large rotations to be treated. It should be noted that λ_α and λ_β are the same as the quantities β_1 and β_2 of Eq. (5.32). The vector integral given by Eqs. (5.44) through (5.48) of Chapter 5 apply also for the present problem.

It is convenient to replace the eccentricity by a new variable φ defined as the arc sign of the eccentricity, Eq. (7.5). Its corresponding Lagrange multiplier is given by Eq. (7.6)

$$\varphi \equiv \sin^{-1} e \tag{7.5}$$

$$\lambda_\varphi = \lambda_e \sqrt{1 - e^2} \tag{7.6}$$

In terms of this new variable, the averaged Hamiltonian is now given by Eq. (7.7).

$$\tilde{H} = \frac{a}{2\gamma} \; 4\lambda_a^2 a^2 + \frac{5}{2}\lambda_\varphi^2 + \frac{1 + 5\cot^2\varphi}{2}\lambda_\theta^2 + \frac{1 + 5\tan^2\varphi}{2}\lambda_\alpha^2 + \frac{1}{2}\lambda_\beta^2 \tag{7.7}$$

It should be noted that the rates of change of the semimajor axis and the variables φ and β are independent of the eccentricity. Only the rates of change of the rotations around the major axis and in the orbit plane depend upon the eccentricity. By averaging the Hamiltonian of Chapter 5, another integral given by Eq. (7.8) is obtained.

$$\tilde{H} = \frac{\tilde{\lambda}^2}{2} = \text{const.} \tag{7.8}$$

This integral may also be obtained by noting that the Hamiltonian is independent of the independent variable, time. This implies that the averaged value of the square of the thrust acceleration is a constant throughout the motion. Equation (7.8) may be immediately integrated to determine an integral for the payoff given by Eq. (7.9).

$$J = \tilde{H}\, t \tag{7.9}$$

Because the averaged acceleration is a constant, the cost increases linearly with time. Another integral may be found by averaging Eq. (5.18) and (5.49) to yield the results given by Eq. (7.10).

$$\lambda_a a = \lambda_a^o a^o - \tilde{H}\, t = \lambda_a^o a^o - J \tag{7.10}$$

Another integral may be found by writing down the rates of change of the semimajor axis and its Lagrange multiplier. The averaged Hamiltonian possesses the conventional canonical equations in terms of the averaged values of the orbit elements and their Lagrange multipliers.

$$\frac{da}{dt} = 4\lambda_a \frac{a^3}{\gamma} \tag{7.11}$$

$$\frac{d\lambda_a}{dt} = -\frac{\tilde{H}}{a} - \frac{4\lambda_a^2 a^2}{\gamma} \tag{7.12}$$

By dividing Eq. (7.12) by (7.11) these equations may be integrated to yield Eqs. (7.13) and (7.14)

$$\lambda_a^2 = \frac{\tilde{H}\gamma}{2a^3} - \frac{\tilde{H}\gamma - 2\lambda_a^{o2} a^{o3}}{2a^o a^2} \tag{7.13}$$

$$\frac{a^o}{a} = 1 - \frac{4\lambda_a^o a^{o2} t}{\gamma} + \frac{2a^o \tilde{H} t^2}{\gamma} \tag{7.14}$$

Equation (7.10) may be verified directly from these equations. The notation x^{on} is defined as the initial value of x raised to the n th power.

The explicit solution for the semimajor axis and its Lagrange multiplier allows the elimination of these variables and the reduction of the problem from a five-dimensional problem to a four-dimensional problem. In order to do this, it is convenient to rewrite Eq. (7.7) in terms of the rates of change of the orbital elements rather than in terms of the Lagrange multipliers. The equations of motion such as Eq. (7.11), may be solved for their Lagrange multipliers in terms of the rate of change of the corresponding orbital element. This can easily be done in the present case because of the lack of cross-product terms to yield Eq. (7.15).

$$\tilde{H} = \frac{\gamma}{2a}\left[\frac{\dot{a}^2}{4a^2} + \frac{2}{5}\dot{\psi}^2 + \frac{2\dot{\theta}^2}{1+5\cot^2} + \frac{2\dot{\alpha}^2}{1+5\tan^2} + 2\dot{\beta}^2\right] \tag{7.15}$$

A new payoff variable ψ whose rate of change is defined by Eq. (7.16) is now introduced.

$$\dot{\psi}^2 \equiv \frac{\dot{\varphi}^2}{5} + \frac{\dot{\theta}^2}{1+5\cot^2} + \frac{\dot{\alpha}^2}{1+5\tan^2} + \dot{\beta}^2 \tag{7.16}$$

It will now be possible to separate the original optimization problem into two parts. The first part is to determine the cost for given changes in the semimajor axis and ψ. The second part will be to minimize ψ for given changes in the remaining four orbit elements. Eq. (7.16) shows that this second problem may be interpreted geometrically as the problem of determining a minimum length trajectory or geodesic in a four-dimensional orbit element space.

In terms of this new variable, the Hamiltonian of Eq. (7.7) is now given by Eq. (7.17).

$$\tilde{H} = \frac{a}{2\gamma}\left[4\lambda_a^2 a^2 + \frac{\lambda_\psi^2}{2}\right] \tag{7.17}$$

The rate of change of ψ is given by Eq. (7.18) where it should be noted that λ_ψ is a constant.

$$\dot{\psi} = \frac{\lambda_\psi a}{2\gamma} \tag{7.18}$$

Equation (7.18) may be integrated by use of Eq. (7.12) and (7.13) to yield Eq. (7.19).

$$\sqrt{\frac{a}{a^o}} = \cos\sqrt{2}\psi + \sqrt{8}\,\frac{\lambda_a^o a^o}{\lambda_\psi}\sin\sqrt{2}\psi \tag{7.19}$$

The constants of Eqs. (7.19) and (7.14) may be eliminated to determine the payoff explicitly in terms of the initial and final values of the semimajor axis and the total change in ψ, Eq. (7.20).

$$J = \frac{2}{t}\left[\frac{\gamma}{a^o} - \frac{2\gamma\cos\sqrt{2}\psi}{\sqrt{a^o a}} + \frac{\gamma}{a}\right] \tag{7.20}$$

This equation has an interesting physical interpretation. The cost is the same as the cost of transfering in field free space from the mean orbital velocity of the initial orbit to the mean orbital velocity of the second orbit with an angle of the $\sqrt{2}\psi$ between the

two velocity vectors. By the definition of ψ this will provide a complete solution for problems where the eccentricity is changed but there is no rotation of the elliptic orbit. In such problems, the variable ψ will be equal to the total change in the orbit element φ divided by $\sqrt{5}$.

7.2 Coplanar and Coaxial Transfers

It is possible to solve the four-dimensional problem of minimizing ψ in terms of the remaining four-orbital elements explicitly. However, the solution of this general orbit transfer problem is rather complex and only 2 two-dimensional problems will be considered in this chapter. These two problems are the important cases of coplanar and coaxial transfers. In both cases there is only a rotation around a single axis. In the coplanar case, the rotation is around an axis perpendicular to the orbit plane. In the coaxial case the rotation is around the major axis of the orbit. The coplanar and coaxial cases are obtained from the general case by means of the following definitions.

Coplanar

$$\theta = \omega \qquad \lambda_\theta = \lambda_\omega$$

$$i \equiv 0 \qquad \lambda_\alpha \equiv 0$$

$$\Omega \equiv 0 \qquad \lambda_\beta \equiv 0$$

Coaxial

$$\omega \equiv 0 \qquad \lambda_\theta \equiv 0$$

$$i = \alpha \qquad \lambda_\alpha = \lambda_i$$

$$\Omega \equiv 0 \qquad \lambda_\beta \equiv 0$$

Because of the particular form of the Hamiltonian, Eq. (7.7), the coplanar and coaxial cases can be transformed into one another so that it is only necessary to solve one of these problems to obtain the solution of both. The following transformation equations will take the solution of one problem into the solution of the other problem.

Coplanar		Coaxial
a	$\longleftrightarrow$	a
φ	$\longleftrightarrow$	$\varphi - \pi/2$
ω	$\longleftrightarrow$	i
$i \equiv 0$	$\longleftrightarrow$	$\omega \equiv 0$
$\Omega \equiv 0$	$\longleftrightarrow$	$\Omega \equiv 0$

The Hamiltonian for the coplanar problem is given by Eq. (7.21).

$$\tilde{H} = \frac{a}{2\gamma}\left[4\lambda_a^2 a^2 + \frac{5}{2}\lambda_\varphi^2 + \frac{1 + 5\cot^2\varphi}{2}\lambda_\omega^2\right] \tag{7.21}$$

The equations of motion and the Euler Lagrange equations are given by Eqs. (7.22) through (7.25).

$$\dot{\varphi} = \frac{5}{2}\frac{\gamma}{a}\lambda_\varphi \tag{7.22}$$

$$\dot{\omega} = \frac{1 + 5\cot^2\varphi}{2}\frac{\gamma}{a}\lambda_\omega \tag{7.23}$$

$$\dot{\lambda}_\varphi = \frac{5}{2}\frac{\gamma}{a}\cot\varphi\csc^2\varphi\,\lambda_\omega^2 \tag{7.24}$$

$$\dot{\lambda}_\omega = 0 \tag{7.25}$$

A first integral of these equations may be obtained from the constancy of λ_ψ as Eq. (7.26).

$$\lambda_\varphi^2 = \lambda_\varphi^{02} + \lambda_\omega^2(\cot^2\varphi^0 - \cot^2\varphi) \tag{7.26}$$

Dividing Eq. (7.23) by Eq. (7.22) and utilizing Eq. (7.26), Eq. (7.27) is obtained.

$$\dot{\omega} = \frac{(1 + 5\cot^2\varphi)\lambda_\omega}{5\sqrt{\lambda_\varphi^{02} + \lambda_\omega^2\cot^2\varphi^0 - \lambda_\omega^2\cot^2\varphi}}\dot{\varphi} \tag{7.27}$$

Equation (7.27) is readily integrated to yield Eq. (7.28).

$$\omega = \left[\cos^{-1}\left(\frac{\cot\varphi}{\cot k_1}\right) - \frac{4}{5}\sin k_1 \cos^{-1}\left(\frac{\cos\varphi}{\cos k_1}\right)\right]_{\varphi^0}^{\varphi} \tag{7.28}$$

The variable k_1 in Eq. (7.28) is defined by Eq. (7.29).

$$\lambda_\omega^2 \cot^2 k_1 \equiv \lambda_\varphi^{02} + \lambda_\omega^2 \cot^2\varphi^0 \tag{7.29}$$

By utilizing the definition of the rate of change of ψ given in Eq. (7.16) and integrating, Eq. (7.30) for ψ is obtained.

$$\psi = \left[\frac{\sqrt{1 + 4\cos^2 k_1}}{5}\cos^{-1}\left(\frac{\cos\varphi}{\cos k_1}\right)\right]_{\varphi^0}^{\varphi} \tag{7.30}$$

Equations (7.28) and (7.30) provide a parametric representation of the solution for ψ and ω in terms of ψ and the initial conditions on φ and the Lagrange multipliers.

$$\varphi = \varphi(\psi, \lambda_{\varphi}^{0}, \lambda_{\omega}, \varphi^{0}) \tag{7.31}$$

$$\omega = \varphi(\psi, \lambda_{\varphi}^{0}, \lambda_{\omega}, \varphi^{0}) \tag{7.32}$$

This type of representation can be explicitly solved for in the present case. The structure of the resulting extremals is shown in Fig. 7.1. The values of ω are limited to the range between 0 and π. Larger rotations need not be considered. The values of φ are limited to the range between 0 and 2π. Values of φ greater than π represent elliptic orbits having the opposite sense of rotation to the initial orbit. The direction of rotation is reversed by passing through a unit eccentricity ellipse having zero angular momentum but a finite semimajor axis.

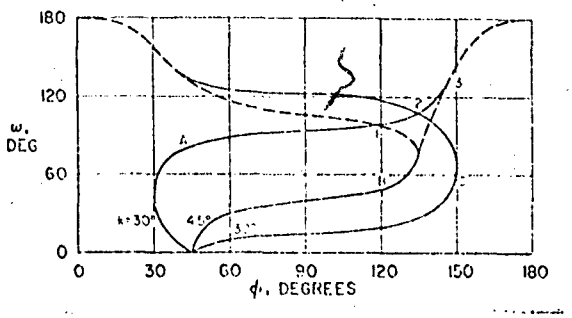

Fig. 7.1

Structure of the extremals for $\omega 0 = 45^{0}$.

If the desired terminal value of φ is also 90° there will be no change in the eccentricity during the transfer if the total change in the angle ω is less than 36°. The vertical line for $k_1 = 90^{\circ}$ in Fig. 7.2 is a minimizing extremal until it becomes tangent to the envelope at this point. Beyond 36° the ellipses decrease in eccentricity and then increase it to produce the extremals shown for other values of k_1. While this transfer is somewhat academic the corresponding coaxial transfer is the more interesting case of transfer between inclined circular orbits. For inclinations of less than 36° the orbital transfer will involve no change in the eccentricity of the intermediate orbits while for angles greater than 36° the intermediate orbits will become eccentric.

The extremals and payoff curves for two other initial values of φ, 45° and 0° are shown in Figs. 7.3 and 7.4.

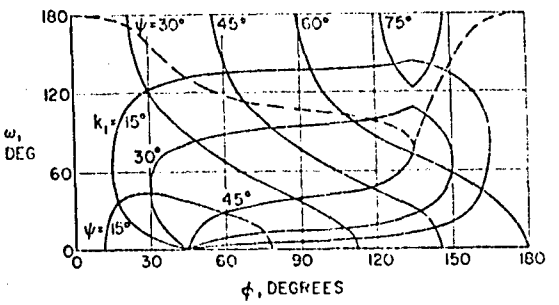

Fig. 7.3 Extremals and payoff curves for coplanar transfer with $\omega 0 = 45^{\circ}$.

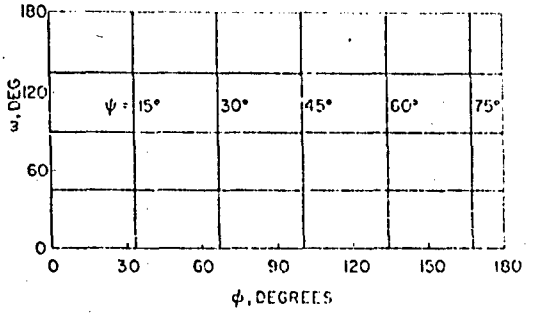

Fig. 7.4 Extremals and payoff curves for coplanar transfer in the degenerate case $\omega 0 = 0^{\circ}$.

In Figure 7.1 three sample extremals, A, B, and C, are shown representing different values of the constant k_1 for a value of φ^o of 45^o. If extremal A is followed from its start at $\psi = 0$, it will first pass through a region in which there are no other extremals which go to the same point. Up to point 1, extremal A will represent a unique solution of the boundary value problem for any point it passes through. At point 1, extremal A first crosses an envelope of extremals shown as the dotted line. Beyond point 1, there is another family of extremals such as extremal C which goes to every point along extremal A. The boundary value problem no longer has a unique solution. Between point 1 and point 2, extremal A represents the absolute minimum value of ψ to reach any point along it. At point 2, extremal A has the same cost as extremal C. A point where two extremals of different families have the same cost is known as a Darboux point. Between points 2 and 3, extremal A still represents a locally minimizing solution of the optimization problem but does not represent the absolute minimum which occurs with extremals of the other family. At point 3, extremal A first becomes tangent to the envelope of extremals. Such a point is called a conjugate point. At the conjugate point, the Jacobian of the state with respect to the initial values of the Lagrange multipliers becomes equal to 0.

$$J^{0}_{(\lambda_\varphi, \lambda_\omega)}(\varphi, \omega) \equiv \begin{vmatrix} \frac{\partial \varphi}{\partial \lambda_\varphi^0} & \frac{\partial \varphi}{\partial \lambda_\omega} \\ \frac{\partial \omega}{\partial \lambda_\varphi^0} & \frac{\partial \omega}{\partial \lambda_\omega} \end{vmatrix} = 0 \qquad (7.33)$$

If extremal A is continued beyond point 3, it ceases to be even locally minimizing. That is, there are curves in the immediate neighborhood of extremal A which will have a lower cost. At point 3, extremal A violates an additional necessary condition for optimality of the classical calculus of variations that is known as the Jacobi condition. The Jacobi condition is simply that a minimizing extremal must possess no conjugate points between its initial and final points. For problems in the classical calculus of variations where the control never lies on a boundary, the combination of the strong forms (without equality) of the maximum principle and the Jacobian condition is sufficient for an arc to be locally minimizing. It should be noted that these sufficiency conditions do not guarantee that the extremals represent an absolute minimum as is shown by the example of extremal A between points 2 and 3. On extremal C, the three points 1, 2, and 3 become coincident.

A set of extremals and constant cost lines for the minimizing extremals is shown in Fig. 7.2 for an initial value of ω of 90°.

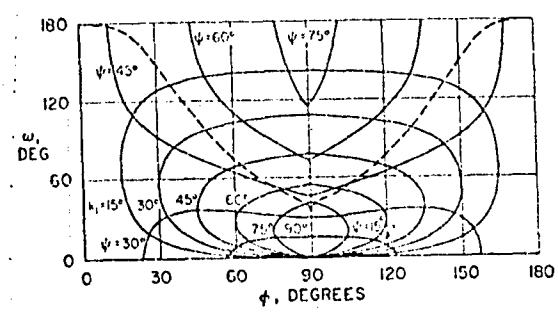

Fig. 7.2 Extremals and payoff curves for coplanar transfer with $\omega 0 = 90^{\circ}$.

In Fig. 7.4, the problem becomes degenerate because the argument of perigee of a circular orbit is undefined. In this case, the fuel consumption depends only upon the changes in eccentricity and semimajor axis between the initial and final orbits.

CHAPTER 8: LINEARIZED IMPULSIVE TRANSFER IN THE VICINITY OF A CIRCULAR ORBIT

8.1 The Primer Vector on a Circular Orbit

The conventional orbit elements used in Chapter 5 to derive the equations for the primer vector have singularities at zero eccentricity and zero inclination. It is desirable to use another set of orbit elements which is well behaved for this case to represent the primer vector on a circular orbit. One such set of orbit elements is defined by Eqs. (8.1)

$$\left.\begin{aligned} e_x &\equiv e\cos(\omega+\Omega) & e_y &\equiv e\sin(\omega+\Omega)\\ i_x &\equiv i\cos\Omega & i_y &\equiv i\sin\Omega\\ M_x &\equiv M+\omega+\Omega & E_x &\equiv E+\omega+\Omega \end{aligned}\right\} \tag{8.1}$$

For the particular case of zero eccentricity the rates of change of these orbit elements are given by Eqs. (8.2) to (8.7).

$$\frac{da}{dt} = 2\sqrt{\frac{a^3}{\gamma}}\,\frac{F_\varphi}{m} \tag{8.2}$$

$$\frac{de_x}{dt} = \sqrt{\frac{a}{\gamma}}\left(\frac{F_r}{m}\sin E_x + \frac{F_\varphi}{m}\,2\cos E_x\right) \tag{8.3}$$

$$\frac{de_y}{dt} = \sqrt{\frac{a}{\gamma}} \left(- \frac{F_r}{m} \sin E_x + \frac{F_\varphi}{m} 2 \cos E_x \right) \tag{8.4}$$

$$\frac{di_x}{dt} = \sqrt{\frac{a}{\gamma}} \frac{F_z}{m} \cos E_x \tag{8.5}$$

$$\frac{di_y}{dt} = \sqrt{\frac{a}{\gamma}} \frac{F_z}{m} \sin E_x \tag{8.6}$$

$$\frac{dM_x}{dt} = \sqrt{\frac{\gamma}{a^3}} - 2 \sqrt{\frac{\gamma}{a}} \frac{F_r}{m} \tag{8.7}$$

The primer vector in terms of this set of orbital elements is given by Eqs. (8.8) through (8.10) and the rate of change of the primer vector is given by Eqs. (8.11) through (8.13).

$$\lambda_r = \sqrt{\frac{a}{\gamma}} \left(\lambda_{e_x} \sin E_x - \lambda_{e_y} \cos E_x - 2\lambda_{M_x} \right) \tag{8.8}$$

$$\lambda_\varphi = \sqrt{\frac{a}{\gamma}} \left(2\lambda_a a + 2\lambda_{ex} \cos E_x + 2\lambda_{ey} \sin E_x \right) \tag{8.9}$$

$$\lambda_z = \sqrt{\frac{a}{\gamma}} \left(\lambda_{i_x} \cos E_x + \lambda_{i_y} \sin E_y \right) \tag{8.10}$$

$$\dot{\lambda}_r = \frac{1}{a} \left(-2\lambda_a a - \lambda_{e_x} \cos E_x - \lambda_{ey} \sin E_x \right) \tag{8.11}$$

$$\dot{\lambda}_{\varphi} = \frac{1}{a}(-\lambda_{ex} \sin E_x + \lambda_{eg} \cos E_x + \lambda_M) \tag{8.12}$$

$$\dot{\lambda}_z = \frac{1}{a}(-\lambda_{i_x} \sin E_x + \lambda_{i_y} \cos E_x) \tag{8.13}$$

As for the elliptic orbit, all the Lagrange multipliers will be constant except the Lagrange multiplier for the semimajor axis which will vary linearily with time or with the central angle. Eqs. (8.14) and (8.15).

$$\lambda_a = \lambda_a^o + \frac{3}{2}\lambda_{M_x}\sqrt{\frac{\gamma}{a^5}}(t - t^o) \tag{8.14}$$

$$\lambda_a = \lambda_a^o + \frac{3}{2}\lambda_{M_x}\frac{E_x - E_x^o}{a} \tag{8.15}$$

It is somewhat easier to visualize the behavior of the primer vector by transforming the origin of the polar coordinate system to yield Eqs. (8.16) to (8.19).

$$\lambda_r = \sqrt{\frac{a}{\gamma}}\left(\sqrt{\lambda_{ex}^2 + \lambda_{ey}^2} \sin\varphi - 2\lambda_{M_x}\right) \tag{8.16}$$

$$\lambda_\varphi = \sqrt{\frac{a}{\gamma}}(2\lambda_a^o a + 2\sqrt{\lambda_{ex}^2 + \lambda_{ey}^2} \cos\varphi + 3\lambda_{M_x}\varphi - 3\lambda_{M_x}\varphi^o) \tag{8.17}$$

$$\lambda_2 = \sqrt{\frac{a}{\gamma}}\left(\frac{\lambda_{ey}\lambda_{i_x} + \lambda_{e_x}\lambda_{iy}}{\sqrt{\lambda_{ex}^2 + \lambda_{ey}^2}} \cos\varphi + \frac{\lambda_{ex}\lambda_{iy} - \lambda_{ey}\lambda_{ix}}{\sqrt{\lambda_{ex}^2 + \lambda_{ey}^2}} \sin\varphi\right) \tag{8.18}$$

$$\varphi = E_x - \tan^{-1}\frac{\lambda_{ey}}{\lambda_{ex}} \tag{8.19}$$

This form for the primer vector on a circular orbit may be used to treat transfers between neighboring near-circular orbits. The geometric properties of the primer vector are of considerable importance in this analysis and will be illustrated in the following sections.

8.2 Time-Open Case--Nodal Solutions

For the time-open case, the Lagrange multiplier for the mean anomaly is 0 and the components of the primer vector may be written as Eqs. (8.20) through (8.22).

$$\lambda_r = \sqrt{\frac{a}{\gamma}} \sqrt{\lambda_{ex}^2 + \lambda_{ey}^2} \sin \theta \tag{8.20}$$

$$\lambda_\theta = \sqrt{\frac{a}{\gamma}} (2\lambda_a^o a + 2\sqrt{\lambda_{ex}^2 + \lambda_{ey}^2} \cos \theta \tag{8.21}$$

$$\lambda_z = \sqrt{\frac{a}{\gamma}} \frac{\lambda_{ey}\lambda_{ix} + \lambda_{ex}\lambda_{iy}}{\sqrt{\lambda_{ex}^2 + \lambda_{ey}^2}} \cos \theta + \frac{\lambda_{ex}\lambda_{iy} - \lambda_{ey}\lambda_{ix}}{\sqrt{\lambda_{ex}^2 + \lambda_{ey}^2}} \sin \theta \tag{8.22}$$

These equations represent the equations of an ellipse in three space. This ellipse is formed by the intersection of a 2:1 elliptical cylinder parallel to the λ_z axis and a plane which passes through the intersection of the cylinder axis with the $\lambda_r\lambda_\theta$ plane. A typical case is illustrated in Fig. 8.1 which also shows the projection of the ellipse on the $\lambda_r\lambda_\theta$ plane.

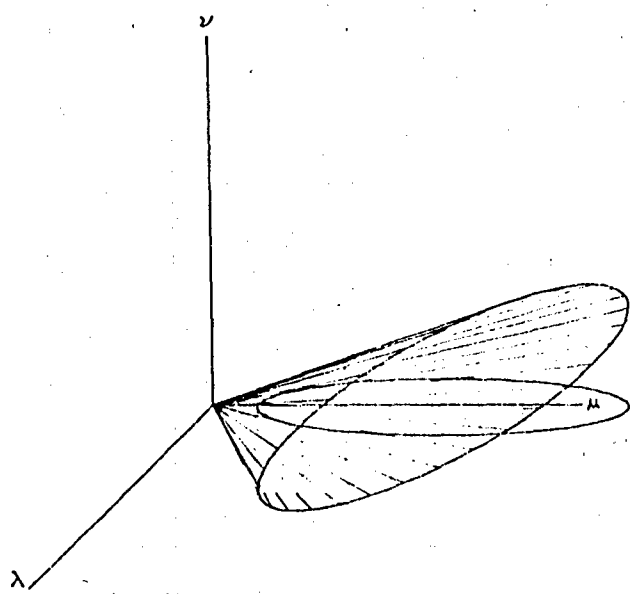

Primer Locus Diagram

Fig. 8.1

For transfers with more than one impulse, this elliptical primer locus must have more than one equal maxima. There are only three configurations of this elliptical primer locus which allow the primer vector to have more than one maximum. The first configuration, to be treated in this section, represents a family of solutions where the center of the ellipse is located at the origin. (Fig. 8.2) In this case the two equal maxima occur on the major axis of the ellipse and are separated by 180^{o}. For this case the components of the primer vector at the second impulse will be equal in magnitude but opposite in sign to the components of the primer vector at the first impulse.

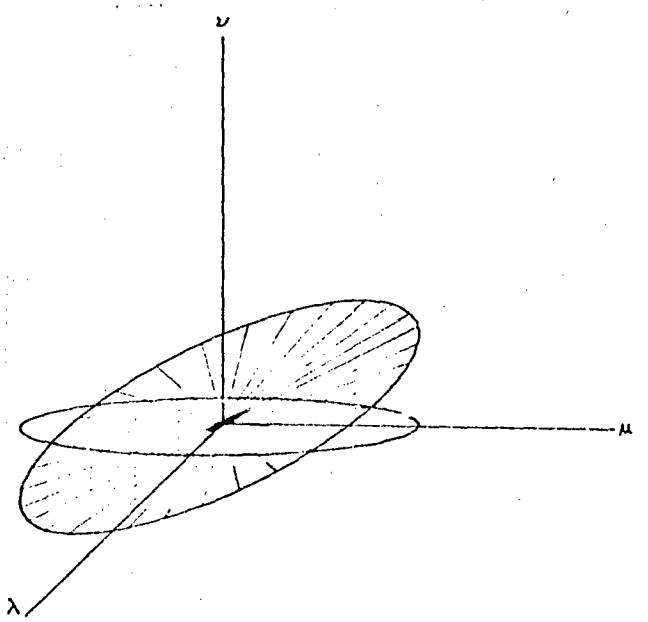

Primer Locus Diagram

Fig. 8.2

As the two impulses are separated by 180^{o}, both impulses must occur on the line of intersection or line of nodes between the initial and final orbit planes. If they do not, then the second impulse could not remove all of the inclination between the two planes. As a result, this case will be referred to as the nodal case. The total ΔV for the nodal case is given by Eq. (8.23).

$$\Delta V = \sqrt{\frac{\gamma}{a^o}} \sqrt{\Delta i^2 + \frac{\Delta e_x^2}{4} + \Delta e_y^2} \qquad (8.23)$$

It should be noted that the fuel consumption is independent of the change in semimajor axis for this case. In order for the primer vector to h ve two equal maxima for this case, the two inequalities given by Eqs. (8.24) and (8.25) must be satisfied.

$$\left(\frac{\Delta a}{a^o}\right)^2 \leq \Delta e_x^2 \qquad (8.24)$$

$$\Delta i^2 \leq 3 \Delta e_y^2 \qquad (8.25)$$

For the equations, the x axis has been assumed to be aligned with the line of nodes.

8.3 Time-Open Case: Nondegenerate Solutions

A second configuration which allows two equal maxima of the primer vector corresponds to cases where the ellipse passes through the λ_θ axis and the primer vectors again lie in single plane. (Fig. 8.3)

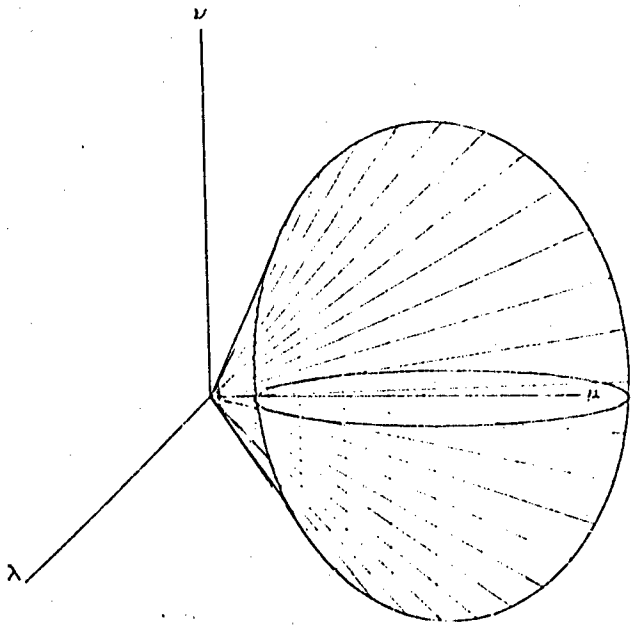

Primer Locus Diagram

Fig. 8.3

This case will be referred to as the nondegenerate case as the fuel consumption will depend upon the changes in all of the orbital elements. For this case the radial and out of plane components of the primer vector have equal and opposite values at the two impulses, while the circumferential components have equal values. For this case, the central angle is not restricted to 180^{o}. The total fuel consumption for the nondegenerate case is given by Eq. (8.26).

$$\Delta V = \sqrt{\frac{\gamma}{2a^{o}}} \sqrt{\Delta i^2 + \Delta e_x^2 + \Delta e_y^2 - \frac{\Delta a^2}{2a^{o2}} + \sqrt{(\Delta i^2 - \Delta e_x^2 - \Delta e_y^2 + \frac{\Delta a^2}{a^{o2}})^2 + 4\,\Delta i^2 \Delta e_y^2}} \tag{8.26}$$

For the primer vector to have two equal maxima for this case, the following two inequalities must be satisfied.

$$\frac{\Delta a^2}{a_o^2} \geq \Delta e_x^2 \tag{8.27}$$

$$\frac{\Delta a^2}{a_o^2} \geq \Delta e_x^2 + \Delta e_y^2 + \frac{2}{\sqrt{3}} \Delta e_y \Delta i - \Delta i^2 \tag{8.28}$$

8.4 Time-Open Case: Singular Solutions

The third configuration of the primer vector locus which allows for more than one maxima of the primer vector is a combination of the two previous cases where the primer locus passes through the λ_θ axis and where the center of the ellipse is located at the origin of the coordinate system. This particular locus is tilted so that the primer vector has unit magnitude at all points. This is an example of a singular solution where the orbital location of the impulses can not be determined from the primer vector solution. In fact, for this linear problem, the singular solution is ununique in that there are an infinite number of transfers involving different numbers and locations of impulses all of which have the same total fuel consumption. This particular locus (Fig. 8.4) is only one of two that occur for circular reference orbits.

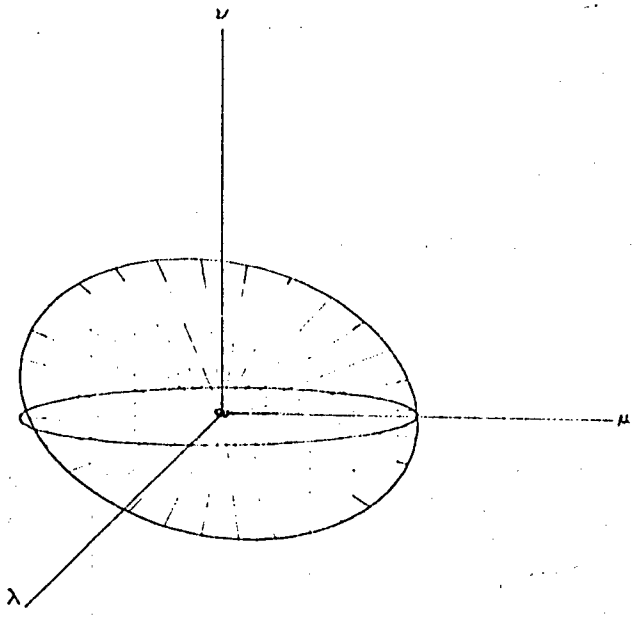

Primer Locus Diagram

Fig. 8.4

The other singular locus is a special case of the nondegenerate case where the ellipse shrinks to a point located at plus or minus one on the λ_θ axis. For the singular case illustrated in Fig. 8.4, the total ΔV is given by Eq. (8.29).

$$\Delta V = \sqrt{\frac{\gamma}{4a^o}} \sqrt{(\sqrt{3}\Delta i + \Delta e_y)^2 + \Delta e_x^2} \tag{8.29}$$

Once again, there are two inequalities which must be satisfied to distinguish the singular case from the two other cases which can occur.

The fuel consumption of the different cases is illustrated in Figs. 8.5 through 8.10. In each case, the total change in semimajor axis and eccentricity are

plotted with contours of constant values of the total change in inclination. All three elements are normalized by dividing them by the total ΔV assuming a gravitational constant of unity. The total change in inclination contours range from a numerical value of one at the origin to a value of zero at the edges of the square figures. Each contour represents a change of .05 in the normalized inclination change.

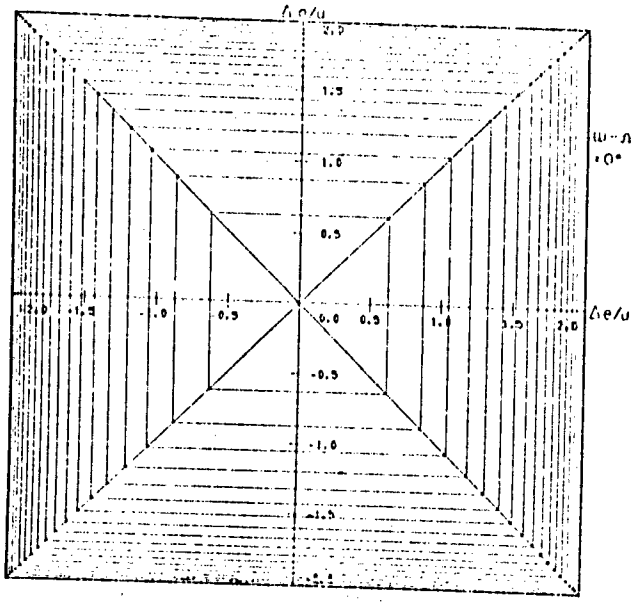

Fig. 8.5

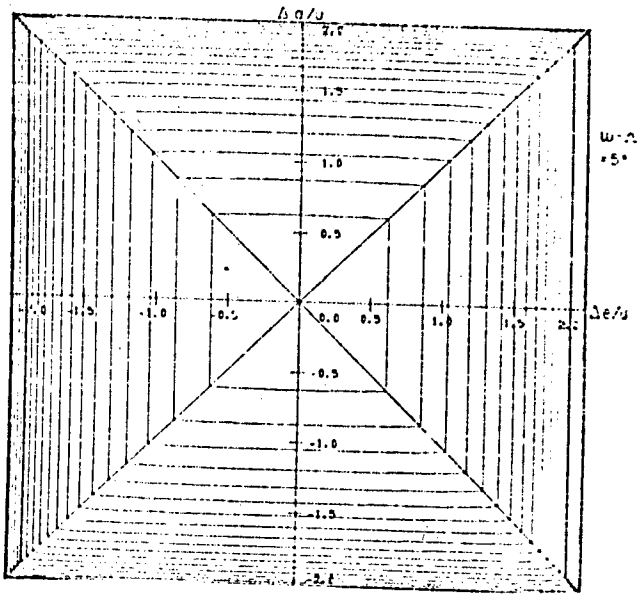

Fig. 8.6

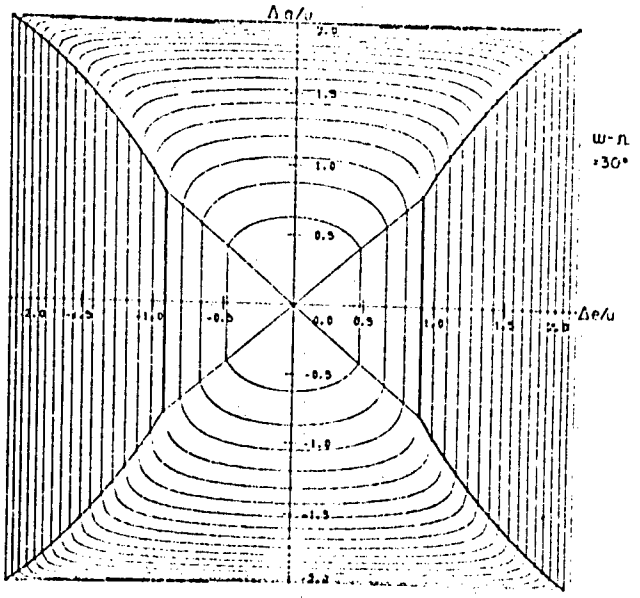

Fig. 8.7

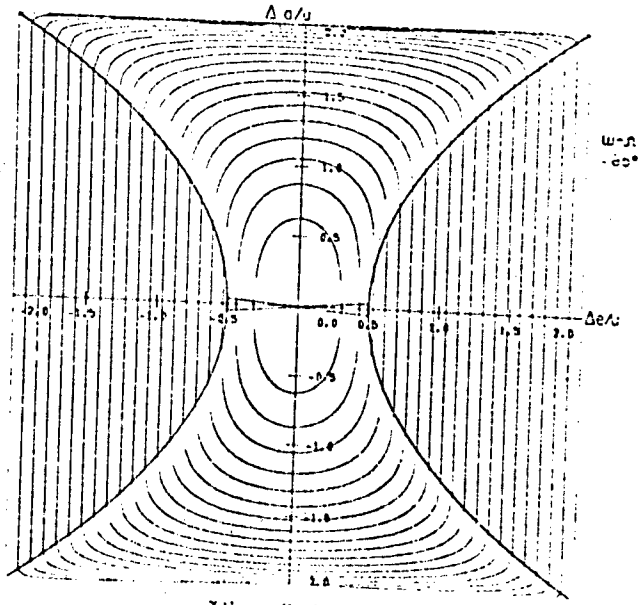

Fig. 8.8

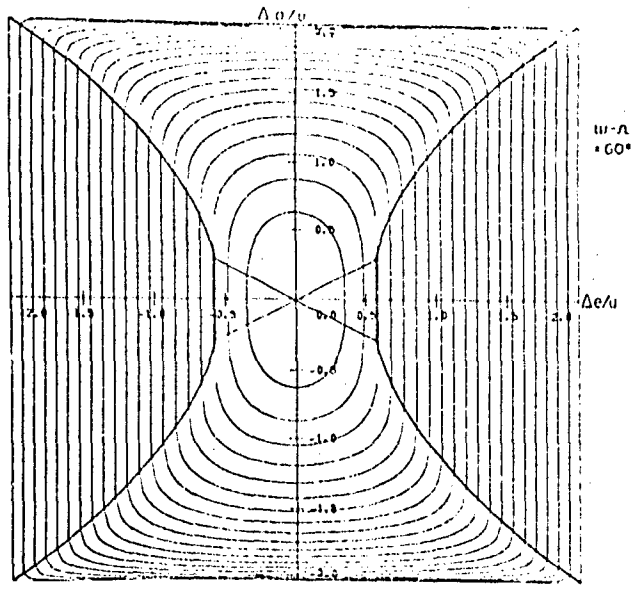

Fig. 8.9

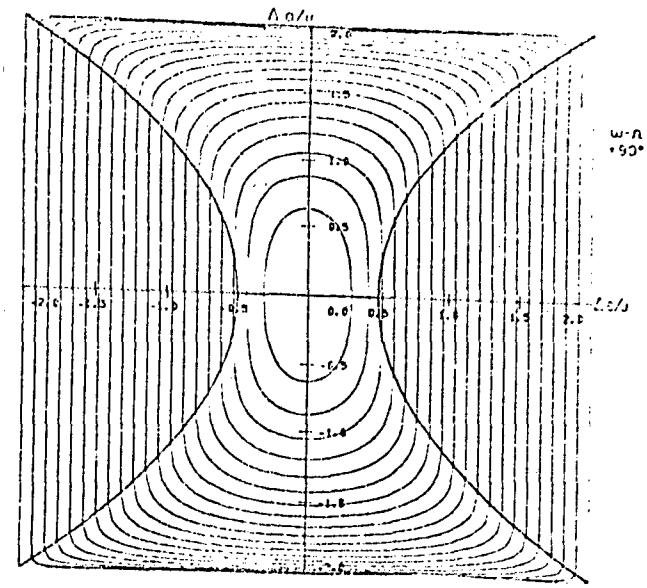

Fig. 8.10

The angular variable shown to the right of each figure represents the angle between the line of nodes and the desired direction of the change in eccentricity. In Fig. 8.5, we have the coaxial case in which the change in eccentricity is alligned with the line of nodes of the two orbits. In this case, the singular case does not arise and only the nodal case and the nondegenerate case occur. In Fig. 8.6, ther is a 5^{o} angle between the eccentricity change vector and the line of nodes and the singular case starts to appear at the left and right sides of the figure. The curves for both the singular case and the nodal case are indepdndent of the change of semimajor axis and are straight lines whereas the curves for the nondegenerate case start to develop some curvature.

As the angle between the eccentricity change vector and the line of nodes increases, the nodal region decreases and the singular region grows until in Fig. 8.10 the nodal region has completely disappeared.

8.5 Time Fixed Cases

For these cases we must return to Eqs. (8.16) through (8.18) including the Lagrange multiplier for the mean anomaly. When this term is included the elliptic locus becomes stretched out to form a cycloid-like curve in three dimensions. It is as though one took an elliptic coil of wire and stretched it out uniformly in the λ_θ direction. In this case it is possible to have transfers with up to six impulses in the three dimensional case and up to four impulses in the two dimensional case. There is a general result that linear transfers require a number of impulses no greater than the number of states. In the time-open case this means that transfers between neighboring near-circular orbits may require up to five impulses. However, these cases, in fact, require no more than two impulses even in the singular case. However for time-fixed rendezvous, it is easy to construct two dimensional transfers which use the maximum number of four impulses. Three dimensional transfers which use the maximum number of six impulses have been determined by Marec and by Breakwell.

For the two dimensional case, Prussing has considered the four impulse transfers and has shown that all of these transfers have symmetry properties. He constructs these transfers by taking the two dimensional cycloid-like locus and drawing a circle which is tangent to the locus at two points. As long as these tangencies produce local maxima of the primer vector, he has determined the stationary interior maxima of the primer vector. The next intersections of the circle with the primer locus yield the nonstationary terminal maxima of the primer vector. Prussing has shown that these solutions exist with both odd and even numbers of loops of cycloid-like curves included in the circle. The single loop transfers even exist for transfer angles slightly below 180°.

Prussing further considered the fixed time rendezvous between neighboring circular orbits. He found that these rendezvouses may require four impulses, three impulses with initial of final coast periods; three impulses, two impulses with an initial or final coast period and two impulses. There is also a class of singular cases corresponding to the coplanar singular case which may have any distribution of impulses and coasts. His results show that the structure of the minimum fuel rendezvous solutions in even this simple case is very complex. The extensions of this work to some special three-dimensional cases by Breakwell and by Maree show that the extra dimension adds proportionally to the complexity of the solutions.

CHAPTER 9: OPTIMUM IMPULSE TRANSFER IN AN INVERSE SQUARE FIELD

9.1 Time Open Transfer Between Coplanar, Coaxial Ellipses

There are four different classes of coplanar, coaxial transfer problems depending upon whether the ellipses intersect or not and upon whether the apoapsis of the ellipses point in the same or opposite directions. If the orbits intersect, then the optimum transfer is always a Hohmann transfer from the highest apsis to the opposite apsis. For the intersecting orbit case one impulse will always be an accelerating impulse and the other impulse will always be a decelerating impulse. The primer vector solution corresponding to this transfer is the solution corresponding to the Lagrange multiplier for the eccentricity in Chapter 6. These two-impulse transfers must be compared with a transfer that goes out to infinity and comes back again. If the axes are aligned, then the optimum transfer via infinity will be via two parabolas which are tangent to the periapses of the two ellipses. Transfer from the first to the second parabola is via an infinitessimal impulse at infinity. If the orbits are not aligned, the same two transfer parabolas to infinity are used but these parabolas must be connected by an elliptic orbit at infinity. Marchal has given a number of results which indicate whether the optimal transfer is a two impulse transfer or via infinity.

If the orbits are non-intersecting and the axes are aligned, the optimal two-impulse transfer is again from the highest apsis to the opposite apsis of the second ellipse. If the orbits are non-intersecting and the apses are opposed, then the Hohmann transfer from either apsis of the outer orbit must be considered to determine the true

optimum two-impulse transfer. The primer vector solution corresponding to the non-intersecting case has both impulses either accelerating or decelerating the velocity and has a primer vector solution corresponding to the Lagrange multiplier for the semi-minor axis. Once again there is a three impulse transfer via infinity (the bi-elliptic transfer) if the axes are aligned, and a four impulse transfer via infinity if the axes are not aligned. For the aligned case, the optimal transfer is always through infinity if the ratio of the two periapsis radii is greater than 11.938 and is always two impulse Hohmann if the ratio of these periapsis radii is less than nine.

9.2 Time Open Transfer Between Non-Coplanar Coaxial Ellipses

As for the coplanar case, all of the impulses for coaxial transfer should be on the line of apsides (which is also the line of nodes) and should have no radial components. In the non-planar case, there is an additional type of transfer possible which does not occur in the planar case. Namely, a three impulse transfer where the third impulse is giving at a finite radius. One important class of transfers for which the finite radius three-impulse transfer is always optimal is for transfer between circular orbits of the same radius for inclination angles between zero and 60.185 degrees. Marchal has once again given a number of rules for determining whether the transfer should be a two impulse transfer, a three impulse transfer with a finite periapsis radius or a transfer via infinity. For all of the transfer most of the inclination change is done at the largest apoapsis radius. The other impulses always lie within about six degrees of the orbit plane of the initial and final ellipse. The optimum inclination change for each of the impulses can readily be determined either from the primer vector solution or from an analysis by Sun which reduces the problem to the well known spider fly problem.

9.3 Time Open Transfer Between Coplanar Ellipses

Time open transfer between coplanar but non-coaxial ellipses fall into three different categories. Two impulse transfers, three impulse transfers with all impulses occurring at finite radii, and transfers via infinity. The three impulse transfers occur rarely and only for highly eccentric initial and final ellipses over a small range of orientation angles. The two impulse transfers are of two different families. One family has both impulses either increasing or decreasing the energy. For this family both impulses occur on one side of the major axis of the transfer ellipse. The limiting members of this family are the Hohmann transfer whose primer vector solution corresponds to the Lagrange multiplier for the semi-minor axis and which has a transfer angle of 180°; and the primer vector solution corresponding to the Lawden spiral which has a transfer angle of 0°. The other family of two impulse transfers has one impulse being an accelerating impulse and the other impulse being a decelerating impulse. For this family, the two impulses lie on the opposite sides of the semi-major axis of the transfer ellipse and the transfer angle is always in the vicinity of 180°. The limiting members of this family of two impulse transfers are the reverse Hohmann transfer corresponding to the Lagrange multiplier for eccentricity and the symmetric transfer corresponding to the Lagrange multiplier for changing the argument of perigee.

At every point on the ellipse there is only a small range of angles in between the local horizontal and the local direction of the velocity vector in which impulses may be directed for an optimal transfer. The limiting values of this set are deter-

mined by the members of the two different families of two impulse transfers mentioned in the last paragraph. A single impulse transfer from the initial ellipse or onto the final ellipse from the transfer ellipse must lie within this range of useful angles. For all eccentricities below a critical eccentricity of 0.925 there is a positive range of useful angles at every point on the ellipse. Above this critical eccentricity, there is a range of positions between periapsis and the semi-minor axis for which there is no positive range of useful angles and which cannot be employed in optimal transfer. Above this critical eccentricity it is possible to have transfers between the two different families of two impulse transfers so that infinitessimal three impulse transfers in the vicinity of these highly eccentric ellipses become possible. At an eccentricity of unity, the range of forbidden positions where no optimal impulse may be applied extends all the way from periapsis to the semi-minor axis.

9.4 Time Open Transfer Between an Ellipse and a Hyperbola

This is one transfer problem which is completely solved in the time open case. Unfortunately the optimal solution requires infinite time. This optimal solution is useful for generating the optimal finite time transfer for long transfer times by means of a perturbation analysis. The optimum time open transfer requires five impulses. The first impulse is a tangential impulse at the periapsis of the initial ellipse which puts the vehicle onto an escape parabola. The second impulse is an infinitessimal impulse at infinity on the escape parabola and it transfers the vehicle onto an ellipse at infinity which transfers the vehicle to a different position on the celestial sphere. The third impulse is an infinitessimal impulse at infinity and it transfers the vehicle back

onto a parabola which will have its periapsis radius at the minimum allowable radius determined by the planetary radius and atmosphere. At the periapsis of the second parabola, a second finite impulse is applied tangentially to transfer the vehicle onto an escape hyperbola having the proper energy and the proper direction of the asymptotic velocity vector. The fifth and final impulse is an infinitessimal impulse at infinity on the escape hyperbola to produce the correct angular momentum vector for this hyperbola.

9.5 Time Open Transfer Between Two Hyperbolas

The optimum time open transfer between two hyperbolas is completely solved only in the case where the radius of the attracting body is zero so that impulses may be applied at the center of attraction. In this case the optimal transfer is a six impulse transfer where all the impulses are of infinitessimal magnitude and the transfer time is infinite. For the case where there is a minimum allowable radius, the transfer problem becomes quite complicated. By applying infinitessimal impulses at infinity, the problem is reduced to the problem of transfer between two asymptotic velocity vectors. The optimal transfer always lies in the plane of these two velocity vectors. This problem has been partially solved by Marchal in some recent papers. For some cases the optimal transfer requires four impulses and the use of an intermediate ellipse at infinity. This type of transfer requires the spending of an infinite amount of time in the vicinity of the planet. The other optimal transfers only require spending a finite time in the vicinity of the planet and involve energies which are always above the parabolic energy level.

When the transfer is not made through the parabolic level, there are never more than two finite impulses. If there is more than one finite impulse, at least one of these impulses always occurs at infinity. The other impulse will generally occur somewhat above the minimum allowable radius. It will only occur at the minimum allowable radius if a transfer between the two asymptotic velocity vectors may be made by means of a tangential impulse at the minimum allowable radius. If this is not the case, the impulse at a finite radius will not be tangential. The transfer hyperbolas may or may not descend to the minimum allowable radius.

9.6 Coplanar Time-Open Angle-Open Transfer

This is one transfer which has been completely solved analytically for the two impulse case. The problem is stated as optimal two impulse transfer between two different radii and between fixed radial and circumferential components of initial and final velocity. It may be looked upon as transfer between specified locations on initial and final orbits with the argument of periapsis of the orbits being left open. This solution is useful for re-entry and for ascent trajectories and has guidance applications since it can be written down in closed form. In general these transfers can be improved by adding an extra degree of freedom and not specifying the points of arrival and departure on the terminal orbits. In this latter case, the optimal orientation is always coaxial with the periapsis pointing in the same direction.

9.7 Time Open Transfer Between Fixed End Points

The problem of time-open two-impulse transfer between fixed positions on fixed initial and final orbits has been considered by a number of authors. The solution

has been reduced to finding the roots of an eighth degree polynomial. It has been shown that for some initial and final positions on elliptic orbits, the optimal two impulse transfer may involve a hyperbolic intermediate orbit. In this case, as well as in some other cases, the fuel consumption of the two impulse transfer may be reduced by going to a transfer through infinity. If the constraints that a finite impulse must be applied at the specified initial and final positions is dropped, then, by allowing coasting in the initial and final orbits, this problem may be reduced to the problem of optimal transfer between specified initial and final orbits. The problem with specified positions does have some application to ascent and descent trajectories where there may be a minimum allowable radius.

9.8 Time Fixed Transfer

Very little has been done on the problem of time fixed transfer and rendezvous. The work that has been done has shown that the problem is one of considerable complexity. The work with neighboring orbits has shown that the optimal transfer may involve up to six impulses. The work with singular arcs has shown that in the time fixed case there may exist optimal coplanar singular arcs so that singular arcs as well as a large number of impulses must be considered in finding the minimizing extremal for these transfers. The major contribution has been an iterative technique which allows the determination of an optimal n-impulse transfer from the non-optimal two-impulse transfer between the initial and final positions. However, this method is only a method for (hopefully) finding a locally minimizing solution. In general it will not be known if there are other n-impulse transfers or if there are other trans-

fers which may involve one or more singular arcs. This problem is a fruitful area for future research.

CHAPTER 10: SINGULAR ARCS

10.1 Necessary and Sufficient Conditions for Singular Arcs.

For optimal rocket trajectories with constant exhaust velocity, a phenomenon known as a singular arc may occur. A singular arc occurs when the coefficient of the thrust acceleration in the Hamiltonian remains identically zero over a finite thrust arc for a finite time. In these cases, the optimum magnitude of the thrust acceleration can not be determined from the Hamiltonian. Imposing the condition that the coefficient of the thrust acceleration in the Hamiltonian remains identically zero will allow the derivation of a magnitude for the thrust acceleration at each point on a singular arc. For the case where the thrust acceleration may become unbounded, this will correspond to the magnitude of the primer vector being unity along such an arc. Considerable information about such arcs may be determined by taking the successive derivatives of the magnitude of the primer vector, all of which will be zero. If the optimal thrust magnitude is bounded then the magnitude of the primer vector will be constant on a singular arc. As has been pointed out earlier, for linear problems singular arcs correspond to nonunique solutions with undefined acceleration magnitudes. However, for the nonlinear problem the acceleration magnitude on the singular arcs become well defined. Such arcs may be candidates for portions or all of a minimizing extremal.

The literature on the classical calculus of variations provides very little information on singular arcs. In recent years the discovery that singular arcs

may occur in minimizing solutions has lead to renewed interest in this problem. This recent work has culminated in necessary and sufficient conditions for singular arcs although the problem of coupling singular extremals to nonsingular extremals is still not in a satisfactory state. The first of the new necessary conditions was generalized or transformation of the Legendre-Clebsh condition of the calculus of variations. The extension was carried out by a number of investigators including Kelley, Tait, Robbins, Gurley, Goh, and Speyer. An additional necessary condition for singular arcs was then developed by Jacobson. More recently necessary and sufficient conditions have been obtained by Jacobson, Speyer and Jacobson, and McDanell and Powers. These conditions allow the testing of a singular arc for local optimality.

10.2 Junction Conditions

Kelley, Kopp and Moyer have shown that optimal junctions between singular and nonsingular arcs can be very complex. For example, they have shown that for the rocket problem with a bound on the thrust magnitude, an optimal junction between a singular and an arc of maximum thrust must involve a well-defined infinite sequence of switches between maximum thrust and zero thrust. This infinite sequence of switches takes place in a finite time. However, if impulses are allowed, it is apparently possible to have a simple junction between a singular arc and an impulsive thrust. Not much work has been done on this problem and it remains as a topic for future investigation.

10.3 Singular Arcs for an Inverse Square Field.

One of Lawden's many contributions to space trajectory optimization was his treatment of the coplanar singular arcs, and his analytical integration of the

time-open arc which has become known as the Lawden spiral. The generalized Legendre-Clebsh condition was subsequently applied to these arcs by Robbins and by Kopp and Moyer to yield the result that the optimal thrust direction must point in toward the center of attraction and that the square of the sign of the angle with the horizontal must be less than or equal to 1/3. This result rules out the Lawden spiral as on this singular arc the thrust always has a radial component directed away from the center of attraction. This is a very important result as it indicates that for the time-open coplanar problem the minimizing solution can never have a singular arc. However, Robbins has shown that for the time-fixed case a significant protion of the phase space is filled by singular arcs which do satisfy the generalized Legendre-Clebsh condition. Among these singular arcs is one considered by Fraeijs de Veubeke which corresponds to the fixed-time angle open case. This particular arc can be integrated analytically as can the Lawden spiral and a portion of this arc is minimizing. Robbins uses an argument similar to an argument in the classical calculus of variations to show that sufficiently short segments of singular arcs satisfying the generalized Legendre-Clebsh condition are locally minimizing. With the development of the new sufficiency conditions for singular arcs, this argument is no longer necessary and it remains as a topic for future investigation to apply the additional necessary and sufficiency conditions to the singular arcs of an inverse square field. Another problem for future investigation is the determination of composite extremals in an inverse square field involving both singular and nonsingular arcs.

The case of singular arcs in three dimensions has been treated by Christian Marchal. Two of his co-workers, Contensou and Marec, have also considered an academic type of singular arc which may occur in the time-open case. This

peculiar type of extremal involves applying a finite acceleration for an infinitisimal time and then coasting through an angle of 360^{o} before applying another infinitisimal pulse. These arcs do not appear to be of much interest because of their somewhat esoteric nature and partially because they appear to be nonminimizing.

CHAPTER 11: INTERPLANETARY TRAJECTORIES

11.1 Impulsive Trajectories

The problem of calculating optimum trajectories from one planet to another is an n-body problem. For preliminary analysis this n-body problem can be simplified by considering only the attraction of the sun and of those celestial bodies to which the space craft makes a close approach including the launch and the arrival planets. Lawden has made an approximate analysis of this n-body problem by utilizing what is essentially a low order matched asymptotic expansion. This type of analysis has been widely used for mission planning purposes and has been found to be sufficiently accurate for preliminary design purposes. In this analysis the radii of the spheres of influence of the planets are neglected. The trajectory from one planet to another is calculated as a heliocentric two body trajectory from the position of the first planet to the position of the second planet. The relative velocities of arrival and departure are then regarded as the asymptotic velocities on two body approach and departure hyperbolas relative to the planets. The time from one planet to another is based only upon the heliocentric two body transfe . The time inside the planetary spheres of influence is neglected.

A higher order analysis by Perko and Breakwell of the matched asymptotic expansion shows that the errors in calculating propulsion requirements from this model are acceptably small.

In calculating the primer vector for this approximate n-body trajectory a change must be made in the magnitude of the primer vector necessary to trigger an

impulse at the approach departure planets. The primer vector on the heliocentric trajectory is calculated in the normal fashion except that its boundary conditions are somewhat different. Lawden has shown that the magnitude of the primer vector at the start of the heliocentric arc should be smaller than unity by the ratio of the asymptotic velocity on the initial departure hyperbola to the periapsis velocity at the beginning of this departure hyperbola. A similar condition holds for the arrival hyperbola. These two conditions define the magnitude of the primer vector at the two ends of the heliocentric trajectory. The direction of the primer vector is the same as the direction of the relative velocity vector to the planets. The primer vector on the escape hyperbola has the solution corresponding to the Lagrange multiplier for changing the semi-major axis or the energy of the hyperbola. The primer vector is coincident with the direction of the velocity vector and its magnitude is proportional to the magnitude of the velocity vector.

The analysis of the heliocentric trajectory is conducted exactly as the analysis of the normal two-body orbit except for the changed condition on the critical magnitude of the primer vector at the launch and arrival planets. For an intermediate impulse given in heliocentric space the magnitude of the primer vector must again have a stationary maximum of unity.

Two impulse transfers from one planet to another are readily calculated by solving Lambert's problem for given launch and arrival dates. If contours of constant total delta v are plotted as a function of the launch and arrival dates the well known "pork-chop" curves are obtained. These trajectories may readily be checked for

local optimality by calculating the necessary conditions on the primer vector along the trajectory. During any single opposition only portions of the two impulse "pork-chop" curves will represent optimal transfers. In many cases it will be necessary to go to an additional mid course impulse or to initial or final coasting periods in order to have an optimal transfer from one planet to another. For some planets such as Mars or Venus the optimal transfer during any given opposition (the transfer requiring the lowest total delta v for any launch and arrival dates during the opposition) will be a two impulse transfer. For other planets such as Mercury an optimum rendezvous will generally require three impulses. An approximate first order theory of the optimum transfer to any planet during any opposition has been given by Marchal. Numerical calculations indicate that this first order theory is sufficient to be used to determine initial conditions for numerical processes to find the true optimum but is not sufficiently accurate to be a good approximation to the true non-linear minimum. Numerical calculations of optimum multiple impulse transfer from the earth to other planets have been carried out by Lion, Doll and Gobetz. These calculations show that mid course burns can be used to open up launch windows, and for planets such as Mercury to significantly reduce the delta v required for rendezvous missions.

11.2 Power Limited Trajectories

Many calculations have been made of optimum low thrust trajectories between various planets. These optimum trajectories must at the present time be found by numerical methods as none of the approximate analytic theories have proven sufficiently accurate. Several fairly efficient numerical techniques have been developed

and such trajectories can be routinely calculated for arbitrary launch and arrival dates. These trajectories have been calculated for various assumptions including constant power, constant thrust, constant acceleration, constant specific impulse and either solar electric or nuclear electric power supplies. The typical practice is to reduce the n-body problem to an approximate sequence of two body problems as is done for the impulsive case. An approximate theory of the influence of the departure planet's gravity on the heliocentric departure trajectory has been developed by Melbourne and by Edelbaum by using a low order matched asymptotic expansion. This analysis shows that a correction to the heliocentric trajectory due to the planeocentric gravity field is necessary, particularly for the larger planets. The treatment of the planeocentric phases depends on whether the energy to escape from the planet is provided by a high thrust or a low thrust propulsion system. For the case where the space craft spirals away from the planet under low thrust propulsion, the time spent during this escape maneuver must be considered. A refined analysis of this problem has been developed by Breakwell and Rauch. For the early electric propulsion systems it is generally more desirable to use high thrust systems to provide the planetary escape and capture propulsion. In these cases the aforementioned analysis of Melbourne and Edelbaum should be utilized. If curves of constant fuel consumption are plotted against launch and arrival dates some similarities are obtained with the corresponding results for high thrust propulsion. One difference is that in a low thrust case the fuel consumption generally decreases monotonically with the total transfer time. However, for any given transfer time, there is an optimum launch date and the optimum launch dates for low thrust

propulsion tend to be close to those for high thrust propulsion with about the same transfer times.

11.3 Swingbys

In one of Lawden's early papers he considered was referred to as a perturbational maneuver, where a space craft on its way to Mars would swing by the moon in order to pick up some additional delta v, for free, from the Moon's gravitational field. He found that the delta v that could be added by the moon was not very large and this idea was neglected for about 10 years. Even then, the idea was not a new one, as it had long been known that Jupiter could change the energy of comets and cause them to escape permanently from the solar system. In the early 60's it was discovered that for round trip missions to the near planets it was often desirable to use swingbys of Venus en route to Mars or vice versa. It was also discovered that the enormous gravitational field of Jupiter could be advantageously used to perform various missions throughout the solar system including the grand tour missions, close solar probes, and probes far out of the ecliptic plane. The analysis of optimum swingby missions falls within the general theory of optimal rocket trajectories treated in this monograph. The analysis is conducted by using matched asymptotic expansions as was the case with planetary escape and arrival trajectories. The analysis of optimal swingby missions can be carried out both for high thrust systems and low thrust power limited rocket systems. The effect of the swingby is to cause a discontinuous change in the direction of the primer vector at the swingby time at the two ends of the heliocentric approach and departure trajectories from the planet.

The angle that the primer vector rotates through is the same as the angle through which the hyperbola relative to the planet rotates its asymptotic velocity vectors. It is possible to treat both powered and unpowered swingby missions in this fashion. During a powered swingby mission an impulse is applied at a point close to the planet. For the powered swingby missions with high thrust it is possible to use the analysis of transfer between hyperbolic asymptotes treated in the chapter on inverse square force fields. The analysis of low thrust trajectories during swingbys is very similar to the analysis of low thrust trajectories during the approach and departure phases from the terminal planets.

CHAPTER 12: COMBINATION PROPULSION

12.1 Field Free Space

Early work on low thrust propulsion systems assumed that the low thrust system would be placed into orbit by a high thrust system and that all subsequent propulsion would be provided by the low thrust system. Later work on the utilization of low thrust propulsion systems indicated that it was often desirable to utilize high thrust in conjunction with low thrust for additional mission phases. It has been found that combinations of high thrust and low thrust propulsion systems can often provide better performance than either system when used alone. The simplest such missions to analyse are missions in field free space. The simplest of the field free space missions is the problem of changing only velocity. For this mission the payload with pure high thrust is independent of the mission duration while the payload with pure low thrust increases monotonically with mission duration. For mission times in the vicinity of the time for which the low thrust and the high thrust system have the same payload, the combination of both propulsion systems will provide higher payloads.

The optimum combination load may be described as follows: a high thrust impulse is first used to accelerate the vehicle to some fraction of the final desired velocity. Then the low thrust engine is turned on and operates until a later time when the power supply is dropped. After the power supply is dropped, a second high thrust impulse accelerates only the payload to the final velocity. For this mode

of operation, the payload is independent of the split between the initial and final impulses. It is possible to provide all of the high thrust impulse initially and then continue with low thrust so that the power supply is retained at the end of the mission. Alternately, the low thrust may be used first after which the power supply is dropped and all the high thrust is used at the end. This is a special result which only applies to this particular mission. For this case where the primer vector is constant in magnitude the benefits of combination propulsion are only significant when the payload is quite small.

A second interesting mission in field free space is a transfer between two positions of rest in field free space. Such a transfer may be considered as an approximation to a fast transfer to the outer planets with a nuclear electric propulsion system. The velocities required for fast transfers in this case are so high that the influence of gravitational fields and terminal velocities may be neglected. The optimum mode with pure high thrust is to provide an initial impulse, coast for a given time and then decelerate at the target position back to zero velocity with a second impulse. In this case the high thrust payload is a function of the flight time and increases monotonically with the flight time as does the low thrust payload. For short transfer times the payload with the high thrust system will be larger than the payload of the low thrust systems while for long transfer times the payload with the low thrust system will be larger. Once again combination propulsion is advantageous in the region where both systems have about the same performance. The combination mode for this mission is to first provide an initial velocity impulse , and then turn on the low thrust which has an acceleration magnitude that decreases linearly with time. The acceleration magnitude

passes through zero and then increases to its initial acceleration magnitude. A second and equal high thrust impulse is then provided after the power supply has been dropped. Once again the combination propulsion system can provide appreciable payload increases where the payload of either system alone is quite small and about equal to the payload of the other system.

12.2 Inverse Square Force Fields

In more complicated gravitational fields such as inverse square fields the difference between the maximum and the average values of the primer vector along the optimum trajectory maybe much greater than for the cases in field free space. By utilizing high thrust systems in those regions where the primer vector has its maximum values, much greater benefits from combination operation are possible than for the missions in field free space. If the inverse square field is a strong field then the analysis of Chapter 7 may be used for the low thrust phases of the mission. The high thrust phases may use the analysis in Chapter 9. Since the high thrust will be used impulsively the low thrust system may be assumed to be on all the time except possibly at the final impulse before which the power supply will be dropped. If there is more than one high thrust impulse it might be advantageous to drop portions of the low thrust power supply during the mission. This will also be true if the payload for the low thrust portion of the system becomes very small so that optimal staging of the low thrust power supply becomes desirable. The optimal mission modes in inverse square fields become very complicated and in different regions different combinations and sequences of low thrust and high thrust become optimal. It is necessary to assume different modes and check the local optimality by calculating the primer vector in order

to determine the local optima. These local optima must then be compared by determining which of the different modes tends to lead to the absolute minimum. The mission that has been analysed in most detail is escape from an inverse square field with a given hyperbolic velocity. The optimum mode for this mission has generally been found to be an initial period of low thrust which increases the semi-major axis of the initial circular orbit and also increases the eccentricity. At the end of the first low thrust phase the vehicle will be in an elliptic orbit, usually with a minimal allowable periapsis radius and a fairly high apoopsis radius. At this point a high thrust impulse is applied at periapsis to accelerate the vehicle beyond escape energy. A second period of low thrust may then be used if the final desired hyperbolic velocity is fairly large.

For transfer between co-planer, co-axial elipses the optimum mode may require from zero to two initial impulses. A second impulse, if it occurs, being given at the second apsis of the first transfer elipse. And there may also be from zero to two terminal impulses. Usually, there will be no more than two high thrust impulses in combination with the low thrust system, although, occasionally three impulses may be required. For the cases with two high thrust impulses, both impulses might occur at the beginning, one may occur at the beginning and one at the end, or both impulses may occur at the end depending upon the particular initial and final orbits.

BIBLIOGRAPHY

Chapter 1

Grodzovsky, G.L., Ivanov, Y.N., and Tokarev, V.V., Mechanics of Cosmic Flight with Low Thrust, Nauka, Moscow, 1966 (in Russian).

Ruppe, H.O., Introduction to Astronautics, Vol. 1, Academic Press, New York and London, 1966; Vol. 2, Academic Press, New York and London, 1967.

Sutton, George P. Rocket Propulsion Elements, 2d ed., pp. 128-158, John Wiley & Sons, Inc., New York 1956.

Jahn, Robert G., Physics of Electric Propulsion, McGraw-Hill Book Co., New York, 1968

Stuhlinger, E. Ion Propulsion for Space Flight, chap. 1, McGraw-Hill Book Company, New York 1964

Seifert, Howard S., Space Technology, John Wiley & Sons, Inc. , New York, 1959

Koelle, Heinz H., Handbook of Astronautical Engineering, McGraw-Hill Book Company, New York 1961

Bussard, R.W., and DeLauer, R.D. Nuclear Rocket Propulsion, McGraw-Hill Book Company, Inc., New York 1958.

Chapter 2

Bryson, Arthur E., Jr. and Ho, Yu-Chi, Applied Optimal Control, Blaisdell Publishing Company, Waltham, Mass. 1969

Pontryagin, L.S., Boltyanskii, V.G., Gamkrelidze, R.V., and Mishchenko, E.F., The Mathematical Theory of Optimal Processes, John Wiley & Sons, Inc. New York, 1962

Athans, M. and Falb, Peter L., Optimal Control, McGraw-Hill Book Company, New York, 1966

Chapter 3

Grodzovsky, G.L., Ivanov, Y.N., and Tokarev, V.V., Mechanics of Cosmic Flight with Low Thrust, Nauka, Moscow, 1966 (in Russian).

Lawden, D.F., Optimal Trajectories for Space Navigation, Butterworths, London, 1963

Luric, A.I., "Thrust Programming in a Central Gravitational Field", Chapter 4 of Topics in Optimization (Mathematics in Science and Engineering), Vol. 31, Academic Press, New York, 1967, pp. 104-146.

Chapter 4

Lawden, D.F., Optimal Trajectories for Space Navigation, Butterworths, London, 1963.

Preston-Thomas, H., "Some Design Parameters of a Simplified Ion Rocket," J. BIS, 16, 1958

Preston-Thomas, H., "A Note on 'A Nuclear Electric Propulsion System'," J. Brit. Interplan. Soc., 16, 1958, pp. 508-517.

Leitmann, G., "Minimum Transfer Time for a Power-Limited Rocket, "J. Appl. Mech., 28 1961, pp. 17-1178.

Leitmann, G., "On a Class of Variational Problems in Rocket Flight," J. Aero/Space Sci., 26, 1959, pp. 586-591.

Chapter 5

Lawden, D.F., Optimal Trajectories for Space Navigation, Butterworths, London, 1963.

Lurie, A.I., "Thrust Programming in a Central Gravitational Field", Chapter 4 of Topics in Optimization (Mathematics in Science and Engineering), Vol. 31, Academic Press, New York, 1967, pp. 104-146.

Edelbaum, T.N. and Pines, S. , "The Fifth and Sixth Integrals For Optimum Rocket Trajectories in a Central Field, AIAA Paper No. 69-904.

Pines, S., "Constants of the Motion for Optimum Thrust Trajectories in a Central Force Field", AIAA Journal, Vol 2, No. 11, Nov. 1964, pp. 2010-2014

Chapter 6

Edelbaum, T.N., "Optimum Low-Thrust Rendezvous and Stationkeeping," AIAA Journal, 2, 1964, pp. 1196-1201.

Chapter 7

Edelbaum, T.N., "Optimum Power-Limited Orbit Transfer in Strong Gravity Fields," AIAA Journal, 3, 1965, pp. 921-925.

Edelbaum, T.N., "An Asymptotic Solution for Optimum Power Limited Orbit Transfer," AIAA Journal, 4, 1966, pp. 1491-1494.

Chapter 8

Marec, J., "Transferts Infinitesimaux Impulsionnels Economiques Entre Orbites Quasi-Circulaires Non Coplanaires, "(Optimum Impulse Transfer Between Near Circular Non-Coplanar Close Orbits) Pres. XVIIth Int. Astronautical Cong., Madrid, Oct. 1966.

Marec, J., "Optimal Impulse Rendezvous of Long Duration Between Near-Circular Noncoplanar Close Orbits," Pres. Liege Colliquium on Advanced Problems and Methods for Space Flight Optimization, June 1967.

Edelbaum, T.N., "Minimum Impulse Transfer in the Near Vicinity of a Circular Orbit," AAS J., Vol, XIV, No. 2, March 1967, pp. 66-73.

Chapter 9

Gobetz, F.W. and Doll, J.R., "A Survey of Impulsive Trajectories" AIAA Journal, Vol. 7, May 1969, pp. 801-834.

Breakwell, J. V., "Minimum -Impulse Transfer," Paper 63-416, 1963, AIAA; also AIAA Progress in Astronautics and Aeronautics: Celestial Mechanics and Astrodynamics, Vol. 14, edited by V. G. Szebehely, Academic Press, New York, 1964, pp. 583-589.

Breakwell, J. V., "Minimum-Impulse Transfer Between a Circular Orbit and a Nearby Non-Coplanar Elliptic Orbit," Proceedings of the Liege Colloquium on Advanced Problems and Methods for Space Flight Optimization, Pergamon Press, to be published.

Contensou, P., "Etude Theorique Des Trajectories Optimales Dans un Champ de Gravitation Application au Cas d'un Center d'Attraction Unique," Astronautica Acta, Vol. 9, 1963, pp. 134-150; also "Theoretical Study of Optimal Trajectories in a Gravitational Field. Application in the Case of a Single Center of Attraction," TR-22, transl. by Paul Kenneth, Aug. 1962, Research Dept., Grumman Aircraft Engineering Corp.

Culp, R. D., "Contesou-Busemann Conditions for Optimal Coplanar Orbit Transfer," AIAA Journal, Vol. 5, No. 2, Feb. 1967, pp. 371-372.

Edelbaum, T. N., "Some Extensions of the Hohmann Transfer Maneuver," ARS Journal, Vol. 29, No. 11, Nov. 1959, pp. 864-865.

Edelbaum, T. N., "How Many Impulses?" Paper 66-7, 1966, AIAA; Astronautics & Aeronautics, Vol. 5, No. 11, Nov. 1967, pp. 64-69.

Gobetz, F. W., Washington, M., and Edelbaum, T. N., "Minimum Impulse Time-Free Transfer Between Elliptic Orbits," CR-636, Nov. 1966, NASA.

Horner, J. M. "Optimum Two-Impulse Transfer Between Arbitary Coplanar Terminals," ARS Journal, Vol. 32, No. 1, Jan. 1962, pp. 95-96.

Marchal, C., "Transferts Optimaux Entre Orbites Elliptiques (Duree Indifferente)," Presented at 16th International Astronautical Congress, Athens, September 1965. Also "Optimum Transfers Between Elliptical Orbits (Time Open)," Redstone Scientific Information Center Translation RSIC-515, March, 1966, Redstone Arsenal, Ala.

Marchal, C., "Transferts Optimaux Entre Orbites Elliptiques Coplanaires (Duree Indifferente)," Astronautica Acta, Vol. 11, No. 6, Nov.-Dec. 1965, pp. 432-435.

Marchal, C., "Transferts Optimaux Entre Orbites Hyperboliques (Rayon Planetaire Non Nul)," presented at 17th International Astronautical Congress, Madrid, Oct., 1966.

Marchal, C., "Synthesis of the Analytical Results on Optimal Transfers Between Keplerian Orbits (Time-Free Case)," TP 482, 1967, ONERA. Also presented at the Liege Colloquim on Advanced Problems and Methods for Space Flight Optimization, June 1967.

Marchal, C., Marec, J.-P. and Winn, C. B., "Synthese Des Resultats Analytiques Sur Les Transferts Optimaux Entre Orbites Keplériennes," presented at the 18th International Astronautical Congress, Belgrade, Sept. 1967.

Moyer, H. G., "Necessary Conditions for Optimal Single Impulse Transfer," AIAA Journal, Vol. 4, No. 8, Aug. 1966, pp. 1405-1410.

Moyer, H. G., "Minimum Impulse Coplanar Circle-Ellipse Transfer," AIAA Journal, Vol. 3, No. 4, April 1965, pp. 723-726.

Sun, Fang-Toh, "On Optimum Transfer Between Two Terminal Points for Minimum Initial Velocity Vector," CR-622, Nov. 1966, NASA.

Winn, C. B., "Minimum Fuel Transfers Between Arbitrary Coaxial Ellipses," presented at the Liege Colloquium on Advanced Problems and Methods for Space Flight Optimization, June 1967, proceedings to be published by Pergamon Press.

Chapter 10

Robbins, H. M., "Optimality of Intermediate Thrust Arcs of Rocket Trajectories," AIAA Journal, Vol. 3, No. 6, June 1965, pp. 1094-1098.

Robbins, H. M., "Optimal Rocket Trajectories with Subarcs of Intermediate Thrust," presented at the 17th International Astronautical Congress, Madrid, Oct. 1966. Also Rept. 66-825-2009, IBM Federal Systems Division.

Kelley, H. J., Kopp, R. E., and Moyer, H. G., "Singular Extremals," Topics in Optimization, Mathematics in Science and Engineering, Vol. 31, Academic Press, New York, 1967, Chap. 3, pp. 63-101.

Lawden, D. F. Optimal Trajectories for Space Navigation, Butterworths, London, 1963.

Fraeijs, de Veubeke, B. , "Canonical Transformations and the Thrust-Coast-Thrust Optimal Transfer Problem," Astronautica Acta, Vol. 11, July-Aug. 1965, pp. 271-282.

Chapter 11

Doll, J. R. and Gobetz, F. W., "Three-Impulse Interplanetary Rendezvous Trajectories," Proceedings of the Southeastern Symposium on Missiles and Aerospace Vehicle Sciences of AAS, Vol. II, Dec. 1966, pp. 55-1-55-14.

Jezewski, D. J. and Rozendaal, H. L., "An Efficient Method for Calculating Optimal Free-Space N-Impulse Trajectories," MSC Internal Note 67-FM-170, Nov. 1967, NASA.

Lion, P. M. and Handelsman, M., "The Primer Vector on Fixed-Time Impulsive Trajectories," Paper 67-54, Jan. 1967, AIAA; also AIAA Journal, Vol. 6, No. 1, Jan. 1968, pp. 127-132.

Chapter 12

Edelbaum, T. N., "The Use of High- and Low-Thrust Propulsion in Combination for Space Missions," The Journal of the Astronautical Sciences, Vol. 9, No. 2, Summer, 1962., pp. 49-60.

Fimple, W. R., "An Improved Theory of the Use of High- and Low-Thrust Propulsion in Combination," The Journal of the Astronautical Sciences, Vol. 10, No. 4, Winter, 1963, pp. 107-113.

Grodzovsky, G. L., Ivanov, Y. N., and Tokarev, V. V., Mechanics of Cosmic Flight with Low Thrust, Nauka, Moscow, 1966 (in Russian).

PROBLEMS

1. A body moves in a central force field where the force is directed towards the origin and is proportional to the distance from the origin. What shape does an unpowered orbit have in such a force field? How many periapses and apoapsides are there in one revolution? What is the period of the orbit? (Rectangular coordinates are suggested for this and the following two problems.)

2. Assume that the optimum impulsive transfer between a circular orbit and a coplanar elliptic orbit in the above force field requires two tangential impulses at the apsides. What is the minimum ΔV required for transfer from a circular to an elliptic orbit? Does the transfer to the apoapsis or to the periapsis require less fuel? Both the periapsis and the apoapsis of the ellipse may be either larger or smaller than the radius of the circular orbit.

3. Derive the optimum thrust program for a power-limited vehicle in the linear central force field of Problem 1. Express this program in terms of the initial values of the Lagrange multipliers and the time by integrating the Euler-Lagrange equations.

4. A power-limited vehicle is moving along the x axis towards the y axis in field-free space. What is the minimum J to transfer from velocity u^o and position x^o to a final velocity v_1 directed along the y axis in the time t_1? What is the optimum value of y at t_1 for this J? What is the optimum value of x^o?

5. Synthesize the optimal control for transfer from any state to the final state of problem 4.

DOCUMENT CONTROL DATA - R & D

Analytical Mechanics Associates, Inc
179 Fifth Street
Cambridge, Massachusetts 02141

UNCLASSIFIED

3. REPORT TITLE

OPTIMAL SPACE TRAJECTORIES

4. DESCRIPTIVE NOTES (Type of report and inclusive dates)
Scientific Final

5. AUTHOR(S) (First name, middle initial, last name)

Theodore N. Edelbaum

6. REPORT DATE	7a. TOTAL NO. OF PAGES	7b. NO. OF REFS
~~January 1970~~ December 1969	156	

8a. CONTRACT OR GRANT NO	9a. ORIGINATOR'S REPORT NUMBER(S)
AFOSR 49(638)-1648	
b. PROJECT NO 9749-01	
c. 61102F	9b. OTHER REPORT NO(S) (Any other numbers that may be assigned this report)
d. 681304	AFOSR 70-0299TR

10. DISTRIBUTION STATEMENT

1. This document has been approved for public release and sale; its distribution is unlimited.

11. SUPPLEMENTARY NOTES	12. SPONSORING MILITARY ACTIVITY
TECH, OTHER	Air Force Office of Scientific Research (SR 1400 Wilson Boulevard Arlington, Virginia 22209

13. ABSTRACT

The proliferation of papers published on various aspects of optimum space trajectories has made it desirable to produce a unified treatment of this subject that will contain the major results of these papers. This monograph on optimal space trajectories is addressed to this goal. The monograph includes Chapters on space propulsion systems, the maximum principle, general theory of optimum rocket trajectories, trajectory optimization in field free space, trajectory optimization in an inverse square-field, linearized power-limited transfer in the vicinity of an elliptic orbit, optimum power-limited orbit transfer in strong gravity fields, linearized impulsive transfer in the vicinity of a circular orbit, optimum impulse transfer in an inverse square field, singular arcs, interplanetary trajectories, and combination propulsion.

DD FORM 1 NOV 65 1473

Security Classification